INFORMATION TO USERS

This manuscript has been reproduced from the microfilm master. UMI films the text directly from the original or copy submitted. Thus, some thesis and dissertation copies are in typewriter face, while others may be from any type of computer printer.

The quality of this reproduction is dependent upon the quality of the copy submitted. Broken or indistinct print, colored or poor quality illustrations and photographs, print bleedthrough, substandard margins, and improper alignment can adversely affect reproduction.

In the unlikely event that the author did not send UMI a complete manuscript and there are missing pages, these will be noted. Also, if unauthorized copyright material had to be removed, a note will indicate the deletion.

Oversize materials (e.g., maps, drawings, charts) are reproduced by sectioning the original, beginning at the upper left-hand corner and continuing from left to right in equal sections with small overlaps.

ProQuest Information and Learning
300 North Zeeb Road, Ann Arbor, MI 48106-1346 USA
800-521-0600

Surface-Enhanced Raman Spectral study of Pyridine, Heme Proteins in the Presence and Absence of Surfactants Adsorbed on a Silver (Ag) Electrode Surface.

by
Richard Foucault

A Dissertation Submitted to the Graduate Faculty in Chemistry in partial fulfillment of the Requirements for the Degree of Doctor of Philosophy, The City University of New York.

2003

UMI Number: 3103110

ProQuest Information and Learning Company
300 North Zeeb Road
P.O. Box 1346
Ann Arbor, MI 48106-1346

This manuscript has been read and accepted for the Graduate Faculty in Chemistry in satisfaction of the dissertation requirement for the degree of Doctor of Philosophy.

5-28-03
date

Chairman of Examining Committee

May 29, 2003
date

Executive Officer

Supervisory committee

The City University of New York

Abstract

SURFACE-ENHANCED RAMAN SPECTRAL STUDY OF PYRIDINE, HEME PROTEINS IN THE PRESENCE AND ABSENCE OF SURFACTANTS ADSORBED ON A SILVER (Ag) ELECTRODE SURFACE.

by

Richard Foucault

Advisors: John R. Lombardi, Patricia A. Broderick, and Ronald L.Birke

Surface-enhanced Raman spectroscopy is one of the spectroscopic techniques used to investigate the orientation, and conformational changes of pyridine, heme proteins and surfactants adsorbed on a silver (Ag) electrode.

For pyridine, its SERS was studied in different electrolyte solutions and compared with theoretical calculations. We showed that the adsorbate has no effect on the metal-nitrogen band at approximately 230 cm^{-1}, that is, when the SERS was taken in different electrolyte solutions. In addition, a very negative voltage results in changed orientation of water molecules and solute toward the electrode surface.

Heme proteins such as horse skeletal muscle myoglobin and horse heart cytochrome c were also investigated for the oxidation state, spin state, and the orientation of the iron atom of the heme chromophore. It was found that at a specific voltage, the iron of the heme chromophore can exist as Fe^{2+} or Fe^{3+}; the chromophore can have an orientation in the plane or out of the plane of the tetrapyrrole ring.

The structure of surfactants and their interaction with the electrode surface were also investigated SERS. The interaction between the electrode surface

and the surfactants was found to be dependent on the charge of the head group and electrode potential applied. Over a range of voltage from -0.1V to –0.9V, most of the surfactants have a head-on orientation toward the electrode surface using a saturated calomel electrode (SCE) as a reference electrode. However, at a relatively more negative voltage, the polar head group of the surfactants is directed away from the electrode surface. With the exception of cetylpyridinium chloride (CPC), all of the surfactants have the ability to form a protective layer of film that prevent hydrogen evolution at a very negative voltage, i.e., beyond –0.9V.

Finally, we have incorporated heme proteins inside DDAB surfactant, and an increase in electron transfer has been observed using cyclic voltammetry and SERS. The increase in electron transfer can be explained by the fact that the DDAB surfactant has provided a specifically favorable orientation of the protein toward the electrode surface facilitating electron transfer between the electrode and the molecules.

Acknowledgements

The first experience that motivated my desire to become a scientist was very strange and bizarre at the same time. It all started when I was a ten-year-old boy during a summer vacation in my native country, Haiti. At that time, I was at my grandmother's house located in the countryside. One day, it was raining while the sun was shining; my grandmother told every one of us (grandchildren) to go outside to take a shower in the rain because she had her own belief regarding rain. My grandmother has always believed that rain is a process by which God urinates and blesses all the creatures on earth and that belief was the main reason that prompted her to tell us (grandchildren) to go outside and take a shower whenever it was raining. At the age of ten, one of the relevant questions that immediately crossed my mind was: How big is God so that he can urinate over such a wide area that can cover an entire city and even a country? At the end of the summer vacation, I had to go back to the capital city of Port-au-Prince for school and rejoined my immediate family (mother and siblings). At my elementary school, every student had to share their summer experience with the class by standing up in front of the class and telling their stories while classmates and the teacher were listening attentively. After listening carefully to every student's summer's experience, including mine, my elementary school teacher approached me and told me my experience was very funny. The only explanation that he gave me was: "It is all science". I had to wait until high school to get a detailed and satisfactory explanation of rain.

One explanation was closer to the truth while the other one was hiding it. However, both of them had really shaped my life since I strongly believe in the existence of a supreme being (God) while the other explanation (It is all science) can be considered the main reason for my decision to become a scientist. For a good part of my adolescent life, I had to struggle to reconcile both explanations that regarding rain because in Haiti parents and teachers are regarded in very high esteem and should always be trusted. Indeed, my strong belief in God originates mainly from my grandmother's belief about rain.

The educational background that I have received in high school in Haiti had really provided me with a good foundation which served me well in college and graduate school in the United States of America. At the City College, I was exposed to a variety of great professors, and they have really contributed to my intellectual improvement. My studies at the City College of New York dated back to the fall of 1989 when I was enrolled as a freshman majoring in Biochemistry and Mathematics. Students at the City College of New York, as is the case in every college and university in America, must be totally dedicated in order to survive. I will always remember City College and the names of so many great professors who contributed to my intellectual career.

I would like to thank my entire family for their support: my mother who never stopped sacrificing herself in order to provide her children with a top quality education, my two brothers, and unique sister, for their love and words of encouragement.

Finally, I have to thank the National Institutes of Health (NIH) for its financial support throughout my graduate studies at City College and at the Graduate Center of CUNY. The financial support that I have received from the NIH through the MBRS (RISE program) at the City College of New York really made my dream become a reality. Once again, thank you so much, NIH.

TABLE OF CONTENTS

List of Figures

List of Tables

Chapter 1

Introduction to SERS from a Silver Electrode Surface.

A. Raman scattering and its origin

Raman spectroscopy is one of the techniques used to study the transition between various vibrational states of a specific molecule. It is essentially a scattering technique while IR (Infrared) is resonance absorption of IR radiation. The difference between Raman spectroscopy and its counterpart IR spectroscopy is the mechanism which gives rise to the two techniques. A major difference between Raman and infrared techniques is that there is no infrared analog of the resonance Raman (RR) effect. The latter occurs when the laser wavelength, used to excite the Raman spectrum, lies under an intense electronic absorption band of a chromophore. Under these conditions, tremendous intensity enhancement of certain Raman bands may occur with the result that the absolute intensities are increased by a factor of 10^3 to 10^5. Raman and infrared spectroscopies are both complementary to each other and the reason for this lies in the different natures of the physical process involved in the two effects. Raman spectroscopy is essentially a scattering effect involving an induced dipole moment μ, which in turn, depends on a change in molecular polarizability during vibration. In contrast, infrared spectroscopy is an absorption process caused by a change in the permanent molecular dipole with change in bond length during vibration. In addition, infrared and Raman spectroscopies have different selection rules and as a results, homonuclear molecules (S_2, O_2, N_2) have no IR spectrum since these molecules have no net dipole moment while the

Raman spectra for these molecules exist because they have experienced a change in their permanent molecular dipole.

Raman spectra help in the study of the structural changes of molecules by giving detailed information about the vibrational motions of atoms in the molecules since these vibrations are sensitive to chemical changes. The vibrational spectrum can be used as a probe to monitor molecular chemistry. The vibrational motion that produces the peaks in Raman spectra are similar to the vibrational motion that also produces the absorption peaks in infrared spectra. Therefore, the methods are complementary and most of the basic or trivial information gathered from infrared studies can be used for Raman spectroscopy and vice-versa. Differences between infrared and Raman techniques exist in the physical aspect of the two methods and these dissimilarities have important implications for the applications of vibrational spectroscopy to such areas as biochemistry. For example, spectroscopic analysis of biochemical molecules in water is possible using Raman spectroscopy since water is a weak Raman scatter while this same analysis cannot be done using the infrared technique since water strongly absorbs in the infrared region and as a result it interferes greatly with the study of biochemical molecules in water. Therefore, under these conditions, the Raman data are the sole source of information.

Mechanism

IR- electric dipole mediated transitions
Raman- inelastic light scattering

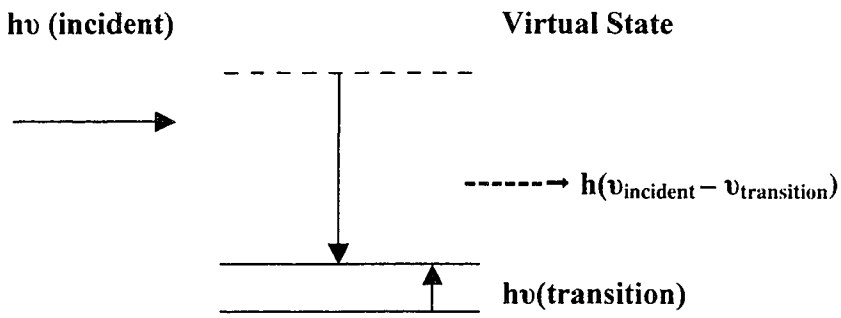

B. The Raman effect and Raman spectroscopy

Raman spectroscopy is primarily concerned with the phenomenon in which a shift in frequency occurs when light is scattered by molecules. For example, if incident light with a specific wavelength (λ) and frequency (ν_0) impinges on a molecular system the component of Raman scattered light will have a frequency of ν_r. Then, the frequency shift $\nu_r - \nu_0 = \Delta\nu$ may be either positive or negative. Its magnitude is referred to, as a Raman frequency and the set of Raman frequencies of the scattering species constitute its Raman spectrum.

A shift in frequency characterized by the symbol $\Delta\nu$ implies a change in energy $\Delta\nu/h$. Usually, the Raman spectrum is measured as intensity versus wavenumber instead of frequency. A frequency is defined as a number of

vibrations per seconds, whereas wavenumber (ν) is the number of waves per centimeter, and so is related to ν by the equation $\nu = \nu/c$, where c is the velocity of light.

Radiance per molecule (I) is defined according to Furtak [4] as $I = A (\omega)^4 (\hat{e} \mu)^2$ (1) where A is a constant, ω is the scattered angular frequency, μ is the induced dipole moment and $\hat{e}$ is the unit vector identifying polarization selected in the scattered beam. The induced dipole moment is related to the incident field through the effective polarizability (α) and is related to how hard or easy it is to move electrons in a molecule and it depends on the size and shape of the molecule.

(2) $\mu_{Induced} = \alpha * E$ where E is the incident electric field and since the molecule is an oscillating dipole, we can say the electric field is oscillating with an initial electric field (E_0) defined by equation (3).

(3) $E = E_0 \cos(2\pi\omega_0 t)$ and by replacing equation (3) into (2) , we have

(4) $\mu_{induced} = \alpha * E_0 \cos(2\pi\omega_0 t)$

The polarizability tensor α, which is a physical quantity written as a matrix, and it can be defined and expanded the following way:

(5) $\alpha = \alpha_0 + (\delta\alpha / \delta Q_i)*Q_i$ where Q_i are the normal coordinates of the system.

(6) $Q_i = A\cos(2\pi\omega t)$

Thus, we have the induced dipole moment equal to:

(7) $\mu_{Induced} = \alpha * E_0\cos(2\pi\omega_0 t) + (\delta\alpha / \delta Q_i) * A_\nu E_0\cos(2\pi\omega_0 t) \cos(2\pi\omega t)$

finally eq (7) can be rearranged and gives the dipole moment as a function of ω_0 , $\omega_0 + \omega$ and $\omega_0 - \omega$.

$\mu_{induced} = \alpha^* E_0 \cos(2\pi\omega_0 t) + 1/2(\delta\alpha / \delta Q_i)^* A_v E_0\{\cos[2\pi(\omega_0 - \omega)t + \cos[2\pi(\omega_0+\omega) t]\}$

where ω_0 : Rayleigh scattering

$\omega_0 + \omega$: Stokes scattering

$\omega_0 - \omega$: Anti- Stokes scattering

Quantum mechanically the polarizability α (Raman scattering) is described by the second order time- dependent perturbation theory:

$$\alpha_{0 \to n}(\omega) = \Sigma \frac{\langle n|\mu|k\rangle\langle k|\mu|0\rangle}{E_0 + \hbar\omega - E_k + i\Gamma}$$

The above expression is in fact the Kramers- Heisenberg- Dirac (KHD model) where $\langle n|\mu|k\rangle = \int \Psi_n^* \mu \Psi_k \, d\tau$ and the sum is over all the excited states, n, of the system. E_0 and E_k are the energies of the initial and final states and $i\Gamma$ is inversely proportional to the lifetime of the excited states n.

C. Chemisorption and Physisorption

Normal Raman scattering is very weak and can not be used to study molecules on surfaces, however, Surface-Enhanced Raman Scattering (SERS) provides a large enhancement to molecules adsorbed on a coinage metal surface. Since most of the time SERS is used to monitor a specific molecule's behavior as a function of voltage, it can have different

orientations on the metal surface depending upon the applied voltage. At some specific voltage, the metal surface can be positively or negatively charged and as a result, molecules that we want to study might form some type of bond with the metal surface. We can take the case of one of the simplest and earliest molecule (pyridine) that spectroscopists used in the past to illustrate the chemisorption and physisorption phenomena. At potentials positive to the point of zero charge (P.Z.C.), the silver electrode surface is positively charged; pyridine is adsorbed to silver via its nitrogen and in an aqueous acidic environment. And, in that case the water molecules are orientated in such a way that the oxygen atoms of each water molecule are pointed toward the metal surface (chemisorbed). However, at potentials negative to the (P.Z .C), the silver electrode is negatively charged and pyridine is adsorbed in an aqueous environment in which the two hydrogens of each water molecule are pointing toward the electrode surface (physisorbed). We can also assume that part of the surface enhancement in SERS is due to a chemisorption induced increase of the molecular polarization. There exist many theories [6,27,31] that suggest possible mechanisms for such an enhancement, but unfortunately, most models are such that their quantitative predictions are not very reliable and the qualitative ones are numerous which makes it harder for experimental identification.

D. Characteristics of the Surface-Enhanced Raman Scattering

i) The interaction between the metal surface and molecules

Surface-Enhanced Raman Spectroscopy is a phenomenon that is mostly dependent on the submacroscopic surface roughness of the metal and the geometrical shape of metal nanoparticles. Upon adsorption, it is believed that some molecules make a very weak chemical bond with the metal surface. Three types of interaction have been proposed between molecules and a SERS active surface and they are the following: physisorption, adsorption through an ion pair or a direct chemical bond between the metal and the adsorbate.

Physisorption occurs when a molecule does not have specific chemical bonding interactions with the metal surface. The type of interaction involved in physisorption is an electrostatic attraction or dipole-dipole interaction, but no real chemical bond is involved and as a result, there is no sharing of electrons between a molecule and the electrode surface. The mechanism for this attraction can be perceived in the following way: as the adsorbate gets closer to the surface the dipole moment of the adsorbate induces an image dipole, like a reflection on the metal surface on the opposite side of the surface of opposite polarity. The two, oppositely polarized, dipoles attract each other through dipole-dipole interaction and generate an electromagnetic field on the surface. It is also worthy to mention that in this kind of interaction, a weak electromagnetic enhancement is the only predominant effect that is involved. An illustration involving metal complexes with

different types of ligands that may be physisorbly adsorbed on an electrode surface has been shown by S.Farquharson et al [3] , he has elaborated more on the differences that exist when the complex possesses ligands that contain available lone pairs of electron as opposed to those ligands that do not have a remote pair of electrons located on a nitrogen atom. In one case (when there exist no available lone pair of electron) the complex interacts with the surface through dipole-dipole interaction, while in the second case it interacts with the surface through a weak bond.

Another type of interaction between the surface and adsorbate molecule involves molecules that do not possess nitrogen's atom lone pair, but are ions. In this case, the ion pair theory can be used in an attempt to explain the interaction of those adsorbates with the metal surface. Sun et al [16] have shown that the pyridinium ion and its derivatives are an example of this type of interaction; they have also shown that the adsorption of pyridinium is related to the adsorption of a halide counter ion. The mechanism that supports the ion pair theory can be perceived as the metal surface is being pretreated in an electrolyte, the surface becomes positively charged making an ion pair with any halide ion (negatively charged ion such as Cl^-, Br^-, I^- originating from the electrolyte used) and the pyridinium ion can bind with the adsorbed halide ion through the conjugated π orbital system or through dipole-dipole interaction.

The third type of interaction involves unsaturated molecules that possess a double or triple bond in their structure. In this case, some π bond interaction

is believed to take place between the adsorbate and the metal surface. The SERS spectra of some aromatic molecules such as benzene and its derivatives [47] have been shown to bind through their π-orbital system when they are adsorbed on a gold electrode surface and it has been shown that these molecules take a flat orientation on the metal surface. SERS has also been observed for ethylene whereas ethane does not have any SERS spectrum. That observation has been supported by the findings of Moscovits [12,14,17] who was one of the first Raman spectroscopists to obtain the spectra of ethylene and acetylene on colloidal silver particles formed by gas aggregation and isolated at low temperature in solid adsorbate/argon matrices. Since no SERS signal has been observed for ethane, it has been concluded with certainty that the molecule was not chemically bound to the surface and the only way that ethylene could interact with the metal surface is through its π bond.

ii) The effect of surface roughness

A roughened electrode surface is considered as one of the major contributors to the SERS enhancement and also it is a necessary requirement leading to a SERS signal. Van Duyne et al [9, 29] , affirmed that the surface roughness contributes a factor of 10^2 of the overall 10^6 enhancement , and in some cases a SERS signal has been taken without roughening the metal surface. The process of roughening the electrode surface in SERS is called a pretreatment during which an oxidation-reduction cycle (ORC) is used to oxidized/reduced the metal surface and it is achieved with a double potential step or triangular

sweep. Varieties of methods are at our disposal when we want to obtain surface roughness but the most commonly used method involves performing an ORC while the electrode is submerged into an electrolyte solution. The silver electrode, most of the time, is roughened in a 0.1M potassium chloride (KCl) solution by applying a potential step from – 0.6V to + 0.3V and then back to – 0.6V for a period of a few seconds (usually only two seconds) and all the potentials are relative to the saturated calomel electrode (SCE) . Our electrode system consisted of a working electrode (Ag, Au, Cu) , a counter electrode made up of platinum wire and a reference electrode that was a saturated calomel electrode (SCE) . During the pretreatment, the potential was held at a positive potential for a very specific period of time ranging between one to ten seconds. Surface roughness could be seen with the naked eye by removing the electrode from the electrochemical cell and the shiny texture of the metal before pretreatment was replaced by a colored surface after pretreatment and usually one cycle was enough to give an intense spectra. However, since the oxidation-reduction cycle involves a number of charged particles per area (mC/cm^2), it has been shown by some of the pioneers of SERS that the number of charges per surface area has a direct effect on the SERS intensity. It has been postulated that more than 50 mC/cm^2 will lead to a SERS spectrum with a very low intensity. It is also worthy to mention that the most common electrolytes used in this research for SERS were the halide salts (KCl, KI, KBr and KF), sodium chloride, potassium and sodium sulfates.

Since each metal possesses its own intrinsic chemical and physical properties, it has been observed that other metals such as gold and platinum did not give an intense and reproducible SERS. In fact, a new pretreatment technique was developed whenever gold electrode had to be roughened in an electrolyte. Weaver [11] has demonstrated that reproducible SERS can be obtained using gold electrode under certain conditions and Busby [23] has used a method for producing SERS active gold electrodes involving electroplating from a solution of $KAuCl_4$. However , it remains a fact that the most commonly used method to roughen an electrode involves an ORC electrochemical roughening of the metal surface.

iii) Experimental procedures for SERS

A modern SERS apparatus has the same basic elements used in a normal Raman or resonance Raman instrument. Figure 1. shows an experimental set up for a photon counting SERS experiment .An intense monochromatic radiation originating from a laser source was focused onto or into a sample. After hitting its target, the intense beam of light is scattered and gathered by collecting optics directed to a dispersing system usually a double monochromator. At the exit part of the monochromator the Raman spectrum forms an image identical to a series of faint lines and they are in turn detected and recorded by a photomultiplier. The monochromatic radiation source is usually a continuous wave (CW) laser. The most widely used systems that provide such a continuous waves (CW) are the argon and krypton ion gas lasers. They can be adjusted or tuned between various

discrete wavelengths in order to satisfy the resonance condition. Electrochemical SERS measurements at an electrode surface involves a Raman cell which is an electrochemical cell connected to a potentiostat system that allows us to study molecules on the metal surface as a function of voltage. In order to obtain SERS signal, it is generally accepted among Raman spectroscopists that some form of surface roughness has to be achieved and the process is called a pretreatment. In the case of a silver (Ag) electrode, the electrode is usually polished with a finely divided alumina slurry of different sizes (0.3 and 0.05 micron), washed with distilled water and then ultrasonicated to remove any small particles of alumina that could still stay on the electrode surface. Usually, with a silver electrode, an initial potential is set negative to the onset Ag oxidation and then the electrode potential is either stepped or scanned into the positive region where silver oxidation occurs. For a halide-containing electrolyte, insoluble silver halide is formed on the metal surface that is then reduced back to silver (Ag) upon either reversing the potential sweep or stepping back to a potential negative to the region of stable silver halide.

SCHEMATIC DIAGRAM OF A SERS EXPERIMENT

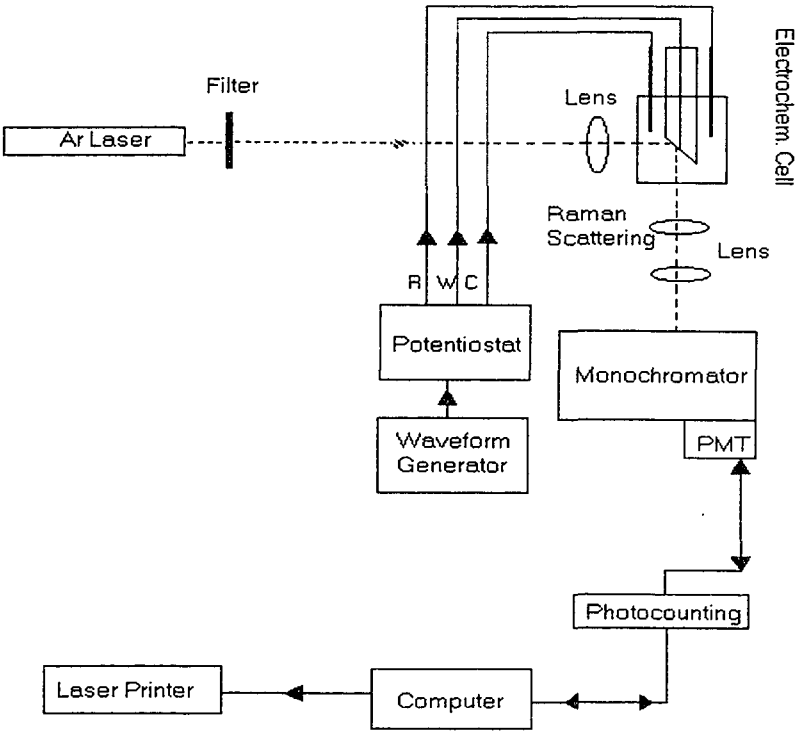

Fig 1.

E. Overview of the Mechanisms Contributing to Surface Enhancement.

Many theories have been proposed in the past in an attempt to explain the enhancement mechanism of SERS. The two main effects that have been proposed by most Raman spectroscopists are the chemical and electromagnetic effects . However, none of the theories have given a complete explanation of all the experimental evidence and it seems that the effects leading to the enhancement mechanism of SERS is a mixture of a few components, each one contributing in a different way to the overall enhancement.

Originating from the work of Fleischmann et al , in 1974[28], SERS has gained tremendous momentum in an unprecedented fashion since then. The enormous increase in the Raman scattering in a SERS spectrum has proved to be responsible for the growing interest in this technique that allows in-situ surface vibrational spectroscopy of a variety of molecules. An increase in intensity can be as high as 10^{14} fold that of the intensity seen from the same number of molecules in the bulk solution. Some workers in the field have proposed a theory called the "Giant Raman effect" to elucidate the causes for that large increase in intensity for SERS and their efforts have lead to several publications and reviews[17, 24]; however, a complete and perfect mechanism which leads to the "Giant Raman effect" is still under scrutiny and the subject of controversy. The study of SERS requires the interplay of many

fields such as spectroscopy, electrochemistry, analytical and physical chemistry, solid state and surface chemistry. Surface-enhanced Raman spectroscopy allows us to probe in- situ for detailed and unique vibrational patterns of molecules adsorbed on metal surface. High resolution can be obtained using the visible range (0.1 cm^{-1}) that is better than other types of spectroscopy such as IR (infrared) spectroscopy and EELS (electron energy loss spectroscopy) and it allows us to measure a frequency mode as low as 5 cm^{-1}.

i) Chemical enhancement

It has been reported that one of the effects that contribute to SERS is a chemical effect in which a metal surface is immersed in an electrolyte solution, therefore establishing a solid-solution interfaces[81]. Before elaborating more on the chemical effect in SERS, it is also worthwhile to mention SERS is not only limited to metal/solution interfaces[24,25,27,31] but it has also been observed at a metal/gas interface[25] (metal/metal) , at metal-island film / liquid interfaces[27], at metal grating / thin film interfaces[31], at a silver and gold metal sol/ liquid interfaces[18], on dried electrodes and in ultra high vacuum experiments[24].

The chemical enhancement occurs when the actual Raman scattering matrix element of light interacting with an adsorbed molecule is altered by the presence of the surface. This type of enhancement involves direct charge transfer between the molecule and the metal, which in turn, induces modulation of the surface tunneling barrier for electrons. The contribution

of the chemical enhancement to SERS is mostly limited to the molecules located in the first monolayer in direct contact with the surface or on specific active sites. During the charge transfer process an incident photon causes an intraband transition from the Fermi level state of the molecule or from the ground state of the molecule to the Fermi level of the metal. For molecules physisorbed on the surface, the process occurs through tunneling while for chemisorbed molecules the process occurs by virtue of a weak chemical bonding between the molecule and the metal surface . Charge transfer can also occur by emission of photon and in that case the charge is transferred back from the excited state of the molecule to the metal resulting in the molecule being left in a higher vibrational state. This process involves charge transfer from metal to molecule and the reverse process can also take place. The charge transfer theory is the basic theory which explains the resonance Raman excitation and the resonance potential dependence. The charge transfer mechanism is supported by the following expression[27]:

$I = [\, 8\pi (\omega + \omega_{FI})^4 I_L / 9C^4 \,] \Sigma \, |\alpha_{\rho\sigma}|^2$ and it can be used to explain some SERS phenomena .This expression gives the intensity, which is dependent on the polarizability of Raman scattering for a transition from initial state I to final state F. I_L is the intensity of the exciting light operating at a frequency ω while ω_{FI} is a molecular transition frequency between states I and F . In order to get the $\alpha_{\rho\sigma}$ component of the polarizability for transitions between states I and F, we may use the second- order perturbation theory defined as follows:

$$\alpha_{\rho\sigma} = \Sigma_{k \neq I,F} \{ \frac{\langle I|\mu_\sigma|K\rangle\langle K|\mu_\rho|F\rangle}{E_K - E_I - \hbar\omega} + \frac{\langle I|\mu_\rho|K\rangle\langle K|\mu_\sigma|F\rangle}{E_K - E_F + \hbar\omega} \}.$$

In the above expression, μ_σ and μ_ρ are the dipole moment operators for the polarization directions σ and ρ, while E_I and E_F are the energies of the initial and final states and E_K represents the energies of all the other states with the exception for I and F. The notation $\langle I|\mu_\rho|K\rangle$ represents the dipole moment matrix element.

For most of the molecules involve in our study, we may make the zero- order Born – Oppenheimer approximation in order to separate the nuclear from electronic motions. But in the treatment of Raman intensities it is necessary to consider the small deviations in the electronic wave functions with nuclear motion.

Surface-Enhanced Raman spectroscopy in an electrochemical environment is reported in a study in which a silver electrode is immersed in an electrolyte solution, thus forming a solid-solution interface. The interface is very dependent on the silver metal and of the adsorbed species, and the ionic constituents of the electrolyte solution[59]. When submerged into an aqueous electrolyte solution, water molecules are adsorbed on a metal surface as it is exposed to the solution. Interactions between the ions in solution with the electrode surface have a distance of closest approach that is restricted by the hydration sheath of the electrode and by the hydration spheres of the ions[79]. Since the electrode is normally charged, there exist a potential distance profile which depends on the nonhydrated ions, held tightly to the metal, and

the nonrigidly held hydrated ions in the diffuse layer, which extends into the bulk solution[53]. Differences that exist between normal and surface Raman are very striking at some point when it comes to the electrochemical environment that is potential dependent[78]. During Surface-Enhanced Raman Scattering (SERS), molecules in solution are adsorbed on a metal surface and as the voltage is varied, so does the number of molecules on the electrode surface[30]. This potential dependence can be seen as due to the accumulation of species within the double layer.

At each specific voltage, the number of molecules and their orientation on the metal surface are different since molecules in the double layer will contribute to the intensity of the spectrum and the molecules can be parallel or perpendicular to the electrode surface[21]. At the point of zero charge (pzc) [61], there is no net surface charge on the electrode and this phenomenon occurs at a very specific potential and it gives rise to an increase in intensity. The point of zero charge (pzc) is of major importance to our studies since it influences which species adsorb to the metal and the extent of adsorption at a given potential [(8)] which could be to the positive side of the pzc (the electrode is positively charged) or to the negative side of the pzc (the electrode is negatively charged). Since molecules were studied in aqueous solution, when the applied potential is negative of the pzc, the positive dipole of the water will point towards the metal. Positive ions will displace the water molecules, and will adsorb to the surface, therefore creating the IHP (Inner Helmholtz plane) [45].

At the point of zero charge, the ions in solution are completely solvated, and on the surface, the number of water molecules pointing with the hydrogen or oxygen towards the surface, is equal[28]. Differential capacitance measurements show a peak in the capacity versus potential measurements [33], near the point of zero charge (pzc). At potentials positive of the point of zero charge where anions adsorb specifically, the adsorption of various ions is much more complex [45]. At a position close to the point of zero charge, neutral molecules with a dipole or water orientated with the oxygen to the metal adsorb on the surface. Using the differentiated capacitance measurements with a solution containing specifically adsorbing anions, it has been found that the surface coverage of anions can exceed that of the water when the electrode is very positive of the point of zero charge [40,41]. The water molecules, in that case, are still adsorbed on the electrode surface and are aligned in such a way that the oxygen is pointing toward the electrode.

Since the outer Helmholtz plane (OHP) has any anions and cations solvated by the water molecules, when Na^+ is changed to K^+ and to Li^+ there are shifts in the stretching frequency of water bands, indicating an interaction of the water molecules solvating these cations in the outer Helmholtz plane with the adsorbed water in the inner Helmholtz plane [45,46].

The Coulombic interactions in the inner Helmholtz plane increase as the potential is varied very positive to the point of zero charge creating a very weak covalent bond between the metal and the molecule (adsorbate)[45]. Such interactions between the metal surface and halide or water molecules can

cause frequency shifts of the surface-stretching band of adsorbed molecules to higher values as the potential becomes more positive [42,43].

ii) Electromagnetic enhancement

The electromagnetic enhancement in SERS originates from the interaction between the incident light and the metal surface. Due to the limiting boundary conditions between the metal surface and the incident light, in the proximity of the metal surface, the incident light is modified resulting in a local electromagnetic field, which depends on the optical properties of the substrate and the geometry of the surface. A theoretical explanation that is partly responsible for the electromagnetic enhancement has been suggested by John R. Lombardi and Ronald L. Birke[18]. They state that the shape of the metal particles (spherical or prolate) has to be taken into consideration and as a result, a single isolated sphere or spheroid model has been developed. Upon contact with the metal surface, the incident electric field polarizes the metal particles in such a way that surface charges of opposite sign are developed on either side of the particle which alternate with the frequency of incident radiation producing a localized dipolar surface plasmon, (DSP). The dipolar surface plasmon phenomenon is partly dependent on the size of the metal particles and differences have been observed for metal particles of spherical and prolate spheroid shape. For example, calculations that assume spherical metal particles predict an enhancement of about fifty to five hundred excitation, which is considered much less than the observed enhancement in SERS. However, for a prolate metal spheroid, a much larger

enhancement is predicted from the calculations. These calculations also assume that the electromagnetic enhancement depends upon the distance of the molecule from the metal surface and the electromagnetic enhancement distance from the metal sphere. Another factor that contributes to the electromagnetic enhancement is the oscillating molecular dipole that induces a dipole in the metal particle. In such a case, the metal particles act as receptors for the nearby electromagnetic field of the oscillating molecular dipole , and the emitted Raman radiation from the molecule is thus enhanced by the presence of the metal particles and this is also called the antenna effect

.

The image field effect (IFE), firstly introduced by King et al [27,31] and later expanded by Efrima and Metiu[27], can also be considered as another contributor to the electromagnetic enhancement in SERS. Eesley and Smith[27] have also presented a closely related model, Morowitz, and Koehler[27] proposed a less closely related one. In all of these studies related to the image field effect , a point dipole is used to represent the oscillating dipole moment induced by the applied electromagnetic field in the molecule. The equation that summarizes the SERS enhancement factor ε arising from the image field model is given by:

$$\varepsilon = G \left| 1 - \gamma\, \alpha_0 / 4R^3 \right|^{-4}$$

where $\gamma = \dfrac{(\varepsilon_M - \varepsilon_A)}{(\varepsilon_M + \varepsilon_A)\,\varepsilon_A}$. In this expression, ε_M is the metal

dielectric constant, ε_A is the adsorbate dielectric constant, α_0 is the unperturbed molecular polarizability and R represents the molecule to image plane separation. G is the geometrical factor, which has a numerical value of roughly ten. For Raman scattering from a rough surfaces G incorporates the effect of roughness induced surface electromagnetic field enhancements and its value is correspondingly larger. Since the image field effect requires a very short distance between the adsorbate and the metal surface, thus it is of much of a lesser importance than the other effect that contributes to the electromagnetic enhancement in SERS.

F. Conclusion

We have discussed the origin, theory, characteristics and various aspects and reports of SERS. Since the discovery of the Raman effect in 1928 by Raman and Krishnan[15], this form of spectroscopy is still a growing field that has expanded not only to new theories but also to new systems such as biological and polymeric ones. Indeed, in chapter 3 of this thesis, we will present an investigation that we have done for a biological system (Heme proteins) using SERS as a probe. Although a complete description and the origin of the enhancement in SERS is not fully understood, it is an excellent technique to perform in-situ studies of molecules adsorbed on a metal surface while varying the environmental conditions.

G . References

[1].Albrecht, A . C. *J. Chem. Phys.* 1961 , 34 , 1436 .

[2].Syzmanski, H. A . in " *Raman spectroscopy, Theory and Practice" Vol. 1, Plenum Press, 1967 pages 7& 31.*

[3].Faquharson, S. K .; Guyer, L.; Lay, P. A.;Maynuson, R .H. *Gov.Rep.Announce., Index (U.S)1984, 20, 64 .*

[4].Lombardi, J. R.; Birke, R. L.; Sanchez,L. A.; Bernard, I.;Sun, S. C. *Chem. Phys.Letter.1984, 104 ,240 .*

[5].Lombardi, J. R.; Birke, R. L .;Lu, Tianhong.; Xu, Jia *J. Chem. Phys. 1986, 84 ,4174 .*

[6].Furtak,T. E .;Reyes, J. *Surface Science 1980, 93, 351 .*

[7].Pettinger, B.; Wenning , U.;Wetzel, H. *Chem. Phys. Letter. 1979, 67, 192 .*

[8].Albrecht, M. G.; Creighton, J. A. *J. Am. Chem. Soc., 1977, 99, 5215.*

[9].Jeanmaire, D. J.; Van Duyne, R. P. *J. Electroanal. Chem. 1977,84, 1.*

[10].Manzel, K.; Schutze, W.; Moskovits, M. *Chem. Phys. Letter. 1982, 85, 183 .*

[11].Gao, P.;Weaver, M. J. *J. Phys. Chem. 1985, 89, 5040 .*

[12].Moskovits, M.;Dillela, D.P. *Chem. Phys. Letter. 1983,73,500 .*

[13].Dilella, D. P.;Moskovits, M. *J. Phys. Chem. 1981, 85,2042 .*

[14].Moskovits, M.; and Dilella, D. P. in " *Surface-enhanced Raman Scattering" (R. K. Chang and T. E. Furtak, eds) pages 243-273 Plenum Press. New York (1982) .*

[15].Raman,C. V.; Krishnan, K. S. *Nature 1928, 121, 501 .*

[16].Sun, S. *PhD. Dissertation City University of New York. (1987) .*

[17].Moskovits, M . *J.Chem . Phys. 1960, 44, 310 .*

[18].Lombardi, J. R.; Birke, R. L. in " *Surface- Enhanced Raman scattering " from spectroelectrochemistry: Theory and Practice Edited by R. J. Gale*

[19].Moskovits, M.; Suh, J .S. *J. Phys. Chem. 1984, 88, 5526.*

[20].Creighton, J. A . *Surface Science 1983, 124, 209-219 .*

[21].Fleischmann,M .; Hendra, P. J.;Mc Quillan, A. J. *J. Chem. Soc. Chem. Comm. 1973, 80*

[22].Kimura, F.; Umemura, J.; Takenaka, T. *Langmuir 198, 2 , 96 .*

[23].Busby, C.C.; Creighton, J. A. *J. Electroanal. Chem. 1982 , 140 , 379 .*

[24] .Moskovits, M . in " *Surface roughness and the enhanced intensity of Raman scattering by molecules adsorbed on metals" J. Chem. Phys 1978, 69, 4159.Enhanced Raman Scattering by molecules adsorbed on electrodes. A theoretical Model, Solid State Commun. 32: 59 (197) .*

[25].Weitz, D. A.; Gramila,T. J.; Genack, A. Z.; Gersten, J. I. in "*Anomalous low- frequency Raman Scattering from rough metal surfaces and the origin of surface-enhanced Raman scattering" Phys. Rev. Letter. 1980, 45 , 355 . Inelastic Mie Scattering from rough metal surfaces: Theory and Experiment, Phys. Rev. 1980, B 22, 4562.*

[26].Carey, P. R . in " *Biochemical applications of Raman and resonance Raman spectroscopies" Academic Press Inc. (1982)*

[27].Chang, R . K .;Furtak,T.E. in " *Surface- Enhanced Raman scattering" Library of Congress Cataloging in Publication Data. Plenum Publishing Corporation (1982) .*

[28].Fleischmann,M.;Hendra, P. J.;Mc Quillan A . *J. Chem. Phys. Letter. 1974, 26 ,163 .*

[29].Van Duyne, R . P. in " *Chemical and Biochemical Applications of Lasers" C. B. Moore Editor, Academic Press, New York 1974, 4, Ch. 5 .*

[30].Birke, R .L .;Lombardi, J.R.;Sanchez, L. A. in " *Advances in Chemistry Series" No 201, Karl M. Kadish, Editor, ACS 4 (1982) 69 .*

[31].Furtak, T. E.; Reyes-Corona *J. Surf. Sci. 1980, 93, 382 .*

[32].Otto, A . *Appl. Surf. Sci. 1980 ,6 , 309 .*

[33].Bockris, J. O'M ;Reddy, A . K. N . *in "Modern Electrochemistry" 1970, Vol. 2, Plenum Press, New York .*

[34].Diem, M. in *"Introduction to Modern Vibrational Spectroscopy " New York , John Wiley and Sons: (1993).*

[35].Baranska, H .;Labudzinska, A .;Terpinski, J . in *"Laser Raman Spectroscopy " Trans . J .R .Majer . Chichester (England): Ellis Harwood Ltd: (1987).*

[36].Heller, E . J. in *"The Semiclassical way to Molecular Spectroscopy." Accounts of Chemical Research. 1981, 14 , 368-375 .*

[37].Heller E. J.; Sundberg, R .L. Tannor, D. in *"Simple Aspects of Raman Scattering" Journal of Physical Chemistry. 1982, 86, 1822-1833 .*

[38].Levine, I . N. *"Quantum Chemistry" 4th ed. New York: Prentice Hall : 1991 .*

[39].Merzbacher, E . *"Quantum Chemistry" New York: John Wiley and Sons, 1962 .*

[40].Parson, R . *J. Electroanal. Chem., 1981, 3, 118.*

[41].Valette, G. *J. Electroanal. Chem.,1982, 132, 31 .*

[42].Kotz, R .; Yeager, E . *J. Electroanal . Chem .,1981, 123, 335 .*

[43].Anderson, A. B.; Kotz, R .; Yeager,E . *Chem. Phys. Letter. 1981, 82, 130 .*

[44].King ,F. W.; Van Duyne,R . P.; Schatz, G. C. *J.Chem. Phys. 1978, 69 ,4472 .*

[45].Macomber, S.H .;Furtak, T. M . *Surf. Sci. in press .*

[46].Pettinger, B.; Moere, L . *J. Electroanal. Chem. in press .*

[47].Hosten, C. *Ph.D. Dissertation The City University of New York.* (1991).

[48].Pettinger, B.;Tadjeddine, A .;Kolb, D. M. *Chem. Phys. Lett.1978, 66, 544.*

[49].Furtak, T. E. ; Kester, J.J. *J. Phys. Rev. Lett. 1980, 45 , 1652 .*

[50].Kester, J. J .;Furtak, T. E. *Solid State Commun.1982, 41, 457 .*

[51].Murray, C. A. in *" Surface Enhanced Raman Scattering ", R. K. Chang and T. G.Furtak editors, Plenum, New York 1982, p. 203 .*

[52].Trott, G. R .; Furtak, T. E . *Solid State Commun 1980, 36, 1011 .*

[53].Creighton, J. E. in " *Surface Enhanced Raman Scattering*", *R. K. Chang and T. E . Furtak editors , Plenum , New York , 1982, p. 315* .

[54].Chen, C. K .; de Castro, A . R . B.; Shen, Y. R . *Phys. Rev . Lett .1981, 46, 145* .

[55].Pettinger , B.; Wenning, U.; Kolb, D.M .; Bunsenges, B. *Phys. Chem.1978, 82, 1326* .

[56].Loo, B. H. *J. Phys. Chem. 1982, 86 ,433* .

[57].Fleischmann, M .;Hendra, P. J.;Hill, I . R .; Pemble, M .E . *J. Electroanal. Chem.1981, 117, 243* .

[58].Pettinger, B .; Philpott, M.; Gordon, H . *J. Surf. Sci. 1981, 105 ,469* .

[59].Chen, T. T.; Owen, J. F.; Chang, R . K. *Chem. Phys. Lett. 1982, 89 ,356* .

[60].Macomber, S.H .; Furtak, T. E.; Devine, T. M . *Surf . Sci . in press.*

[61].Macomber, S.H .; Furtak, T. E.;Devine, T. M . *Chem . Phys. Lett .1982, 90 ,439*

[62].Barz, F. G .; Gordon, J. G .; Philpott, M . R. Weaver, M. *J. Chem. Phys. Lett 1982, 91 (4) ,291* .

[63].Chen ,T. T.; van Rabeu, K . U .; Owen, J . F.;Chang, R . K. Laube, B. L . *Chem. Phys. Lett.1982, 91 (6), 494.*

[64].Demuth, J. E .; Sanda Warlaumont, J. M .;Tsang , J . C.Christman, K . in *"Vibrations at Surfaces" editors R . Candano, J. M . Gilles and A . A . Lueas Plenum, New York, 1982, p. 391* .

[65].Woodand,T. H.; Klein, M . V. *J. Vac. Sci. and Tech .1979, 16, 459* .

[66].Furtak,T. E .; Trott, G .;Loo, B . H . *Surf . Sci 1980, 101,374* .

[67].Gersten, J. I .; Birke, R .L.Lombardi, J . R . *Phys. Rev . Lett.1979, 43 ,147* .

[68].Furtak,T. E.;Macomber, S . H. *Chem. Phys. Lett. 1983, 95 , 328* .

[69].Creighton, J . A .;Albrecht, H . G.;Hester, R . E.;Matthew, J .A .D. *Chem. Phys . Lett . 1978 , 55, 55* .

[70].Wenning, U .; Pettinger, B.;Wetzel, H. *Chem. Phys. Lett. 1980, 70 , 49* .

[71].Schmeisser,D.; Demuth, J . E . Avouris, P . H. *Chem . Phys . Lett . 1982,8 , 324 .*

[72].Person, B . N. J . *Chem . Phys . Lett . 1981, 82, 561 .*

[73].Wood, T. H.;Klein, M . V. *Solid State Commun. 1980, 35,263 .*

[74].Furtak, T. E.; Macomber, S . H . *Chem . Phys . Lett . 1983, 95, 328 .*

[75]. Allen, C . S.; Schatz, G . C.; Van Duyne, R . P. *Chem . Phys . Lett . 1980 , 75 ,201 .*

[76].Otto, A. *Surf . Sci . 1978, 75, L 392 .*

[77].Pettinger, B.;Wetzel, H . *Chem . Phys . Lett . 1981, 78, 398 .*

[78].Busby, C. C.;Creighton, J. A. *J . Electroanal. Chem . 1982,133,183 .*

[79].Fleischmann, M .; Hendra, P. J .; Hill, I . R .; Pemble, M .E . *J. Electroanal . Chem . 1981,117, 243 .*

[80].Allen, C . S.; Van Duyne, R. P. *J. Am . Chem . Soc. 1981,103,7497 .*

[81].Wetzel, H.; Gerischer , C. *Chem . Phys . Lett . 1980, 76, 460 .*

[82].Cotton, T . M. *J. Am . Chem . Soc., 1980, 102,7960 .*

[83].Cotton,T. M .; Schultz, S. G.; Van Duyne, R . P. *J . Am . Chem . Soc . 1981, 102, 7960.*

[84].Bernard, I .*Ph.D. Dissertation The City University of New York (1987).*

[85].Gersten , J. I.; Nitzan, C. *J.Chem .Phys.1980, 73 , 3023*

Chapter 2

Ab Initio Frequency Calculations of Pyridine Adsorbed on an Adatom Model of a SERS Active Site of a Silver Surface

A. Abstract

Ab initio and Urey-Bradley calculations of normal modes were carried out to analyze the frequency shifts observed on the SERS spectrum of pyridine obtained on a Ag surface. A molecular model with a Ag atom attached to the pyridine nitrogen was used in the Urey-Bradley calculation. The frequency shifts in the SERS spectrum were calculated by adding K(Ag-N) and F(Ag..C_α) force constants and by adjusting the ring stretches according to how their bond lengths changed in an *ab initio* calculation with a $(Ag-Py)^+$ model. The *ab initio* calculations were done with the HF, MP2 and B3LYP methods using the 3-21G, 6-21G, 6-21G*, 6-21G** and LanL2DZ basis sets. The surface active site was modeled in the calculation by means of Ag^0, Ag^+ atoms and a Ag_4^+ pyramidal cluster structure. The calculations were evaluated on how well they matched the observed frequencies, the ν(Ag-N) stretch , and the frequency shifts for the SERS spectrum in an electrochemical environment. The calculation with Ag_4^+ model yielded the best results although $(Ag-Py)^+$ model also gives reasonable results. All calculations were consistent with an edge-on interaction between pyridine and the electrode surface and a Ag^+ species as part of the surface active site.

B. Introduction

Since the first measurements by Fleischmann et al. in 1974 [1], Surface Enhanced Raman Scattering (SERS) spectroscopy has become a powerful technique for studying the vibrational properties and structure of molecules on SERS active metal surfaces and a powerful tool for chemical analysis of molecules which can be coupled to such surfaces. Indeed, the technique has generated a great deal of interest recently having been used to obtain single molecule Raman spectroscopy (see recent reviews [2]) as-well-as the Raman spectra of molecules adsorbed on nanoparticles [3], to study self-assembled monolayers [4], as probe for trace environmental analysis [5], and as a tracer for DNA and RNA detection [6], to cite a few examples of topical applications. In spite of the widespread use of SERS, relatively few ab initio theoretical studies have been made to elucidate the effect on the SERS vibrational spectra of the molecular interaction between the adsorbate molecule and the metal substrate. It is well known that the so-called chemical enhancement mechanism of SERS, which we believe is essential for observing a SERS spectrum, requires a bonding interaction between the metal substrate and the adsorbed molecule [7]. In principle these theoretical studies could provide the relationship between the molecular level properties of the interfacial structure and the SERS process which in turn could help in the use of SERS spectra to elucidate such properties as the orientation of molecules on various surface sites, the type and strength of the bonds between the molecule and the surface, the reasons for frequency shifts observed with

surface adsorbed molecules, the nature of the surface roughness on the atomic scale, and the very nature of the chemical enhancement mechanism itself.

Herein, we use *ab initio* molecular orbital calculations for a pyridine-Ag metal cluster system as a theoretical approach to investigate some these problems, especially the effect of the bonding interaction at the Ag surface on the band positions of the SERS spectrum of pyridine. Molecular orbital metal cluster-molecule studies have been used to investigate metal to ligand chemical bonding in small metal cluster–ligand systems such as Ag_n–L [8,9] or Cu_n–L [10,11] , where n=1 to 18, in order to model binding on M(100), M(111) , and M(110) metal surfaces. The ligand-metal adsorption geometries investigated were the on-top site where the ligand is directly above a single metal atom, the bridging site where the ligand is directly above a dimer of two metal atoms in the surface, and the hollow site where the ligand is directly above a triangle formed by three metal atoms in the surfaces [8-11].

In order to postulate a chemical model for the molecular orbital frequency calculations, we need to consider the experimental evidence for the structure of the metal/molecule system. A very interesting early paper where pyridine was co-condensed with Ag_2 and Ag_3 in a solid Argon matrix [12] showed a set of vibrational frequencies very similar to the SERS spectrum of pyridine from a Ag electrode in the potential region of –0.2 to –0.6 V vs. SCE. In fact, a 242 cm^{-1} band in the matrix isolation spectrum was assigned to the Ag-N stretch as is usually done for the SERS of pyridine on a Ag surface [13]. In

fact, Creighton *et al.*[14] assigned the ca. 239 cm^{-1} band to a ν(Ag-N) mode because it also showed up in the spectrum of metal-pyridine complexes. However, various other authors claimed that the band was due to a Ag-Cl^- stretch [15, 16]. We showed that the 239 cm^{-1} band still appears in Cl^- free solution SERS spectra of pyridine and various pyridine derivatives adsorbed on Ag sols [13]. Similar results were obtained by Neto *et al.* for bipyrazine [17] also adsorbed on Ag sols. These authors found that the addition of Cl^- ions to the silver sols produced a strong ν(Ag-Cl) band that "masked" the ν(Ag-N) vibration. Furthermore, Muniz-Miranda *et al.*[18] found from potential dependence experiments on a Ag electrode that, at –0.6 V vs. SCE, the Cl^- ion desorbs from the surface and that a ν(Ag-N) stretch is still observed at 220 cm^{-1}. In all, these results show that, in the presence of Cl^- ions, the 239 cm^{-1} band must have at least partially a ν(Ag-N) stretching contribution. This surface-molecule vibration is thus taken as evidence for the edge-on interaction of the pyridine nitrogen with surface Ag.

Of course, for the roughened metal surface the pyridine molecule orientation has been discussed as either edge-on or face-on with respect to a micro-sized Ag particle [19,20,21]. The edge-on binding in an on-top site is predicted to occur by the mostly nitrogen σ– donor orbital, $7a_1$ (σ) , of pyridine interacting with vacant Ag (5s, $5p_z$) orbitals while edge-on binding in a bridge-site occurs more through the π –donor pyridine orbital, $2b_1$, interacting with Ag orbitals [9]. This type of binding should align the molecular axis of pyridine either at a right angle with respect to the extended

surface or at an inclined angle. The face-on binding would occur through the $1a_2$ (π) HOMO orbital of the aromatic ring. This type of binding is expected to align the molecular axis and the molecular plane of pyridine parallel to the Ag surface.

However, various experimental techniques such as angle-resolved ultraviolet photoelectron spectroscopy (ARUPS) and near-edge X-ray absorption fine structure (NEXRAFS) indicate that pyridine bonds to Ag, Cu and Pt surfaces through the nitrogen lone-pair electrons either in a perpendicular manner to the surface or slightly tilted [22,23]. The discussion of the orientation of molecules observed by SERS on a roughened surface is somewhat confusing since it should depend on whether the orientation is with respect to an atomic scale site or the microcrystalline surface particles created by the roughening procedure. A comparison of the frequency shifts in the SERS spectrum with those in the spectrum of a pyridine-Ag ion complex suggests that the molecule bonds to the SERS active surface in the same way that it bonds when coordinating to a Ag ion; that is, edge-on through the nitrogen atom [14].

On the other hand, Creighton [19] later found through the use of the small isolated sphere electromagnetic (EM) surface enhancement rules of SERS that the molecule should be flat on the surface at an electrode potential of –0.5 V versus SCE. Furthermore, we also used the EM selection rules [7,24] for pyridine bands as a function of potential to conclude that the molecule lies flat on the surface at –0.6 V versus SCE, in agreement with Creighton's

results, but that it stands up at –0.9 V. In another study, a theoretical analysis of intensity ratios based on the Pariser, Parr, and Popple semi-empirical method in the surface enhanced hyper-Raman spectrum of pyridine [25] found that pyridine is already standing up at –0.7 V versus SCE. In fact, it is easy to appreciate that the results from the use of the EM selection rules do not give information about the binding geometry at the atomic Ag sites. If the active site is a small Ag cluster on the Ag surface, the pyridine could be bound to a Ag cluster edge-on and still be in a parallel orientation with respect to the micro-sized Ag particles which gives rise to the EM selection rules. In fact, Creighton concluded that σ-bonded pyridine is not incompatible with a parallel orientation to the roughened Ag surface [19]. In spite of the difficulties in probing the roughened metal surface for atomic scale details, some SERS experimental results indicate that interaction between pyridine and a silver surface occurs through a metal adatom. By analyzing the SERS spectrum of cyanide under various conditions during the oxidation-reduction cycle (ORC) pretreatment, Billman *et al.* found that the signal enhancement occurred after the formation of a silver surface that was rough on an atomic scale [26]. They thus concluded that the surface-adsorbate interaction occurred through an adatom on the surface. SERS experiments by Bunding *et al.* in our laboratory with 2,6-dimethylpyridine (lutidine) supported this conclusion [27]. This molecule has its two methyl groups on α carbons to the nitrogen that restricts the interaction with the surface to a single metal atom; yet, a SERS enhancement is still observed providing

evidence that the interaction with the surface adatom does occur. Roy and Furtak [28] went further and proposed that the active site was made up of a Ag_4^+ pyramidal cluster. These authors arrived at this proposition by associating some low frequency vibrations in the SERS spectra with Ag-Ag stretching modes of the pyramidal cluster. This model is consistent with the direct interaction of the scattering molecule with a nearest neighbor adatom since an adatom in this cluster would sit on top of three other Ag atoms that form the base of the pyramid.

Various theoretical models for calculating SERS spectral frequencies have been previously studied involving ab initio methods for the molecule interacting with a metal surface. Recently, Corni and Tomasi treated the molecule at the ab *initio* level whereas the surface was treated by the dielectric properties of a continuous metallic body and by the polarizable dipoles of spherical metallic particles [29,30,31]. Other authors have represented the surface through various metal adatom or small metal cluster models. Kwon *et al.* used a planar Ag_5^+ model with four Ag atoms at the corner of a square and a fifth one at the center with frozen bulk distances to model the energetics for perpendicular and flat orientations of benzoic acid using the LanL1DZ basis set [32]. Cardini and Muniz-Miranda [33] used two Ag atoms at different positions of a pyrazole structure and performed density functional theory, DFT, calculations of the frequencies for pyrazole bonded to silver atoms using a mixed 6-31G(d)//LanL2DZ basis set. Arenas *et al.* [34] represented a Ag surface by two metal atoms aligned along the molecular

axis of pyrazine, using the LanL2DZ basis set and the RHF and CIS level methods to calculate ground and excited state energies and frequencies. SERS spectral bands have also been calculated by Vivoni *et al.* [35] using the model of a single Ag^+ -6-mercaptopurine complex bonded edge-on (semi-empirical PM3 method), while Acoca et al. [36] modeled the SERS spectra for the phthalimide -Ag^+ complex with Hartree-Fock and DFT(S-VWN) theory with the LanL2DZ basis set.

All things considered, there have been relatively few ab *initio* frequency calculations of SERS spectra where the effect of the metal binding site has been explicitly included in the calculation. In fact, even though pyridine was the first molecule whose SERS spectrum was observed [1], there are no ab initio calculations in the literature with a Ag atom or cluster included in the chemical model of the scattering species, although ab initio calculations of the pyridine SERS spectrum have been carried out without explicitly involving the Ag metal [37]. The results cited above from (i) matrix isolation spectroscopy [12], (ii) evidence for adatom involvement [26, 27], and (iii) the low frequency Ag vibrations identified by Roy and Furtak [28] provide good evidence that a small Ag cluster model should be a very adequate representation of the SERS active site for pyridine on a Ag surface. We will also present evidence from empirical normal mode calculations that the SERS spectrum of pyridine is consistent with pyridine binding edge-on to a Ag adatom site on the surface.

We have calculated the vibrational frequency shifts of pyridine bonded to silver using both a Urey-Bradly empirical force field and *ab initio* methods. Recently, various authors have calculated with empirical force fields the differences in vibrational frequencies (or vibrational frequency shifts) between free molecule and surface-enhanced Raman scattering (SERS) spectra by modeling the surface in SERS through metal atoms. Neto *et al.* [17] carried out this kind of calculation with bipyrazine, Muniz-Miranda with 1,10-phenanthroline [38] and Vivoni *et al.* with 6-mercaptopurine [35]. For the ab initio calculations of the effect of the metal (Ag) on SERS spectra of pyridine, we use a model with an on-top geometry site, the model systems being Ag-pyridine, Ag^{+}-pyridine, and Ag^{+}_{4}-pyridine with the pyridine nitrogen directed at a single Ag adatom. The goal of our ab *initio* calculations is to obtain a method that is not too computationally expensive but that yields satisfactory results when compared to experiment. Hartree-Fock and DFT calculations are evaluated according to how well they predict the ν(Ag-N) mode at 239 cm^{-1} and how well they match the frequency shifts on going from a gas phase spectrum of pyridine to the SERS spectrum of pyridine. Initially, normal mode calculations were done with a neutral silver atom-pyridine (Ag-Py) model. But those calculations yielded a ν(Ag-N) mode that was too low. Ab initio calculations with a $(Ag\text{-}Py)^{+}$ model yielded a ν(Ag-N) mode higher than the neutral model, but they are still short of the experimental value. Finally, we obtained a closer value by carrying out a calculation with the

Ag_4^+ cluster model, $(Ag_4\text{-}Py)^+$, that Roy and Furtak proposed for the active site on the surface [28].

C. Experimental

For the experimental part, a concentration of 0.05 M aqueous solutions of pyridine with 0.1 M electrolyte solution was prepared in each case (KCl, KF and K_2SO_4) and they had a pH value of approximately 7.95, 8.15 and 8.25 respectively. Before assembling the electrochemical cell the silver electrode was polished with alumina powders [from Buehler Micropolish (Micron Deagglomerated Alpha Alumina)] of 0.3 and 0.05 microns in size and then the electrode was rinsed in distilled water and sonicated for ten minutes. In KCl solution, adsorption of pyridine on the electrode surface was achieved in-situ (inside of the electrochemical cell) by generating a double potential step sequence of – 0.6V to +0.3V and back to – 0.6V versus the saturated calomel electrode (SCE) with a dwell time of 5 to 10 seconds at + 0.3V. However, in KF electrolyte, adsorption of pyridine on the surface occurred by doing a different oxidation- reduction cycle (ORC) at – 0.5 V to + 0.4 V for 5 seconds. For pyridine in K_2SO_4 the oxidation-reduction cycle was achieved at – 0.2V to + 0.6V for 5 seconds and then back to –0.2V. The formation and reduction of silver chloride for pyridine in KCl resulted in considerable etching of the silver surface which at the end of the pretreatment appeared pale cream in color. In KF electrolyte, at the end of the pretreatment, the silver electrode became purple in color while a black color was observed when it was pretreated in K_2SO_4 . The spectra were

recorded using a Spex model 1401 double monochromator operating with 160-micron slits and with a scan rate of 50 cm^{-1}/min. A Spectra Physics argon (Ar^+) laser operating at 488 nm at approximately 50 mw (on the surface) was the excitation source. All chemicals were reagent grade and all potentials quoted are relative to the saturated calomel electrode. A variety of three electrode cell designs was used[27, 41,42]. A convenient electrochemical cell with a 90° scattering geometry is depicted in figure 2. This cell has an optically flat bottom and side which allowed us to bubble inert gas (N_2, Ar, or He) into the system; this process is called deoxygenation since oxygen can act as a scavenger on the electrode surface especially with those biochemical molecules (myoglobin, hemoglobin, hemin) that react with oxygen at relatively very low concentration.

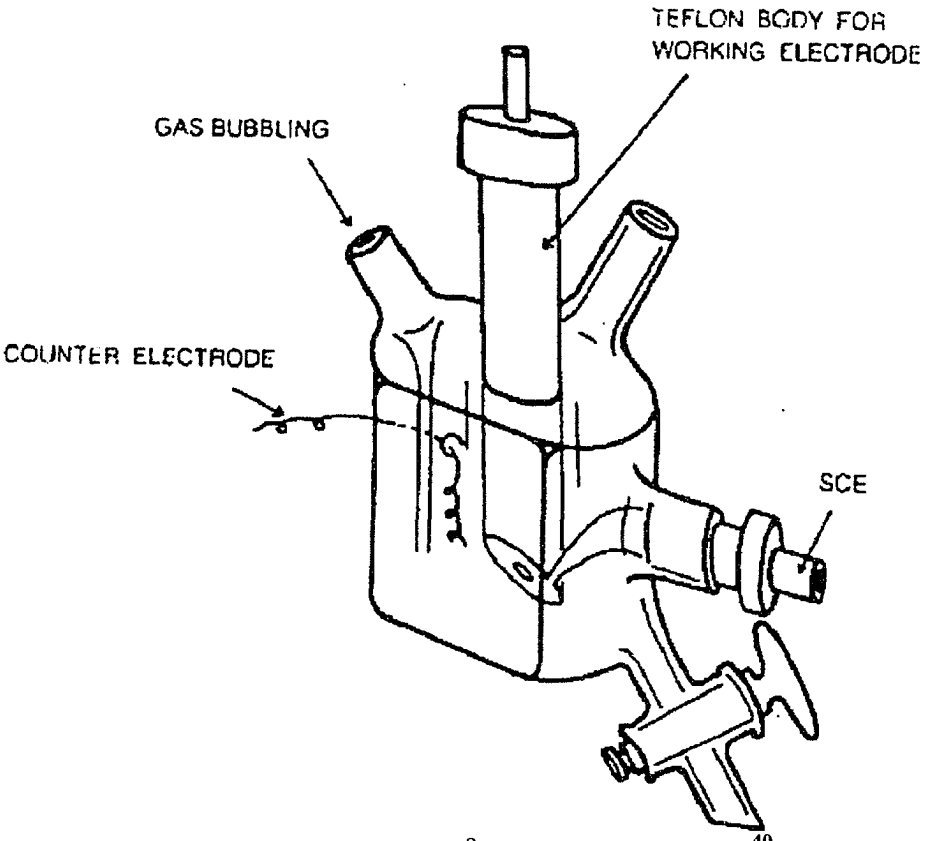

Fig 2. Electrochemical cell with a 90° scattering geometry [40]

Calculation Methods

We performed two types of calculations for this work: Urey-Bradley force field (UBFF) and *ab initio* calculations. The UBFF calculations were carried out using the Diem version of Schachtshneider PC programs adapted for a SIMPLEX refinement of the force constants [39,40]. The calculation of the free pyridine force field was discussed in reference 39. Basically, it consisted of reducing the number of diagonal force constants by treating all angle bends with the same center atom as equal. The number of non-bonded force constants was reduced in a similar manner by treating all non-bonded interactions that had the same corner atoms as equal. The resulting force

field, shown in Table 1, had 12 force constants: 7 diagonal, 4 non-bonded interactions and the aromatic interaction, ρ. These force constants were refined by fitting the gas phase spectra of two isotopomers: pyridine-h_5 and pyridine-d_5. The force field thus obtained was checked against the spectra of four others isotopomers. It reproduced a total of 152 experimental frequencies with an average error of 0.68%. In the present work, we used this force field in order to reproduce the vibrational frequency shifts observed in the SERS spectrum.

Following the Suzuki and Orville-Thomas calculation model [41] we added to the pyridine force field a K(Ag-N) stretching force constant and a F(Ag..C_α) non-bonded interaction. The silver atom was placed at 2.3 Å from the nitrogen along the molecular axis, thus retaining the C_{2v} symmetry. This is the Ag^+-N bond length in the X-Ray crystal structure of tetrahedral $[Ag(Pyd)_4]ClO_4$ [42]. The K(Ag-N) and F(Ag..C_α) force constants were adjusted at 1.10 and 0.40 mdyne/Å respectively such as to match the 239 cm^{-1} band and the vibrational frequency shift of the totally symmetric ring breathing (mode 1) that occurs at 991 cm^{-1} in the gaseous spectrum. The shift of this normal mode is the second largest in the SERS spectrum. The ring force constants were adjusted according to the changes in bond length obtained from a UHF/3-21G calculation that will be described in the next paragraph. The gaseous phase frequencies used were from the results of Stidham and DiLella[1] and the SERS frequencies from those found by Creighton [19] which came from a Ag electrode system at –0.5 V vs. SCE.

The *ab initio* calculations were done with the 94 and 98 version of GAUSSIAN [44]. Initial calculations were carried out with the UHF/3-21G method with the free pyridine molecule and with an Ag atom bonded to nitrogen. These initial calculations were done with neutral and +1 charged models and yielded frequency differences between a gas phase model and an $(Ag\text{-}Py)^+$ model which we associated with the frequency shifts observed in the SERS spectrum. From these calculations we also obtained the changes in bond lengths that were used to adjust the force constants in the UBFF calculation in order to match the vibrational frequency shifts not accounted for by the addition of the K(Ag-N) and $F(Ag..C_\alpha)$ force constants. Subsequent *ab initio* calculations were done free pyridine with the Hartree-Fock method using the 6-31G, 6-31G* and 6-31G** basis sets, with the MP2 method using the 6-31G** and LanL2DZ basis sets, and with the B3LYP method using the LanL2DZ basis set. For calculations including Ag we compared the 3-21G with the LanL2DZ basis set. Each frequency calculation at a given basis set was preceded by a full geometry optimization utilizing the identical basis set. The frequencies of the Ag-Py model were calculated with the HF and MP2 methods and those of the $(Ag\text{-}Py)^+$ model with the HF, MP2 and B3LYP methods. Calculations with the $(Ag_4\text{-}Py)^+$ models were done only with the HF method. The Ag_4^+ cluster was optimized first followed by an optimization of just the pyridine geometrical parameters.

D. Results

i) Empirical Normal Mode Calculations

To the best of our knowledge, Suzuki and Orville-Thomas [41] were the first to perform vibrational frequency shift calculations comparing a molecule in gas phase and when it is bound to a metal ion. In their work, these authors incorporated a metal ion -nitrogen stretching force constant, K(M-N), into the Urey-Bradley force field that they had obtained by fitting the vibrational frequencies in the gas phase spectrum of pyridine. They then adjusted the K (M-N) value to match the M-N stretching frequency, ν(M-N), for a series of pyridine metal ion -complexes. The K(M-N) value thus obtained produced a shift to the calculated frequency of the symmetric ring-bending mode, the Wilson mode 6a, that shows up in the gas phase spectrum at 603 cm^{-1}. (Wilson numbers will be used through out this article to designate the normal modes.) This calculated shift matched the experimental shift observed in the spectra of the pyridine metal ion -complexes. The 603 cm^{-1} band actually has the largest frequency shift in most of the pyridine metal-complexes studied by Suzuki and Orville-Thomas. Since they were able to reproduce that shift as well as the ν(M-N) mode by just incorporating a K(M-N) into the pyridine force field, those authors concluded that the interaction between pyridine and a metal ion on coordination was due mostly to kinetic coupling and that the metal-ligand coordination did not produce a significant redistribution of the electron density in the molecule.

The 603 cm^{-1} band is also the band that shifts the most in the SERS spectrum of pyridine obtained on an Ag electrode surface. Thus, in the present investigation, we followed the calculation method of Suzuki and Orville-Thomas and incorporated a silver atom into a Urey-Bradley force field of pyridine in order to reproduce the ν(Ag-N) mode as-well-as the most significant frequency shifts observed in the SERS spectrum. (By significant frequency shifts we mean those over 10 cm^{-1}.) Those shifts are the ones for the 1581, 1227, 1052, 991, and 603 cm^{-1} bands. These bands correspond to the Wilson modes 8a, 3, 18b, 1 and 6a respectively. In our case, the addition of a K(Ag-N) force constant and a F(Ag..C_α), a non-bonded interaction between a silver atom on the surface and the carbon atoms adjacent to the nitrogen, do not reproduce all of the main frequency shifts. These force constants only yielded significant shifts to the 1581, 991 and 603 cm^{-1} bands. This fact suggested, in contrast to what Suzuki and Orville-Thomas observed for the pyridine-metal ion complexes, that the interaction between pyridine and the Ag electrode surface involved some charge density redistribution. *Ab initio* calculations then provide us a way to determine how the electron density changed, in a relative sense, through the various relations between bond length, bond order and force constant [45,46,47]. Vivoni *et al.* [35] had used this method of adjusting the force constants of 6-mercaptopurine when determining its orientation on a roughened Ag electrode surface.

In the UBFF calculation, a K(Ag-N) value of 1.10 mdyne/Å produced a proper shift of 20 cm^{-1} to the totally symmetric ring breathing mode (1) at

991 cm^{-1} and an overestimated shift of 45 cm^{-1} to symmetric ring bending mode (6a) at 603 cm^{-1}. Yet, it calculated the ν(Ag-N) mode at only 183 cm^{-1}, way short of the experimental value of 239 cm^{-1}. Increasing the K(Ag-N) such as to match the ν(Ag-N) frequency would have grossly overestimated both 1 and 6a modes. By keeping the 1.10 mdyne/Å value for K(Ag-N) and adjusting the F(Ag..C_α) interaction between the Ag atom and the adjacent carbon atoms to 0.40 mdyne/Å , we obtained ν(Ag-N) frequency of 239 cm^{-1}. The F(Ag..C_α) force constant did not affect mode 1, but it further increased the shift of mode 6a to 54 cm^{-1}. This overestimation along with the fact that the calculation underestimated the other significant shifts in the SERS spectrum meant that the electron density redistributed around the molecule as it bonded to the surface. To find out how the electron density redistributed, we turned to the *ab initio* calculations.

The geometry optimization of pyridine compared to a $(Ag\text{-}Py)^+$ model with the HF/3-21G method revealed that the N1-C2 bonds lengthened, that the C2-C3 bonds shortened and that the C3-C4 bonds remained the same when a Ag atom was attached to the nitrogen. Table 2 shows the differences in the bond lengths of the three ring bonds between the free pyridine and the $(Ag\text{-}Py)^+$ calculation. A lengthening of a bond means that the bond looses electron density and becomes weaker. Conversely, the shortening of the bond length means that the bond gains electron density and becomes stronger. Moreover, Majoube [48] showed that magnitude of the bending force constants is inversely proportional to the distances between the corner atoms. The changes in bond

length obtained from the *ab initio* calculation thus justified a decrease in the CNC bending. This force constant contributes significantly to the symmetric ring bending mode 6a and decreasing it by 0.18 mdyne/Å reduced the error in the calculated shift of that band. Similarly, by increasing the K(C2C3) force constants by 0.20 mdyne/Å and decreasing the K(N1C2) by 0.10 mdyne/Å, the shifts to the 1581, 1227 and 1052 cm^{-1} bands approached more closely the experimental shifts. The frequency shifts that resulted from these calculations are shown in Table 3 and the final force constants in Table 1.

ii) Ab Initio Molecular Orbital Calculations

The results of the UBFF calculation just described are consistent with pyridine binding to an adatom on the metal surface by forming a σ-bond through lone pair electrons on the nitrogen. But before performing further *ab initio* calculations for pyridine, we carried out preliminary calculations with benzene and Ag-benzene models, $(Ag\text{-}Bz)^0$ and $(Ag\text{-}Bz)^+$, using the UHF/3-21G method to see if those calculations reproduced the vibrational frequency shifts observed in the SERS spectrum. A comparison between the liquid and the SERS spectra of benzene (Table 4) shows the ring stretching modes are shifted down in the SERS spectrum from their position in the liquid spectrum [49]. Gao and Weaver [50] obtained a SERS spectrum of benzene on a Au electrode that also showed down-shifts of the ring stretching modes. These authors attributed the down shifts to the back-donation of electron density from the surface to the π* antibonding orbitals of benzene as

the molecule binds flat on the surface. The comparison between the solution and SERS spectra of benzene also shows that the hydrogen out-of-plane vibrations are shifted up in the SERS spectrum. These results of the UHF/3-21G calculations of the free benzene molecule and the $(Ag\text{-benzene})^+$ model are shown in Table 4. In the latter case, the Ag atom is placed in the center of the aromatic ring and 2 Å away from it. From this Table, we can see that the calculations with $(Ag\text{-benzene})^+$ model yielded, for the most part, frequency shifts that were analogous to the ones observed in the SERS spectrum, i. e., in the same direction but not necessarily by the same amount.

In the SERS spectrum of pyridine, ring stretching modes shift upward and the out-of-plane modes remained practically unchanged (Table 4). This fact by itself already suggests that pyridine has a different orientation at the surface active site than benzene. As with the benzene calculations, the initial HF/3-21G calculations with a free pyridine molecule and a $(Ag\text{-Py})^+$ model yielded frequency shifts that were analogous to the ones observed in the SERS spectrum. The results of these calculations are shown in Table 4 along those of benzene. The fact that the *ab initio* calculations at the 3-21G level yielded frequency shifts analogous to the experimental shifts for both benzene and pyridine indicates that the single adatom model is an adequate approximation for the molecule/Ag surface interaction. In fact the semi-empirical calculations [9] of a pyridine $/Ag_n$ clusters model (n=10, 13, 14, 15), show that 80% of the bonding is localized between the pyridine N atom and

its nearest neighbor Ag atom. We thus proceeded further with higher level ab initio calculations and turn first to free molecule calculations.

iii) Free molecule calculation

Yang and Schatz [37] have made scaled Hartree-Fock HF/6-311++G frequency calculations for pyridine in vacuum. We repeated these calculations with other basis sets and MP2 and DTF calculations for comparison to results when Ag is included in the chemical model of the scattering species. Our model of pyridine in vacuum was initially constructed with Hartee-Fock, MP2, B3LYP methods and frequencies were subsequently obtained for the 3-21G, 6-21G, 6-31G*, 6-31G** and LanL2DZ basis sets. These calculations followed a full geometry optimization with each basis set. The calculated frequencies were scaled at the HF level by dividing the experimental value for the totally symmetric ring-breathing (mode 1) by the calculated value. Mode 1 is the most intense peak on the pyridine spectrum.

Table 5 shows a comparison of the scaled frequencies of the in-plane normal modes with the experimental frequencies of pyridine. The average relative error does not show much difference between scaled 6-31G, 6-31G*, 6-31G**, 6-311++G at the Hartree-Fock level. Scaled results with the LanL2DZ basis set at the HF level seem to have slightly more error. However, of these basis sets the LanL2DZ has the advantage, for our purposes that it has been extended to include the silver atom. Of the other basis sets only 3-21G includes Ag. Thus, with Ag incorporated in the

chemical model, we used either a mixed basis set with 3-21G for Ag and one of the larger basis sets for pyridine or the LanL2DZ basis set for both with either the HF, MP2, or B3LYP calculational methods.

The unscaled results of the MP2 and B3LYP calculations are also shown on Table 5. It is interesting to point out that the frequencies in the MP2 calculations are not all linearly overestimated as they are in the HF calculations. The low end frequencies tend to be very close to the experimental or slightly underestimated. On the other hand, the upper range frequencies are all overestimated; but even those were not overestimated in a linear fashion as was the case for the HF calculation. On the whole, the MP2 calculation produced a 4.0% average error from the experimental values with the 6-31G basis set and only a 1.4% average error with the LanL2DZ basis set. In comparison the unscaled B3LYP calculation with the LanL2DZ basis set had a slightly larger average of 2.5% error but was found to be computationally more efficient than the MP2 calculation.**

iv) Adatom complex calculation

After calculating the free molecule normal modes, we built the initial Ag-Py model by attaching an Ag atom edge-on to the nitrogen on the pyridine. This model simulates an edge-on interaction of the molecule with an on-top adatom on the Ag surface. We performed the calculations with the HF, MP2, and B3LYP methods using two types of basis sets: the LanL2DZ basis set or a split basis set composed of 3-21G for the silver atom and 6-31G for the**

pyridine molecule respectively. We will heretofore refer to this set as 3-21G//6-31G**. We performed B3LYP calculations with just the LanL2DZ basis set. The results of these calculations are given in Table 6 in terms of a comparison of the observed shift in wavenumbers between the normal Raman scattering spectrum in the gas phase and the SERS spectrum and the calculated shifts between the three chemical models involving pyridine interacting with an Ag adatom in the on-top (σ–bonded) structure and pyridine in vacuum. Table 6 shows that for the strong SERS bands the calculated shifts with the Ag adatom models correspond to the experimentally observed shifts.

First observe the extent to which the Ag-pyridine models reproduce the ν(Ag-N) stretch which appears at ca. 239 cm^{-1} in the SERS spectrum of pyridine. Table 7 shows the Ag-N bond distance and Ag-N stretching vibration for the three models. The neutral Ag-pyridine edge-on model, immensely underestimated the 239 cm^{-1} by 119-143 cm^{-1}. An Onsager SCRF calculation for solvation caused a slight positive shift, but not enough to be of sufficient effect. The calculation of the atomic charges suggested a possible explanation to the underestimated ν(Ag-N) stretch since they showed that both the Ag and N atoms were negatively charged thus resulting in a weak bond. The calculation was subsequently repeated with a positive charge delocalized over the entire Ag-Py model. This calculation improved the calculated value of the 239 cm^{-1} frequency, and for the MP2 and B3LYP methods with the LanL2DZ basis set, the unscaled value was only 40 cm^{-1} on

the low side. To improve the value of the ν(Ag-N) stretch, calculations were carried out with a molecular model that represented the surface active site as a pyramidal Ag_4^+ cluster as proposed by Roy and Furtak. These calculations were made with the HF method using the LanL2DZ basis set. In this manner, the 239 cm^{-1} frequency was calculated at 252 cm^{-1}. Scaling this value by the 0.9227 factor obtained from the gas phase calculation for the LanL2DZ basis set yields a 233 cm^{-1} calculated frequency. This value is quite close to the experimental value. Table 7 gives all of the calculated values for the ν(Ag-N) stretching mode.

In an electrochemical environment, the ν(Ag-N) stretching mode frequency shifts to lower values as the potential at a Ag electrode surface becomes more negative and also shifts with counter anion of the electrolyte. In recent experiments with pyridine in electrochemical environment, we find, on an activated Ag electrode at –0.2 V vs. SCE, the ν(Ag-N) band at 240, 232, and 226 cm^{-1} in 0.1M K_2SO_4, KCl, and KF , respectively. Thus, the above-calculated value is quite close to all of these experimental values. The experimental set-up for these measurements is the same as we used in our previously measurements [51] except that in the present case we use an insitu oxidation reduction cycle. Table 8 shows several assigned bands from these spectra as a function of electrode potential for 0.1 M KCl. We should mention that the spectra obtained in our laboratory are almost identical to spectra recently reported for the same system by Li *et al.* [52] at –0.2, -0.4, -0.6 and –0.8 V. In both studies, the only band position which shifts with

electrode potential is the ν(Ag-N) stretching mode. We note that the lowering of frequency of this band as the potential becomes more negative implies that the Ag-N bond becomes weaker at the more negative potential. We also note that we find similar results for the K_2SO_4 and KF electrolyte systems, i.e., the ν(Ag-N) stretching mode shifts down with a negative shift in voltage but the internal modes do not shift.

We were the first to point out that the so-called surface Ag-molecule band shifts with electrode potential in SERS spectra [53] and we attributed this shift to a vibrational Stark effect. A chemical bonding interpretation of this effect was subsequently given by Anderson et al. [54] for cyanide on a Ag electrode surface. The latter authors made a similar bonding assumption to the one we are making herein, namely that cyanide is bonded to one Ag atom of a Ag cluster, Ag_4-CN. They reasoned that a change in electrode potential is equivalent to a change in the ionization potential of Ag and using semi-empirical calculations found that a positive shift in potential causes more charge donation from a cyanide to Ag in a σ_P orbital with antibonding character which increases both ν(CN) and ν(Ag-C). The same bonding geometry was used by Lin et al [55] using the self-consistent-charge variational Xα(SCC-DV-Xα) calculation method. These workers also found that the dominant charge donation is σ donation from the cyanide to the on-top Ag atom and that a positive charge on the Ag_4 cluster increased the charge donation.[55] A similar situation exits for pyridine on Ag since the surface

bond is formed by charge donation from the nitrogen to a Ag atom of the cluster.

We can interpret differences in the frequency shifts in the SERS spectrum of pyridine obtained at various potentials as being due to the strength of the Ag-N bond. This should not come as a surprise since, as Rodriguez [9,11] demonstrated for cluster models of Ag surfaces, the bond between the pyridine and a metal surface forms by the donation of charge density from the nitrogen to a Ag atom on the surface and a more negative potential on the surface hinders the charge donation thus inducing a weakening of the bond.

While the Ag_4^+ cluster model of the surface best reproduced the ν(Ag-N) frequency, it is still important to consider the effect of pyridine binding to Ag on the other vibrations. From Table 6 we see that the calculations that best reproduce the experimental shifts were those at the MP2/3-21G//6-31G**, MP2/ Lan2DZ, and B3LYP/ LanL2DZ levels for the $(Ag\text{-}Py)^+$ model and HF/LanL2DZ for the $(Ag_4\text{-}Py)^+$ model. The empirical normal mode calculations compared to the HF/3-21G calculations showed that formation of the coordinating bond to the nitrogen of pyridine in turn influenced the SERS spectrum through the redistribution of charge in the ring. We examine this influence by employing natural bond orbital, NBO, calculations implemented in Gaussian 98 using the $NBO BNDIDX NLMO $END keywords. The calculations were done at the restricted B3LYP/LanL2DZ level for pyridine and $(Ag\text{-}Py)^+$ model systems. Below are the Wiberg bond order index (the sum of squares of the off diagonal matrix elements) for the

N1-C2 (C6-N1), C2-C3 (C5-C6), and C3-C4 (C4-C5) bonds obtained from

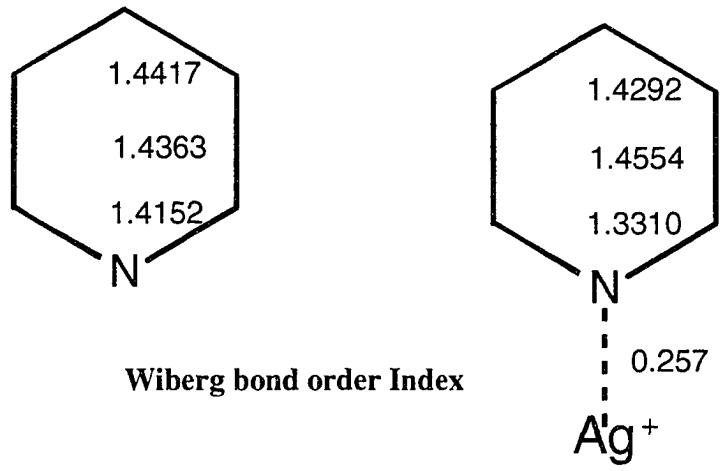

Wiberg bond order Index

the calculation.

We observe that upon interaction with Ag^+ the C2-C3 (C5-C6)) bond order in the pyridine ring increases and the other two decrease. The Wiberg bond order found for N-Ag is 0.257 which is consistent with a weak covalent chemical bonding interaction between Ag and the ring nitrogen, and the natural population analysis, NPA, gives a charge of +0.87 on Ag and –0.68 on N showing that most of the positive charge is on the Ag (Mulliken populations put a much lower charge on both , +0.67 on Ag and –0.29 on N). Another measure of the bonding is the natural localized molecular orbital, NLMO, bond order which gives a bond order of 0.136 with a hybrid overlap of 0.437 between the N –Ag atoms with an atomic hybrid donation of 6.802% from the nitrogen lone pair to Ag orbitals. The percent mixing with the Ag orbitals is 5s (95.85%), 5p (1.65 %), and 4d (2.50%). Thus the bonding of pyridine to an on-top positively charged Ag adatom site on the silver surface involves donation of a small amount of charge from the N lone pair mostly to the vacant 5s Ag orbital. Second order perturbation theory energy analysis of

the Fock matrix in the NBO basis shows that the largest stabilization energy E(2) =28.7 kJ/mol on Ag comes from delocalization of the lone pair NLMO on nitrogen to the NLMO lowest vacant Ag orbital , Ag(5s). Thus, the weakening of the Ag-N bond as the potential is moved negative is consistent with a decrease in this stabilization energy. The second order perturbation analysis also shows a small amount of back donation from Ag (4d) orbitals to N-C antibonding NLMOs with total stabilization energy from this process of 2.6kJ/mol.

E. Discussion

On examining the frequency shifts in the SERS spectrum, we observe that the normal modes that shift the most are the symmetric ring breathing model and the ring bending mode 6a, and the ring stretch mode 18b. Modes 1 and 6a involve the nitrogen vibration and have a_1 symmetry, as seen in Figure 7. Because of their symmetry, the vibration of the nitrogen in those normal modes is along the molecular axis and, thus, in the direction of the Ag atom. The results of the UBFF calculations are therefore as expected since those normal modes were the ones most affected by the K(Ag-N) force constant. The next largest shifts in the SERS spectrum are from the ring stretching modes 18b and 8a which contain contributions from C-H bending. Normal mode 8a has its largest contribution from the C2-C3 stretching motion. As with the modes 1 and 6a, the 8a normal mode has a_1 symmetry and the carbon atoms α to the nitrogen vibrate roughly in the direction of the

Ag atom. While the F(Ag..C_α) did not reproduce the complete shift of this mode, it did reproduce two thirds of it. The rest of the shift was accounted for by the increase of the K(C2C3) force constant. The other two bands that show significant shifts in the SERS spectrum are the gas phase ones at 1227 and the 1052 cm^{-1} corresponding to the Wilson modes 3 and 18b respectively. Both of these normal modes have b_2 symmetry and are mostly ring stretches with a large contribution from the C2-C3 stretch. Because these modes are antisymmetric, the vibration of the α carbons are perpendicular to the direction of the K(Ag-N) and the F(Ag..C_α) force constants and thus not affected by them. The shifts to these normal modes are therefore due to the electron density redistribution within the ring. This fact is also clear from the ab initio calculations on comparing pyridine by itself with Ag adatom - pyridine models using the MP2 and B3LYP calculational methods. The calculations (Table 6) show substantial frequency up-shifts for normal modes 1, 6a, 18b, 3, and 8a which contain a major contribution from C2-C3 (C5-C6) motion. This redistribution of the ring electronic structure leads to an electronic structure with more contribution from a quinoid resonance form as shown by the Wiberg bond order index.

The observations just described are consistent with an edge-on form of attachment of pyridine to the electrode surface. They also provide a justification for including a F(Ag..C_α) force constant in the calculation even though Suzuki and Orville-Thomas did not use it in their pyridine metal ion-complex calculations. Further justification for using the F(Ag..C_α) comes

from the work of Rodriguez [9, 11]. From INDO/S calculations, this author found that the nitrogen provides approximately 80 % of the total charge donated by pyridine and the rest of the charge is donated through the C_α and the hydrogen atoms bonded to the C_α , about 20 % when pyridine is absorbed on cluster models of Ag(100) and Ag(111) surfaces. Our NLMO analysis for $(Ag\text{-}Py)^+$ did not show significant charge donation from C_α orbitals to Ag orbitals. Both our calculations and those of Rodriguez indicate that the Ag -N bond is mostly between the N atom and the nearest-neighbor Ag atom. Moreover, Rodriguez [11] also found that in the case of a Cu(111) surface, the Cu atom bonded to pyridine donates a small amount of charge density into the C-N antibonding orbital (π-backbounding). The second order perturbation analysis for charge donation from filled to unfilled orbitals in the NBO basis showed a delocalization energy of 28.7 kJ/mol for the lone pair orbital on N to the vacant 5s orbital on Ag in comparison with 2.6kJ/mol for donation from filled Ag(4d) orbitals to C-N vacant π-antibonding orbitals. This back bonding should strengthen the nonbonding Ag..C_α interaction; however, its main effect would be to weaken the bond between nitrogen and the adjacent carbons in pyridine.

The frequency shifts observed in the SERS spectrum of pyridine are also observed in comparing pyridine solution and metal ion -complex spectra. From Table 9 we notice the same frequencies shift upward in all of these spectra. The tendency is an increasing frequency shift on going from the solution spectrum to the SERS spectrum and from the SERS spectrum to

the metal ion-complex spectrum. From this tendency, one could surmise that the frequency shifts are directly related to the strength of the bonding at the nitrogen position. Frequency shifts in the case of solution spectra of pyridine were previously noted by Takahasi *et al* [56] and attributed to the formation of a hydrogen bond between the nitrogen and a water molecule. Because of the weakness of the hydrogen bond, the bond that forms between pyridine and a water molecule is expected to be the weakest of the three bonds that the nitrogen can form. The frequency shifts of the pyridine-Ag ion complex are due to the σ-bond between the nitrogen on the pyridine and an Ag^+ ion. This bond is expected to be the strongest in the three types of Raman spectra because it forms with the full positive ion as with all metal ion -complexes. This view is supported by the fact that the ν(Ag-N) band in the $(Ag\text{-}Py_2)^+$ complex is 5 cm^{-1} higher than in the SERS spectrum of pyridine. One deduces that the Ag-N bond is stronger in the $(Ag\text{-}Py_2)^+$ complex than with an adatom on the electrode surface.

Various results of our *ab initio* calculations are also consistent with the relation between magnitude of frequency shifts and the strength of the Ag-N bond. The calculations yielded a higher ν(Ag-N) mode with the a $(Ag\text{-}Py)^+$ model than with the $(Ag\text{-}Py)^0$ model. This should be as expected since +1 charge in the $(Ag\text{-}Py)^+$ model is mostly on the Ag and should enhance the charge donation from the nitrogen to the Ag atom. In fact, the calculation with the neutral model yielded negative partial charges on both the Ag and the N atoms, which made for a weaker bond.

From Table 4 and Table 6 one also sees that, in general, the *ab initio* methods calculated shifts in the same direction as those observed experimentally. Moreover, the neutral model underestimated many of the shifts while the +1 model overestimated many of them. Those results, suggest that the actual charge on the adatom in the surface active site is somewhere between 0 and +1. This inference is supported by the fact that the $(Ag_4\text{-}Py)^+$ model was the one that best fitted the observed frequency of the external mode and the frequency shifts of the internal modes. In this model, the positive charge is distributed mostly throughout the four Ag atoms and, therefore, the Ag atom bonded to the nitrogen of pyridine has a partial charge.

Only the shift of the 19a band to 1483 cm^{-1} was not adequately reproduced by the *ab initio* calculations. This discrepancy is rather small but may due to surface property not accounted for by any of the models used in the calculations. Despite this, a good correlation between the calculated and experimental SERS shifts was observed for all other bands.

One final observation about *ab initio* calculations is the calculated Ag-N bond length (Table 7). Although there is no direct measure of this bond length when pyridine is adsorbed on the electrode surface, that distance is likely to be close to the Ag-N distance of 2.322 Å found from x-ray crystallography for the Ag $(Py)_4^+$ complex ion [42] . Lombardi *et al.* [13] determined that the lower limit of the Ag-N distance for lutidine is 2.5 Å. However, a more accurate lower limit for pyridine is probably closer to the sum of the covalent radii, 2.2 Å, since the Ag-N bond is not expected to be as strong as a covalent bond.

A 2.322 Å Ag-N bond length would also be in accord with the Ag_4^+ cluster model for the surface proposed by Roy and Furtak since the charged experienced by each pyridine will only be one fourth of the total single charge. It should be noticed that all of the $(Ag\text{-}Py)^+$ calculations with the LanL2DZ basis set yielded Ag-N distances less than any of the other calculations. The $(Ag_4\text{-}Py)^+$ model had the most reasonable values for both the ν(Ag-N) frequency and the Ag-N distance.

F.Conclusion

All of the results in this work point towards an edge-on interaction between pyridine and an Ag adatom in the roughen electrode surface. However, the intensity ratio analysis based on surface selection rules [19, 24] indicates that the pyridine molecule can lie flat [19] with respect to the Ag surface so that normal modes are enhanced which have polarizibility tensor elements which couple into the tangential component of the electric field of the exciting light. On the other hand, Creighton [19] also found that the vibrational frequency shifts in the SERS spectrum were characteristic of a pyridine metal-complex spectrum where the molecule binds edge-on to the metal atom. He attempted to reconcile both phenomena by proposing the formation of a pyridine complex, $Ag\ (Py)_2^+$, which might form near the electrode surface and be adsorbed onto the surface during the ORC pretreatment. Since the pyridine molecules are collinear in this complex, they align parallel to the surface when the complex binds to the surface.

We have found that both ex situ and insitu pretreatment give similar SERS spectra suggesting some kind of a pyridine adatom-complex forms on the surface even after ex situ pretreatment. However, our calculations show that it is not necessary to conclude that a complex forms with two pyridine ligands. A single pyridine molecule bound to a Ag adatom of a Ag cluster is certainly an adequate model. In fact, the pyridine could be σ–bonded to the Ag cluster in an in-plane (flat) or above-plane (vertical) configuration. If the active site on the surface is composed of an adatom sitting on top of three other Ag atoms as in the Ag_4 pyramidal structure, the whole pyramidal structure could lie on top of another layer of Ag atoms, perhaps the surface layer. This type of arrangement would allow for the formation of a surface site with the adatom on top of the trigonal pyramid. It would also raise the pyridine ligand just enough over the surface so that it did not show the frequency shift patterns observed in benzene that are characteristic of a face-on interaction with a Ag adatom. At the same time, this structure would keep it close enough to the surface so that it could interact with the electromagnetic field on the surface.

This model explains why pyridine is able to change its orientation with respect to surface potential as we have observed [27]. The pyridine ligand in the adatom complex could go from a linear alignment to an angular alignment, as in the case of the $Ag(Py)_4^+$ ion in the solid state. If it were the case that a $Ag(Py)_2^+$ complex formed on the surface, the two pyridine molecules could not stand up in a completely perpendicular position, as

proposed by several authors for various heteroaromatic molecules that bond to the surface through the nitrogen atom [17,25,38,57,58]. For pyridine to stand up completely perpendicular to the surface, either a pyridine ligand looses its coordination to the adatom upon voltage change or the adatom-complex has only one pyridine ligand.

Our models of the SERS chemisorbed complex have been simplified since if coadsorbed Cl^- and H_2O molecules are nearest neighbors to chemisorbed pyridine, they might need to be considered in addition to more Ag atoms in the surface metal cluster site in order to reproduce all the properties of the SERS spectrum in ab initio calculations. Both Roy and Furtak [28] and Wantanabe et al. [59] provided experimental evidence for a Ag^+ species as a constituent of the Ag electrode SERS active site. The Ag_4^+ cluster was proposed by Roy and Furtak [28] as the dominant active site in an electrochemical environment on the basis of the observation of the Ag cluster vibrational modes whose frequencies are near those calculated by a normal mode analysis. Ag_n^+ clusters produced in the gas phase and mass selected show an odd-even alternation in nuclearity where Ag_3 and Ag_5 are more abundant than Ag_4; and where Ag_6 and Ag_8 are almost absent [60]. On the other hand, if the active site was a Ag_5 cluster, it might be expected to show more low frequency Raman bands [61] than the three observed at the Ag electrode, especially if its Raman spectrum was surface enhanced. Furthermore, Ag_4^+ formed by photoreduction of Ag(I) and aggregation of the metal Ag atoms in H_2SO_4 has been experimentally observed by ESR [62], and

semiempirical MO calculations show that Ag_4^+ is a stable species with respect to Ag_4 [63]. This Ag_4^+ cluster species provides a positively charged metal-molecule chemisorbed system, and our ab initio calculations at the HF level with pyridine binding to this cluster show the up-shifts in Raman bands of the internal modes of pyridine found in the electrochemical environment as-well-as a reasonable value of ν(Ag-N). However, the ab initio calculations with the simple $AgPy^+$ model also reproduce these features almost as well.

Additionally, the fact that the internal modes of pyridine found in the SERS spectra at a Ag electrode do not shift as the voltage is made negative can be explained by the ab initio calculations, since the dominant bonding interaction in this surface complex is the coupling between the lone pair nitrogen electrons and a vacant 5s orbital on the Ag with little contribution from ring pyridine orbitals. Since the bond between the pyridine and the Ag surface forms by the donation of charge density from the nitrogen to the Ag adatom of the cluster, a more negative potential on the surface should hinder the charge donation by shifting the bonding orbitals in such a way as to reduce overlap, thus inducing a weakening of the bond. The experimental SERS results showing a decrease in ν(Ag-N) as the potential is made more negative is consistent with this weakening of the Ag-N bond.

While we originally attributed the lowering of the external mode with voltage to a vibrational Stark effect [53] which is consistent with the effect of electric field on the molecular dipole moment function at the metal-molecule interface [64], the alternate approach of a chemical bonding explanation based

on ab initio calculations may be more productive. In principle such a treatment also has the possibility of calculating enhancement factors for our charge transfer theory [65] and other chemical theories [66] of the SERS enhancement where chemical bonding between the molecule and the surface is required. The main problem is how to quantitatively model the effect of voltage at the molecular level in ab initio calculations. In most cases the charge on the metal cluster has been used to model the effect of electrode potential on bonding and vibrational frequencies, as was done in a relatively recent study of the effect of potential on the SERS spectra of SCN^- adsorbed on an Ag electrode. [67] Here the cluster species, $Ag4SCN^-$, was used with the variational $X\alpha$ calculation method, as in reference 55, to calculate the effect of electrode potential (charge on Ag_4SCN^- species) on bonding and (by implication) on the frequency behavior of the ν(CN) stretching vibration of SCN^-. On the other hand, in order to make very accurate calculations of SERS band positions and the effect of electrode potential on these bands, a model with a much larger number of metal atoms may be necessary. In such a complete model, the active site would have the SERS active molecule and counter ions binding to a small metal cluster which itself is bonded to a larger metal cluster representing the roughened metal surface particle. However, the present small cluster model with calculations at either the HF or B3LYP level and a medium sized basis set like LanL2DZ can reproduce SERS band positions for pyridine at a Ag electrode surface.

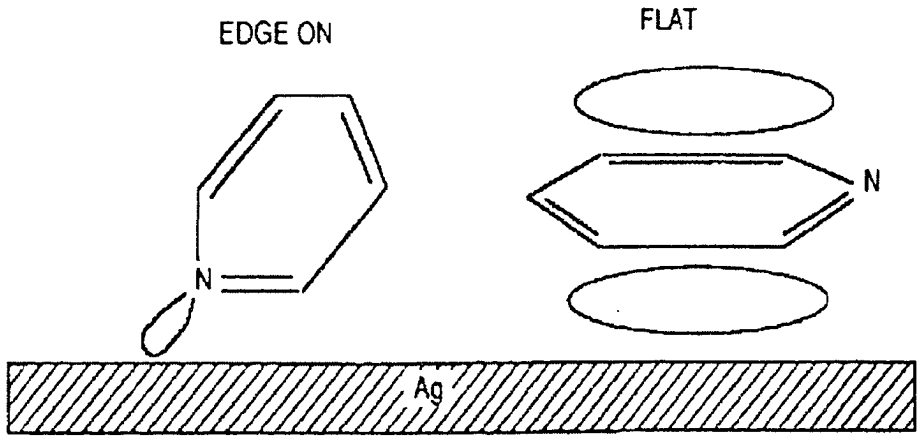

Fig 3. Taken from John R. Lombardi and Ronald L. Birke[40]

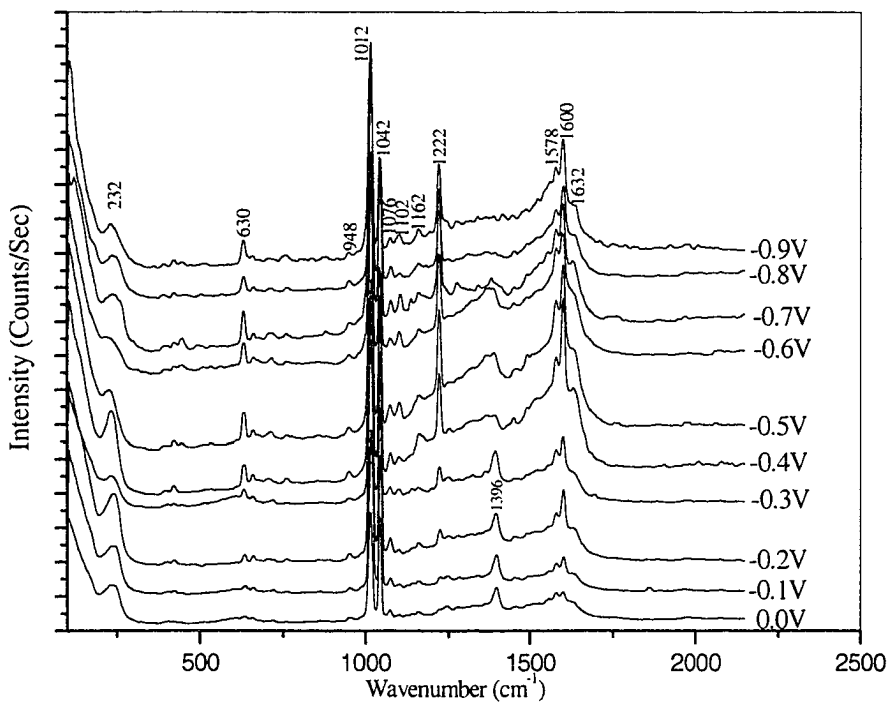

Fig 4. SERS of 0.05M Pyridine in 0.1M K_2So_4 at different voltages.

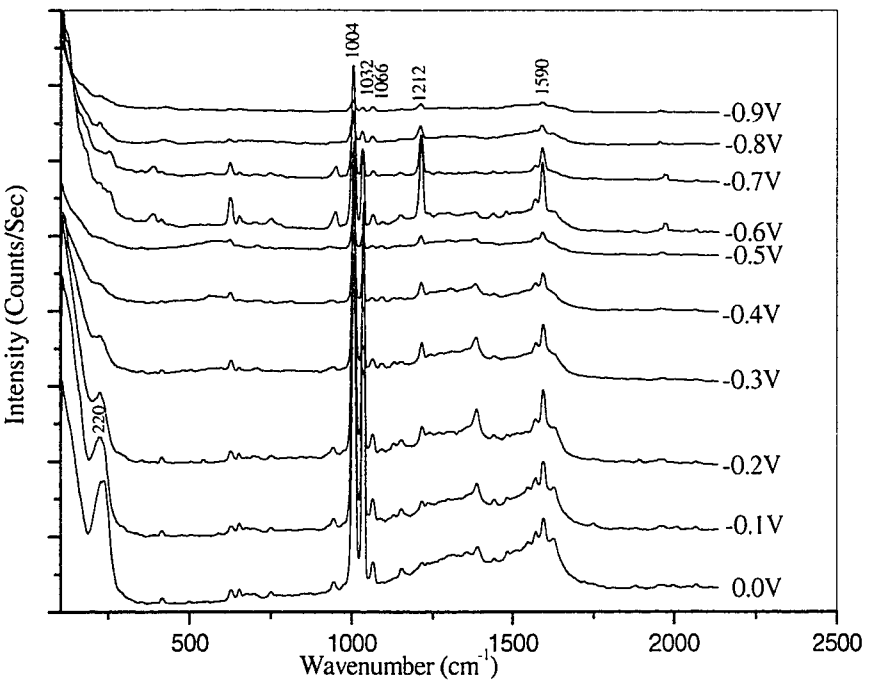

Fig 5. SERS of 0.05M Pyridine in 0.1M KF at different voltages.

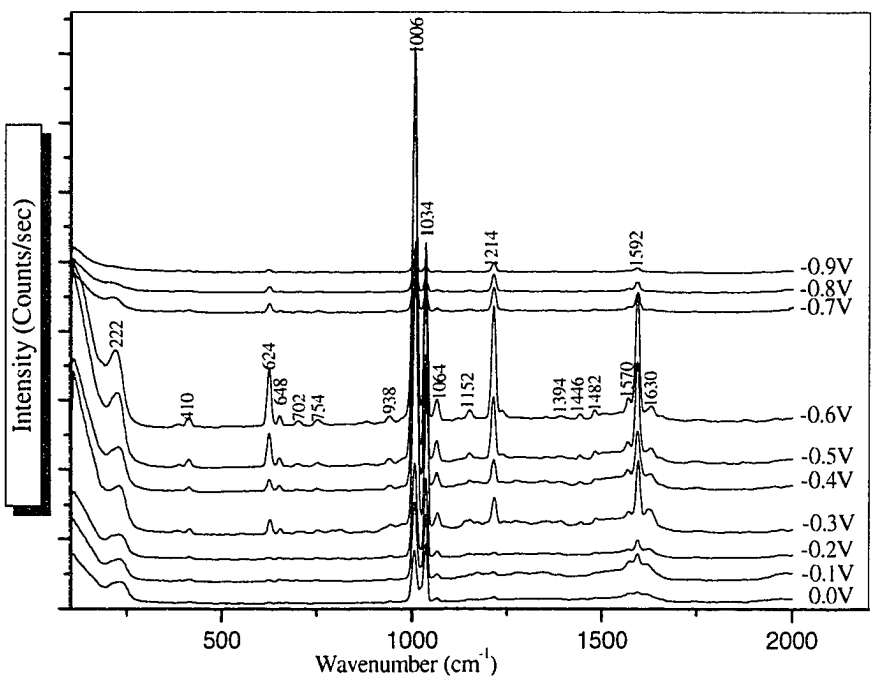

Fig 6. SERS of 0.05M Pyridine in 0.1M KCl at different voltages.

Figure 7 . Normal modes (in Wilson numbers) of the frequencies that shift by more than 10 cm^{-1} in the SERS spectrum of pyridine.

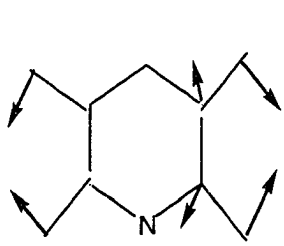

8a

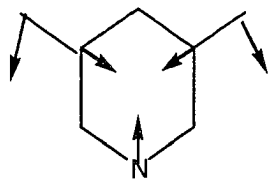

1

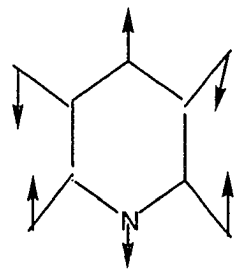

6a

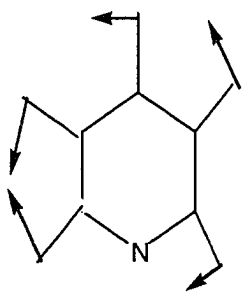

18b

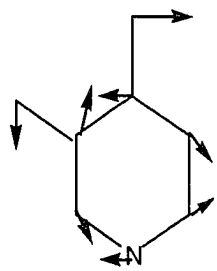

3

Table 1. UBFF force constants of pyridine, in mdyne/Å, obtained by fitting the gas phase frequencies and their modification to fit the SERS frequencies.

force constant type[a]	gas phase	SERS
K(N1C2)	5.58	5.48
K(C2C3)	4.94	5.14
K(C3C4)	4.72	4.72
K(Ag-N)		1.10
H(-CH)	0.33	0.33
H(-C-)	0.82	0.82
H(-N-)	0.28	0.10
ρ	0.37	0.37
F(C..C)	0.72	0.72
F(N..C)	0.38	0.38
F(C..H)	0.38	0.38
F(N..H)	0.59	0.59
F(Ag..C_α)		0.40

K=bond stretch, H=angle bend, F=non-bonded interaction, ρ= aromatic interaction

Table 2. Bond lengths, in Å, of the ring bonds of pyridine and $(Ag\text{-}Py)^+$ model calculated with the HF/3-21G method.

Bond length	Pyridine	$(Ag\text{-}pyridine)^+$
N1-C2	1.331	1.340
C2-C3	1.383	1.377
C3-C4	1.384	1.384

Table 3. Frequency shifts between the gas phase and SERS spectra of the in-plane vibrations of pyridine calculated with a Urey-Bradley force field. All values in cm^{-1}. Observed frequencies obtained from reference 19 and 43.

Wilson no.	symmetry	obsd. freq.	obsd. shift	calcd. shift	assignment
8a	a1	1581	15	16	ring stretch
8b	b2	1574	-2	2	ring stretch
19a	a1	1483	-1	1	C-H deformation
19b	b2	1437	7	8	C-H deformation
14	b2	1355		3	C-H deformation
3	b2	1227	11	7	C-H deformation
9a	a1	1217	1	2	ring stretch
15	b2	1146	7	6	ring stretch
18a	a1	1069	-1	-2	C-H deformation
18b	b2	1052	16	9	ring stretch
12	a1	1030	6	1	trigonal ring breathing
1	a1	991	18	17	totally symmetric ring breathing
6b	b2	654	-3	3	ring deformation
6a	a1	603	24	37	ring deformation

Table 4. Frequency shifts between the liquid and SERS spectra of benzene and between the gas phase and SERS spectra of pyridine calculated with neutral and +1 charged models using the UHF/3-21G method. (Observed frequencies of benzene are from reference 49 and of pyridine from reference 43.)

	benzene				pyridine				
			$(Ag\text{-}Bz)^0$	$(Ag\text{-}Bz)^{+1}$			$(Ag\text{-}Py)^0$	$(Ag\text{-}Py)^{+1}$	
Wilson no.	obsd. freq.	obsd. shift.	calcd. shift	calcd. shift	obsd. freq.	obsd. shift.	calcd. shift	calcd. shift	assignment
In-plane									
8a	1596	-9	-8	-30	1581	15	10	16	ring stretch
8b	1596	-9			1574	-2	-1	-5	ring stretch
19a	1479	-6	-4	-16	1483	-1	3	9	C-H deformation
19b	1479	-6			1437	7	3	5	C-H deformation
3	1346		-1	-8	1355		0	7	C-H deformation
14	1309	2	3	2	1227	11	3	7	C-H deformation
9a	1178	-1	0	-5	1217	1	0	8	ring stretch
9b	1178	-1							ring stretch
15	1149	0	6	-12	1146	7	12	36	
18a	1036	-4	-4	-18	1069	-1	-1	-2	C-H deformation
18b	1036	-4			1052	16	3	0	ring stretch
12	1008		-2	-13	1030	6	8	21	trigonal ring breathing
1	992	-10	-6	-22	991	18	7	12	totally symmetric ring breathing
6b	606	-1	-3	-9	654	-3	-3	-6	ring deformation
6a	606	-1			603	24	15	32	ring

									deformation
Out-of-plane									
5	989		-8	-8	1007	2	9	21	C-H twist
17a	966		0	11	980		8	6	C-H twist
17b	966				941	2	12	16	C-H twist
10a	849	15	8	33	884	-3	2	1	C-H twist
10b	849	15				7	7	13	C-H twist
4	703		-13	-32	747	2	-3	-6	ring twist
11	670	27	14	49	703	8	3	2	C-H twist
16a	404	-7	-11	-1	406	7	-1	-2	ring twist
16b	404	-7			380				ring twist

Table 5. Comparison of observed gas phase frequencies of pyridine (Ref.43) against the scaled calculated frequencies in wavenumbers.

method:		HF	HF	HF	HF	HF[a]	HF	MP2	MP2	B3LYP
basis set:		3-21G	6-31G	6-31G*	6-31G**	6-311++G	Lan L2 DZ	6-31G**	LanL2DZ	LanL2DZ
scale factor:		0.9151	0.9056	0.9059	0.9067	0.90	0.9227			
Wilson no.	obsd. freq.	calcd. freq.	calcd. freq.	calcd. freq.	calcd. freq.	calcd. freq.	calcd. freq.	calcd. freq.	calcd. freq.	calcd. freq.
8a	1581	1600	1617	1631	1631	1583	1633	1662	1573	1610
8b	1574	1594	1609	1622	1622	1577	1628	1652	1567	1616
19a	1483	1513	1503	1505	1501	1475	1510	1537	1479	1499
19b	1437	1470	1462	1457	1453	1435	1471	1501	1448	1469
14	1355	1398	1379	1368	1362	1356	1392	1414	1382	1394
3	1227	1214	1210	1191	1190	1185	1149	1401	1272	1307
9a	1217	1238	1227	1221	1220	1205	1242	1264	1232	1249
15	1146	1090	1135	1074	1073	1101	1070	1199	1187	1195
18a	1069	1097	1080	1072	1070	1060	1086	1110	1077	1090
18b	1052	1060	1064	1054	1051	1040	1071	1098	1057	1079
12	1030	1041	1031	1017	1018	1038	1037	1056	1028	1042
1	991	991	991	991	991	1013	991	1014	947	989
6b	654	685	668	652	653	658	669	666	656	669
6a	603	630	616	597	598	607	617	609	607	615
av. rel. error[b]		2.2	1.4	1.6	1.5	1.1	2.6	4.4	1.4	2.4

[a] Results of Yang and Schatz, *J. Chem Phys.* 97, 1992, 3831.

[b] average relative error = { Σ [abs (calcd. – obsd.) / obsd.] x 100% } / 14

Table 6. Comparison of observed and calculated SERS vibrational frequency shifts in wavenumbers. Observed SERS shifts were calculated by subtracting observed Normal Raman frequencies (Ref.43) from observed SERS frequencies (Ref. 19). Calculated shifts were obtained by subtracting unscaled calculated frequencies of the adatom models from unscaled pyridine values (Table 5).

	model :	$(Ag\text{-}Py)^0$			$(Ag\text{-}Py)^1$					$(Ag_4\text{-}Py)^+$
	method:	HF	HF	MP2	HF	HF	MP2	MP2	B3LYP	HF
Gas phase	basis set:	3-21G//6-31G**	LanL2DZ	LanL2DZ	3-21G//6-31G**	LanL2DZ	3-21G//6-31G**	LanL2DZ	LanL2DZ	LanL2DZ
obsd. freq.	obsd. shift	calcd. shift	calcd. shift	calcd. shift	calcd. shift	calcd. shift	calcd. shift	calcd. shift	calcd. shift	calcd. shift
1581	15	8	6	12	12	15	22	32	28	17
1574	-2	0	0	-2	-8	-7	-2	4	-6	-5
1483	-1	1	4	0	4	11	6	17	11	10
1437	7	3	4	13	6	8	16	18	15	7
1227	11	3	1	1	6	19	7	31	14	6
1217	1	-5	2	5	1	11	5	17	8	10
1146	7	6	6	6	23	16	12	19	18	14
1069	-1	-1	-1		-1	-4	1	-6	-2	-1
1052	16	10	5	10	18	5	16	15	19	14
1030	6	-3	6	9	12	23	4	31	16	5
991	18	9	5	20	15	12	30	34	29	12
654	-3	-3	-2	-1	-6	-5	-5	-2	-7	-3
603	24	12	8	19	28	31	31	39	39	26

Table 7. Calculated Ag-N bond length and Ag-N, stretch observed at 239 cm^{-1} on the pyridine SERS spectrum , with the various *ab initio* methods.

species:	method basis set	(Ag-N) frequency (cm^{-1})	Ag-N bond length (Å)
$(Ag\text{-}Py)^0$	HF 3-21G//6-31**	96	2.58
	HF LanL2DZ	64	2.69
	MP2 LanL2DZ	119	2.45
$(Ag\text{-}Py)^+$	HF 3-21G//6-31G**	170	2.33
	HF LanL2DZ	181	2.29
	MP2 3-21G//6-31G**	177	2.29
	MP2 LanL2DZ	197	2.24
	B3LYP LanL2DZ	198	2.17
$(Ag_4\text{-}py)^+$	HF LanL2DZ	252	2.33

Table 8. Voltage dependence, versus SCE, of the of the vibrational frequencies in the SERS spectrum of pyridine obtained on a Ag electrode.

Wilson no.	-0.2 V	-0.4 V	-0.6 V	-0.8 V
8a	1624	1626	1630	1624
8b	1594	1594	1592	1592
9a	1216	1216	1214	1214
18a	1066	1066	1064	1066
12	1036	1036	1036	1034
1	1006	1006	1006	1006
6b	648	648	648	648
6a	626	624	624	622
16a	414	414	412	410
ν(Ag-N)	232	228	218	206

Table 9. Observed frequency shifts (in cm^{-1}) in the solution, SERS and $Ag(Py)_2^+$ complex spectra of pyridine.

		observed frequency shifts		
Wilson no.	gas phase[a]	solution[b]	SERS[c]	$Ag(Py)_2^+$ [d]
in-plane				
8a	1581	12	15	23
8b	1574	2	-2	-2
19a	1483	4	-1	6
19b	1437	7	7	
14	1355			
3	1227	5	11	
9a	1217	3	1	10
15	1146	7	7	10
18a	1069	2	-1	2
18b	1052		16	
12	1030	6	6	9
1	991	11	18	21
6b	654	0	-3	-7
6a	603	15	24	30
out-of-plane				
5	1007	-5	2	
17a	980			
10b	941	7	2	
10a	884	3	-3	
4	747	13	7	9
11	703	5	2	-2
16b	406	5	8	9
16a	380	5	7	

[a] Ref.43, [b,c,d] Ref.19

Table 10.The vibrational frequencies of 0.05M of Pyridine in different electrolyte solutions (0.1 M K_2SO_4, 0.1 M KCl, and 0.1 M KF) as a function of voltage.

Voltages (V)	Pyridine (K_2SO_4) band freq (cm^{-1})	Pyridine (KCl) band freq (cm^{-1})	Pyridine (KF) band freq (cm^{-1})
0.0V	234	236	234
	420	414	414
	634	624	626
	954	944	944
	1014	1006	1006
	1044	1036	1036
	1074	1066	1066
	1164	1152	1154
	1244	1216	
	1400		1390
	1456	1486	
	1580	1574	1570
	1600	1594	1594
	1622	1620	1624
-0.1V	236	232	226
	420	412	414
	634	624	626
	954	944	944
	1016	1006	1006
	1046	1036	1032
	1076	1066	1068
	1102		
	1164	1172	1156
	1244	1214	1214
	1398		1388
	1582	1572	1570
	1602	1592	1594
	1632	1618	1626
-0.2V	240	232	224
	422	414	412
	634	626	624
	954	944	942
	1016	1008	1006
	1046	1038	1032
	1076	1066	1064
	1102		
	1162	1160	1154
	1228	1216	1216
	1396		1388
	1578	1570	1570
	1602	1594	1592
	1630	1624	1626

Voltages (V)	Pyridine (K_2SO_4) band freq (cm^{-1})	Pyridine (KCl) band freq (cm^{-1})	Pyridine (KF) band freq (cm^{-1})
-0.3V	234	230	220
	420	414	414
	634	624	626
	954	944	942
	1016	1006	1006
	1044	1036	1034
	1074	1066	1066
	1102		1094
	1160		
	1224	1216	1216
	1394		1386
	1580	1570	1570
	1600	1594	1592
	1626	1622	1622
-0.4V	234	228	216
	420	410	412
	636	624	622
	954	942	940
	1016	1006	1006
	1044	1036	1034
	1074	1064	1062
	1100		1092
	1162		
	1222	1214	1214
			1304
			1382
	1580	1568	1570
	1600	1592	1592
	1632	1626	1624
-0.5V	228	222	210
	420	412	412
	634	624	622
	952	940	936
	1014	1006	1004
	1044	1034	1034
	1074	1064	1064
	1102		1092
	1164		
	1222	1214	1214
	1390		1384
	1580	1568	1572
	1600	1592	1590
	1632	1626	1620

Voltages (V)	Pyridine (K_2SO_4) band freq (cm^{-1})	Pyridine (KCl) band freq (cm^{-1})	Pyridine (KF) band freq (cm^{-1})
-0.6V	216	218	212
	438	412	388
	630	624	622
	952	942	948
	1014	1006	1004
	1044	1036	1034
	1074	1064	1066
	1102		
	1162	1152	1150
	1222	1214	1214
	1318		
	1370		
	1388		
	1580	1568	1574
	1596	1592	1590
	1630	1630	1624
-0.7V	236	218	208
	442	410	386
	632	624	622
	954	944	952
	1014	1006	1004
	1044	1036	1034
	1076	1066	1068
	1104		
	1162	1150	1150
	1222	1214	1212
	1276		
	1382		
	1580	1570	1570
	1598	1592	1590
	1630	1626	1628
-0.8V	234	206	220
	420	410	420
	632	624	620
	952	946	940
	1016	1006	1002
	1044	1034	1032
	1076	1066	1066
	1102		
	1162	1152	
	1222	1214	1212
	1580	1570	1568
	1600	1592	1588
	1628	1624	1620

Voltages (V)	Pyridine (K_2SO_4) band freq (cm^{-1})	Pyridine (KCl) band freq (cm^{-1})	Pyridine (KF) band freq (cm^{-1})
-0.9V	232	204	218
	420	420	424
	630	622	622
	950	940	940
	1014	1006	1004
	1042	1034	1032
	1074	1066	1066
	1102	1108	
	1162	1148	1154
	1222	1214	1212
			1272
	1578	1570	1564
	1600	1590	1590
	1632	1618	1622

G. References

[1].Fleishman, M.; Hendra, P.J. ; McQuillan, A.J. *Chem. Phys. Lett.* 1974, 26, 163.

[2].(a) Kneipp, K.; Kneipp, H.; Itzkan, I.; Dasari, R. R.; Feld, M. S. *Chem. Rev.* 1999, 99,2957-2956. (b) Campion, A.; Kambhampati P. *Chem. Soc. Rev.* 1998, 27, 241-250.

[3].Doering, W. H. ; Nie, S. *J. Phys Chem. B* 2020, 106, 311-317

[4].Kennedy, B. J.; Spaeth, S.; Dikey, M.; Carron, K. T. *J. Phys Chem. B* 1999, 103, 3640-3646

[5].Hill, W. ; Fallourd, V.; Klocjow, D. *J. Phys Chem. B* 1999, 103, 4707-4713

[6].Cao, Y-W,; Jin, R,; Mirkin, C. A. *Science* 2002, 297 1536-1540.

[7].Birke, R. L.; Lombardi, J. R. *Spectroelectrochemistry: theory and practice*; Gale, R. J., Ed.; Plenum Publishing Corporation: New York, 1988; pp. 263-347.

[8].Bagus, P. S., Pacchioni, G., Philpott, M. R. *J. Chem. Phys.*, 1989, 90, 4287-4295

[9].Rodrigues, J. A. *Surf. Sci.*, 1990, 226, 101-118

[10].Bagus, P. S., Herman,K., Bauschlicher, C. W. Jr. *J. Chem. Phys.*, 1984, 81, 1966-1974

[11].Rodrigues, J. A. *Surf. Sci.*, 1992, 273, 385-404.

[12].Kasser, W.; Kettler, U.; Bechthold, P.S. *Chem. Rev. Let.* 1982, 86, 223-227.

[13].Lombardi, J. R.; Shields Knight, E. A.; Birke, R. L. *Chem. Phys. Lett.* 1981, *79*, 214-218.

[14].Creighton, J. A.; Albrecht, M. G.; Hester, R.E.; Matthew, J. A. D. *Chem. PhysLett.* 1978, *55*, 55-58.

[15].Van Duyne, R. P. *Chemical and biochemical application of lasers*; Moore, C. B.,Ed.; Academic Press: New York, 1979; Vol. 4, Ch 5, pp. 101-185.

[16].Evans, J. F.; Albrecht, M. G.; Ullevig,, D. M.; Hexter, R. E. *J. Electroanal. Chem.* 1980, *106*, 209-234.

[17].Neto, N.; Muniz-Miranda, M.; Sbrana, G. *J. Phys. Chem.* 1996, *100*, 9911 9917.

[18].Muniz-Miranda, M.; Neto, N.; Sbrana, G. *J. Phys. Chem.* 1988, *92*, 954-959.

[19].Creighton, J. A. *Surf. Sci.* 1983, 124, 209-219

[20].Netzer, F. P.; Bertel, E.; Matthew, J. A. D. *Surf. Sci.* 1980, 92, 43-52.

[21].Surman, M.; Bare, S. R.; Hoffman, P.; King, D. A. *Surf.Sci.* 1987, 179, 243-253.

[22].Dudde, R.; Koch, E. E.; Ueno, N.; Engelhardt, R. *Surf. Sci.* 1986, *178*, 646-656.

[23].Bridge, M. E.; Connolly, M.; Lloyd, D. R., Somers, J.; Jakob, P.; Menzel, D. *Spectrochim. Acta A* 1987, 43, 1473-1478.

[24].Moskovits, M. ; Suh, J. S. *J. Chem. Phys.* 1984, 88, 5526

[25].Golab, J. T.; Sprague, J. R.; Carron, K. T.; Schatz, G. C.; Van Duyne, R. P. *J.Chem. Phys.* 1988, *12*, 7942-7951.

[26].Billman, J.; Kovacs, G.; Otto, A. *Surf. Sci.* 1980, *92*, 153-173.

[27].Bunding, K. A.; Birke, R. L.; Lombardi, J. R. *Chem. Phys.* 1980, *54*, 115-121.

[28].(a) Roy, D.; Furtak, T. E. *Chem. Phys. Lett.* 1986, *124*, 299-303 (b) Roy, D.; Furtak, T. E. *Phys. Rev.* B 1986, *344*, 5111-5117

[29].Corni, S.; Thomasi, J. *J. Chem. Phys.* 2002, *116*, 1156-1164.

[30].Cornis S.; Thomasi, J. *J. Chem. Phys.* 2001, *114*, 3739-3751.

[31].Corni, S.; Thomasi, J. *Chem. Phys. Lett.* 2001, *342*, 135-140.

[32].Kwon, Y. J.; Son, D. H.; Ahn, S. J.; Kim, M. S.; Kim, K. *J. Phys. Chem.* 1994, *98*, 8481-8487.

[33].Cardini, G.; Muniz-Miranda, M. *J. Phys. Chem.* 2002, *106*, 6875-6880.

[34].Arenas, J. F.; Soto, J.; López Tocón, I.; Fernández, D. J.; Otero, J. C. *J. Chem.Phys.* 2001, 116, 7207-7216.

[35].Vivoni, A.; Chen S. -P.; Ejeh, D.; Hosten, C. M. *Langmuir* 1999, *16*, 3310-3316.

[36].Aroca, R. F.; Clavijo, R. E.; Halls, M. D.; Schlegel, H. B. *J. Phys. Chem.* A 2000, *104*, 9500-9505.

[37].Yang, W. H.; Schatz, G. C. J. Chem. Phys. 1992, 97, 3831-3845.

[38].Muniz-Miranda, M. *J. Phys. Chem.* 2000, *104*, 7803-7810.

[39].Barlow, A.; Diem, M. *J. Chem. Ed.* 1991, *68*, 35-39.

[40].Vivoni, A.; Birke, R.; Lombardi, J. *Spectrochim. Acta A* 2001, *57*, 535-544.

[41] .Suzuki, S.; Orville-Thomas, W. J. *J Mol. Struct.* 1976, 37, 321-327.

[42].Nilsson, K.; Oskarsson, A. *Acta Chem. Scand. A* 1982, 36, 605-610.

[43].Stidham, H. D.; DiLella, D. P. *J. Raman Spectrosc.* 1980, *9*, 247-256.

[44].M. J. Frisch, G. W. Trucks, H. B. Schlegel, G. E. Scuseria, M. A. Robb, J. R. Cheeseman, V. G. Zakrzewski, J. A. Montgomery, Jr., R. E. Stratmann, J. C. Burant, S. Dapprich, J. M. Millam, A. D. Daniels, K. N. Kudin, M. C. Strain, O. Farkas, J. Tomasi, V. Barone, M. Cossi, R. Cammi, B. Mennucci, C. Pomelli, C. Adamo, S. Clifford, J. Ochterski, G. A. Petersson, P. Y. Ayala, Q. Cui, K. Morokuma, P. Salvador, J. J. Dannenberg, D. K. Malick, A. D. Rabuck, K. Raghavachari, J. B. Foresman, J. Cioslowski, J. V. Ortiz, A. G. Baboul, B. B. Stefanov, G. Liu, A. Liashenko, P. Piskorz, I. Komaromi, R. Gomperts, R. L. Martin, D. J. Fox, T. Keith, M. A. Al-Laham, C. Y. Peng, A. Nanayakkara, M. Challacombe, P. M. W. Gill, B. Johnson, W. Chen, M. W. Wong, J. L. Andres,

[45].Bürig, H.-B.; Dunitz, J. D. *J. Am. Chem. Soc.* 1987, 109, 2924-2926.

[46].Li, X.-Y.; Zgierski, M. Z. *J. Phys. Chem.* 1991, 95, 4268-4287.

[47].Herschbach, D. R.; Laurie, V. W. *J. Chem. Phys.* 1961, 35, 458-463.

[48].Majoube, M. *J. Raman Spectrosc.* 1985, 16, 98-110.

[49].Moskovits, M.; and Di Lella, D. P. *J. Chem. Phys.* 1980, *73*, 6068-6075.

[50].Gao, P.; Weaver, M. J. J. *Phys. Chem.* 1985, 89, 5040-5046.

[51].Faria, P. A.; Chen, X., Lombardi, J. R.; Birke, R. L. *Langmuir* 2000, 16, 3984-3992

[52].Li, W.-H.; Li, X.-Y.; Yu, N.-T. *Chem. Phys. Lett.* 1999, 305, 303-310.

[53].Vekatesan, S.; Erdheim, G; Lombardi, J. R,; Birke, R. L. *Surf. Sci.* 1980, 101, 387

[54].Anderson, A. B.; Kotz, R.; Yeager, E. Chem Phys. Lett. 1981, 82, 130

[55].Lin, W. F.; Tian, Z. Q.; Sun, S. G.; Tian, Z. W. *Electrochimica Acta* 1992, 37, 211-213

[56].Takahasi, H.; Mamola, K.; Plyler, E. K. *J. Mol. Spectrosc.* 1966, *21*, 217-230.

[57].Arenas, J. F.; Woolley, M. S.; López Tocón, I.; Otero, J. C.; Maecos, J. I. *J.Chem. Phys.* 2000, *112*, 7669-7683.

[58].Carter, D. A.; Pemberton, J. E.; Woelfel, K. J. *J. Phys. Chem.* 1998, *102*, 9870-9880.

[59].Watanabe, T.; Kawanami, O.; Honda, K; Pettinger , B. *Chem. Phys. Lett.* 1983, 102 , 565-569.

[60].Bosnick , K.A., Ph.D. Thesis, University of Toronto, 2000

[61].Haslett, T. L.; Bosnick ,K. A.; Moskovits, M. *J. Chem. Phys.* 1998 108, 3453-3457

[62].Eachus, R.S. ; Symons, M.C.R., *J. Chem. Soc. A 1970, 1329-*

[63].Baetzold, R.C.*J.Chem.Phys. 1971,55, 4363- 4370*

[64].Lambert, D.K. *Electrochimica Acta 1996, 5 ,623-630*

[65].Lombardi, J.R.; Birke, R.L., Lu, T., Xu, J. *J.Chem.Phys. 1986, 84, 4147-4180*

[66].Moskovits, M. *Reviews of Modern Physics 1985, 57, 783-826*

[67].Tian, Z.Q.; Li, W. H.; Qiao, Z.H.; Lin, W.F.; Tian, Z.W. *Russian J. of Electrochem. 1995, 31, 935-940.* From Elektrokhimiya. 1995, 31, 1014-1020

Chapter 3

Surface – Enhanced Raman Spectra of Heme Proteins (Horse Heart Cytochrome C and Horse Skeletal Muscle Myoglobin) as a Function of Voltage.

A. Abstract

Surface –enhanced Raman scattering (SERS), resonance Raman and UV-visible spectroscopy were used to investigate the oxidation state, spin-state, size of the tetrapyrrole ring and the environment of horse heart cytochrome c, and horse skeletal muscle myoglobin as we varied the voltage in a potentiostated system. As the voltage was varied from 0.0V to – 0.9V, it was found that the iron atom of the heme chromophore of both molecules exists as Fe (III) at – 0.2V, while the Fe (III) was reduced to Fe (II) at – 0.6V. For horse heart cytochrome c in the oxidized and reduced state the iron atom is in a low spin state while for myoglobin the iron atom Fe (III) exists in the high spin state at – 0.2V. The change in oxidation state of the iron atom from Fe (III) to Fe (II) is accompanied by a lowering of porphyrin skeletal vibrational frequencies while a change from low spin to high spin iron at constant oxidation state is accompanied by a more marked decreased of vibrational frequencies. The oxidation state and spin state marker bands can be found in the 1100 – 1700 cm^{-1} region in the SERS spectra of these molecules and these bands help us to identify the state of the central iron and the geometry of the heme chromophore. For example, high spin iron of these heme proteins has the iron atom located above the tetrapyrrole ring while a low spin iron has the iron atom located in the plane of the tetrapyrrole ring.

The first SERS study of cytochrome c and myoglobin on a silver electrode surface was reported by T. M. Cotton[1] et al in 1980. In that report, intense SERS spectra were presented as a function of voltage at – 0.2V and –0.6V

respectively. However, in our report, we intend to study these heme proteins in more detail by monitoring their behavior on a wider range of voltage i.e. from 0.0V to – 0.9V. The potential dependence of spectra was used to explain adsorption, denaturation, oxidation state and spin state change of both proteins on surface. This report is just an introduction to chapter five in which some of these proteins, especially myoglobin, will be studied in the presence of surfactants.

B. Introduction

Heme containing proteins, such as cytochromes, hemoglobin and myoglobin, are molecules that can be found in both human and animals as well[3]. They perform a variety of tasks necessary for the metabolic process in many species[15]. These proteins play such diverse roles as reversibly binding molecular oxygen transport by transferring single- electrons in membrane – centered respiratory chains (cytochromes) , reducing peroxidases (catalases and peroxidases) , or acting as the terminal components in multienzymes systems involved in hydroxylation[3] . Since most of the chemical reactions taking place in the human body involve the transfer of electron from one molecule to another, it should not come as a surprise to us that these proteins also perform their task by gaining or losing electrons. Horse heart cytochrome c and horse skeletal muscle myoglobin possesses similar properties found in human cytochrome c and myoglobin[3]. They all have a prosthetic group (tightly and sometimes covalently bound to the apoprotein), which involves an iron atom [Fe (III) or Fe (II)] coordinated to a macrocyclic

tetrapyrrole ring such as protoporphyrin IX. Myoglobin and each of the four subunits of hemoglobin noncovalently bind a single heme group. In addition, the same group occurs in cytochrome where it is bound covalently and in certain redox enzymes such as catalases. Heme is responsible for the characteristic red color of blood and is the site at which each globin monomer binds one molecule of O_2 (globins are the heme –free proteins of Hb and Mb)[3]. The heterocyclic ring system of heme consists of a porphyrin derivative having four pyrrole rings linked by methane bridges. The porphyrin in heme, with its particular arrangement of four methyl, two propionate, and two vinyl substituents, is known as protoporphyrin IX. Therefore, heme is protoporphyrin IX with a centrally bound iron ion. In hemoglobin and myoglobin, the iron atom normally remains in the Fe (II) oxidation state whether or not the heme is oxygenated. In deoxygenated hemoglobin and myoglobin, the iron atom is five – coordinated by a square pyramid of N atoms: four from the porphyrin and one from the histidine side chain of the protein. Upon oxygenation, the O_2 binds to the Fe (II)[15] on the opposite side of the porphyrin ring from the histidine ligand so that the Fe (II) is octahedrally coordinated; that is, the ligands occupy the six corners of an octahedron centered on the Fe atom. The binding of ligands, such as oxygen and water, changes the oxidation state of the iron atom and certain molecules such as CO, NO, H_2S coordinate to the sixth liganding position of the Fe (II) in hemoglobin and myoglobin with much greater affinity than does oxygen[15]. This, together with their similar binding to the hemes of

cytochromes, account for the highly toxic characteristics of these substances. The Fe (II) of hemoglobin and myoglobin can be oxidized to Fe (III) to form methemoglobin (metHb) or metmyoglobin (met Mb) and they do not function as reversible oxygen carriers.

For the cytochromes[1], a variety of them exist but the most intensively studied are the ones found in the mitochondrial membranes in animal cells where they act as electron carriers in the respiratory chain between various iron-sulfur flavoprotein dehydrogenases and molecular oxygen. The cytochromes[15] (a, b, c) have different macrocycles owing to different side-chain substitutions in the basic structure. The variation of the side chains in the cytochromes and differences in the macrocycles themselves are responsible for variations in redox potentials found among them.

The combination of Surface- Enhanced Raman scattering (SERS) and Resonance Raman (RR) has permitted us to observe the vibrational spectrum of the heme chromophore in highly dilute solutions of both, horse heart cytochrome c and horse skeletal muscle myoglobin (Mb). Both of these proteins were chosen for the SERS + RRS experiments because both are structurally well characterized and their conventional resonance Raman spectra have been extensively studied as a function of the central metal oxidation state, spin state, environment and laser excitation[1]. In addition, these two techniques helped us to analyze the structure of the heme chromophore, which considers the backbone of both molecules. The SERS spectra of both molecules (horse heart cytochrome c and horse skeletal

muscle myoglobin) have been investigated and it has been shown that the oxidation state and position of the central iron of the heme chromophore is voltage dependent. The oxidation state and spin state[15] (and as a result the size) of the iron atom bound to the tetrapyrrole ring can play a very important role in the interpretation of the resonance Raman (RR) spectra of hemes, and these properties must be taken into consideration since they have a direct effect on the overall structure of these molecules.

C. Experimental

Horse heart cytochrome c and horse skeletal muscle myoglobin were purchased from Sigma Chemical corporation and used without any further purification. Both molecules had a relatively high percentage purity (95%) and the cytochrome c contained 2.8% water by mass. The SERS stock solutions of these compounds were prepared at one millimolar concentration in distilled and deionized water. Aliquots of these solutions were injected with a pipette into an electrochemical cell that contained degassed 0.1 molar of sodium sulfate (Na_2SO_4) in distilled and deionized water. A dilution of 1 micromolar concentration in distilled water was used for the UV- visible experiment and the resonance Raman spectrum was taken at 0.5 millimolar concentration in 0.1 molar sodium sulfate (Na_2SO_4). The Raman apparatus consists of an argon (Ar^+) laser (514.5 nm line from Spectra-Physics model 2065–7S) operating at approximately 250 mw for SERS (50 mw on surface) while we used a power of 350 mw for RR (70 mw on surface). The spectra of

the molecules were obtained with a Spex model 1401 double monochromator withphoton counting detection. Our electrochemical cell consisted of a silver electrode, a saturated calomel electrode (SCE) called a reference electrode and a platinum counter electrode. These electrodes were connected to a potentiostat that allowed us to monitor the voltage. The anodization procedure consists of a single oxidation and reduction cycle. Oxidation of the silver (Ag) electrode was achieved at + 0.45V vs. SCE, followed by reduction at – 0.6V with a dwell time of 5 seconds. Although we did not use the chronocoulometric technique to determine the amount of charge per surface area for a specific amount of time, we can assume that the charges passed in the oxidation step were between 100 – 150 mC / cm^2.

D. Results and Discussion

i) The UV- vis of the heme chromophore marked by the appearance of the α, β and γ.

Figure 7. illustrates the structure of heme proteins (protoporhyrin IX) and their electronic properties are dominated by the aromatic system of the porphyrin ring . The structure of a resonance Raman (RR) that corresponds to a heme protein is mainly dependent on the absorption band chosen to generate the RR effect. As a result, it is necessary to give detailed information about the general characteristics of heme absorption spectra. Heme proteins have their visible and near ultra –violet spectra dominated by two $\pi - \pi^*$ transitions. Both are of E_U symmetry[3] under the D_{4h} point group which applies approximately to metalloporphyrins. These transitions ($\pi - \pi^*$)

are polarized in the plane of the heme and they undergo considerable interaction with the result that the transition dipoles are additive for the higher energy transition and largely cancel for the lower energy one. Typical UV–Vis spectra for these heme proteins (horse heart cytochrome c and horse skeletal muscle myoglobin) are shown in figure 10 for cytochrome c and myoglobin in the oxidized form. In both figures, the higher energy transition is assigned to the intense absorption band and it is called the Soret or γ band occurring nearly around 400 nm. A much weaker band (by a factor of 10 or more) absorbs approximately at 500 nm and it is called the α band. The lower energy transition, however, can " steal "some of the intensity of the higher energy transition through vibrational interactions. And as a result, these interactions give rise to a vibronic band called β which occurs at an energy in the proximity of 1300 cm^{-1} higher than the α band. The α band is caused by a pure electronic transition in which no change in vibrational quantum numbers take place. However, the β band[3] corresponds to the envelope of all the active vibronic transitions in which the vibrational quantum numbers of the vibronically active modes increase from zero to one.

ii) Oxidation state and spin state marker bands of the heme chromophore as a function of voltage on a silver electrode surface

The SERS as well as the resonance Raman (RR) spectra of heme proteins are dominated by bands between the 1100 – 1650 cm^{-1} region , where one expects in- plane porphyrin ring modes involving the stretching of C-C and C-N partial double bonds and the bending of C-H bonds. Figure 11 illustrates the

reduction Fe (III) to Fe (II) of the heme chromophore of horse heart cytochrome c after adding sodium dithionite that is considered as a reducing agent. Usually, the oxidation state marker bands occurs between 1358 – 1377 cm^{-1} and they are the most widely used oxidation state. In figure 11, the oxidation marker bands occurs at 1360 cm^{-1} which is considered as a lower frequency shift from Fe (III) to Fe (II). Therefore, that band (1360 cm^{-1}) confirms that after the addition of sodium dithionite to the solution, we have Fe (II) present instead of Fe (III). Tables 2 & 3 compare the oxidation –state and spin – state markers of horse heart cytochrome c and horse skeletal muscle myoglobin as a function of voltage. At – 0.2V, in both cases, the iron atom exists in the Fe (III) form and that oxidation band can be seen in the vicinity of 1370 cm^{-1} region while at – 0.6V they exist as Fe (II) and the oxidation band has been shifted to a lower frequency at 1358 cm^{-1} (See figures 12 & 13). In both figures (12 &13) the spectrum is most intense at – 0.6V and this can be attributed to the state of the silver electrode at this specific voltage [close to the point of zero charge (P. Z .C)] .The reduction of Fe (III) to Fe (II), for horse heart cytochrome c, occurs without change in spin –state i.e. both states exist in a low spin state. This can be interpreted in terms of increase back donation of electrons from Fe (II) into π^* antibonding porphyrin orbitals with a slight reduction in the strength of porphyrin bonds. However, horse skeletal muscle myoglobin is present in the high – spin aquamet Fe (III) state, which suggest that the myoglobin undergoes a change in spin state at the electrode surface. Direct interaction of the heme

group with the electrode surface may have caused the shift in frequencies that we have seen in the case of myoglobin.

T. M. Cotton[1] et al had given two possible oxidation reactions; she predicted that at first the myoglobin solution might undergo reduction to the Fe (II) state at – 0.6V and then reoxidation to Fe (III) at – 0.2V. Alternatively, if myoglobin is not reduced at – 0.6V from Fe (III) as it is present in solution, it is conceivable that oxidation to Fe (IV) is found near 1383 cm^{-1}. In our case, the latter possibility seems highly unlikely because in figure 13, the oxidation state marker band does not occur at 1383 cm^{-1}. Thus, we can propose that the reduction of Fe (III) to Fe (II) occurs at – 0.6V for myoglobin adsorbed on a silver electrode surface and is then followed by its oxidation at – 0.2V.

The kind of interaction of the heme protein with the surface is another matter of concern to us since different kinds of interaction are possible. The heme chromophore may interact directly with the electrode either by direct detachment from the protein matrix or due to denaturation of the protein. It is conceivable that cytochrome c is less likely to get denatured which is partly due to its structure since it is covalently bound to the protein while the probability for myoglobin to get denatured and to release its heme is more likely since it has a more labile coordination and hydrogen bonding interactions which attach the heme to the apoprotein. Therefore, the possibility of heme loss or protein denaturation in the case of cytochrome c^1 is remote while one or both phenomenons are possible in the case of myoglobin.

iii) Orientation of the tetrapyrrole ring for a high and low spin iron as a function of voltage .

The spin –state marker bands[15] occur in the 1552 – 1630 cm^{-1} region and they have been the subject of a controversy involving the nature of the structural change in the iron – porphyrin core responsible for bringing about a shift in marker frequencies. We have already mentioned and described in detail the voltage dependence of the iron atom of the heme chromophore, a change in oxidation state implies a change in the size of the iron atom, and this factor will have an effect on the orientation of the tetrapyrrole ring. Thus, there exist a clear correlation between porphyrin structure and band frequencies and it allows us to monitor the chemistry of the iron – porphyrin core in heme proteins. In addition, it also permits us to make some valuable conclusions about important topics such as the effect of the protein matrix on the structure of the tetrapyrrole ring. Various groups of scientists have made considerable effort in this domain to clarify without ambiguity the structure – frequency shift relationship. Thomas. G. Spiro et al.[4, 5,6, 25] can be considered as one of the leading scientists who has made a tremendous contribution in this area and who originally interpreted the frequency decreases observed for high – spin hemes in terms of increased expansion of the core of the ring (Spiro, Stong and Stein, 1979). He and his coworkers have indicated that the large size of the high spin iron results in out – of – plane displacement of the atom toward an axial ligand. As a result, they[3] have proposed two possible structures for the tetrapyrrole skeleton; one with a planar shape and the other having a tilted shape. The out – of – plane

displacement of the iron forces the pyrrole rings to be tilted in order to maintain overlap with the iron orbitals. This tilting results in poorer π conjugation through the porphyrin methine bridges and consequently lowers the observed frequency.

E. Conclusion

We have presented a brief study of the effect of electrode potential on the oxidation – state and spin – state of heme proteins adsorbed on a silver electrode surface. Our results are in agreement with other pioneering scientists, like T. M. Cotton[1] and T. G. Spiro[2], who have performed numerous investigations and published several scientific papers on that subject. Surface – enhanced Raman and resonance Raman were both used to monitor the structure of heme proteins (Horse heart cytochrome c and Horse skeletal muscle myoglobin) as a function of voltage. We have shown that some vibrational modes of these heme proteins are sensitive to changes in oxidation and spin – state of the iron atom, via the attendant changes in porphyrin conformation and electronic structure. As an example, we have illustrated that at – 0.2V the iron atom of both molecules exists in the Fe (III) state and it takes a planar orientation vis- a – vis the tetrapyrrole ring. However, at – 0.6V, both molecules have their iron atom outside of the plane of the tetrapyrrole ring and as a result the entire ring is forced to adopt a new tilted conformation. The data presented in this chapter are of a background nature, and they are considered as a starting point, since in chapter five of this thesis, we will investigate the behavior of myoglobin in the presence of some surfactants such as didodecyldimethylammonium bromide (DDAB), and cetyltrimethylammoniumbromide (CTAB).

Structure of Protoporphyrin IX

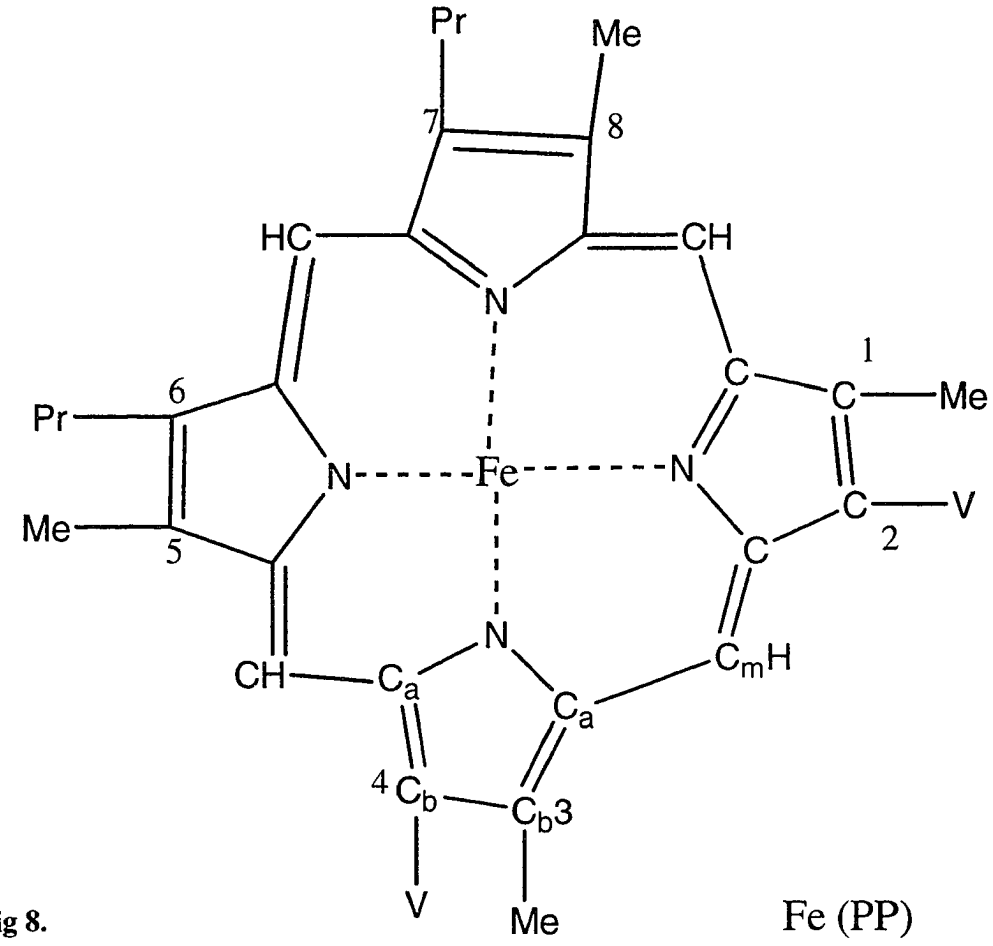

Fig 8. Fe (PP)

Me = Methyl
V = Vinyl
Pr = Propionic acid
PP = Protoporphyrin

Structure of the high spin and low spin iron

Low spin iron :

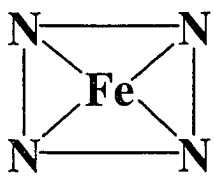

Fig 9.

High spin iron :

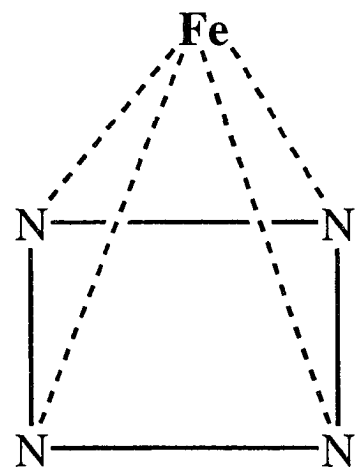

Fig 10.

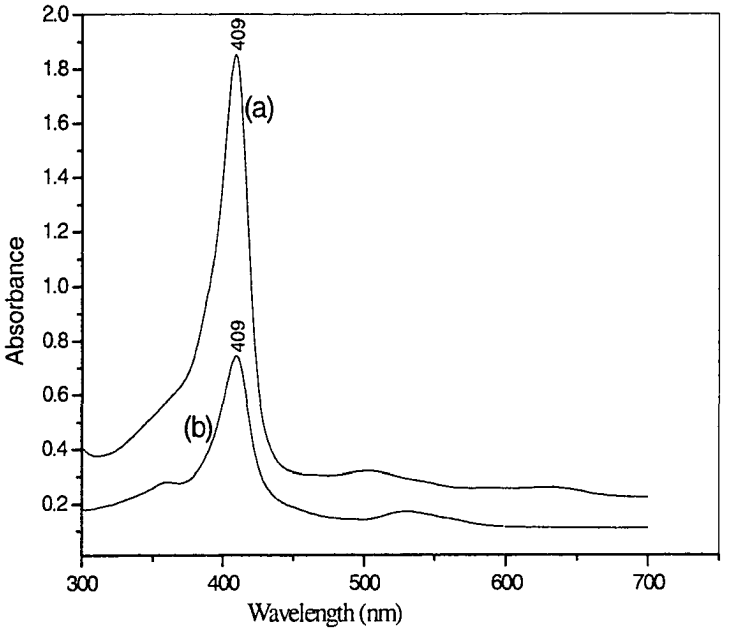

Fig 11. UV -Vis of $1*10^{-6}$ M: (a) Horse skeletal muscle myoglobin and (b) Horse heart Cytochrome C in 0.1M Na_2So_4

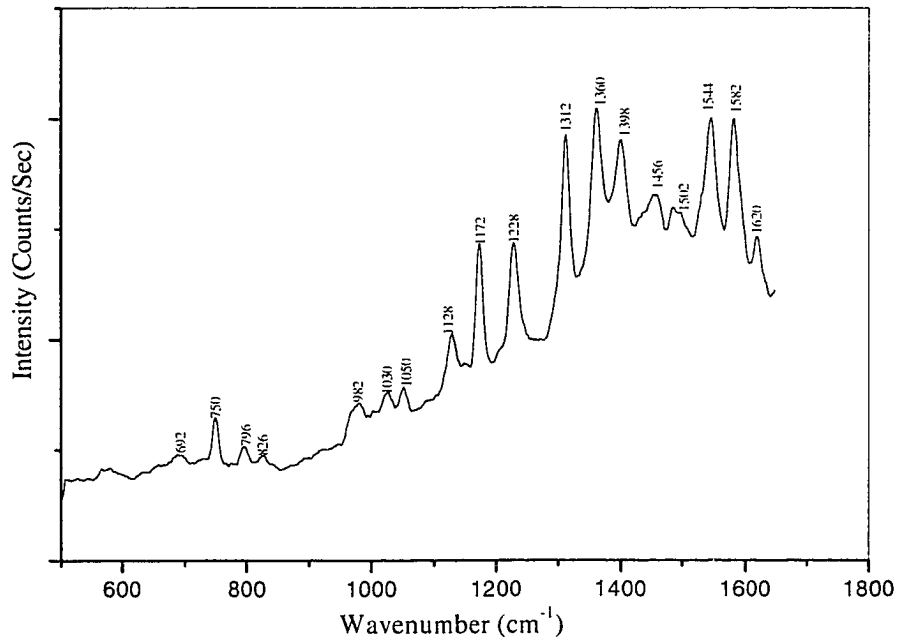

Fig 12 . Resonance Raman (RR) of 0.5mM of Horse Heart Cytochrome C in 0.1 M Na_2So_4 . Sodium dithionite was added to the solution in order to reduce $Fe^{3+}$to Fe^{2+}.

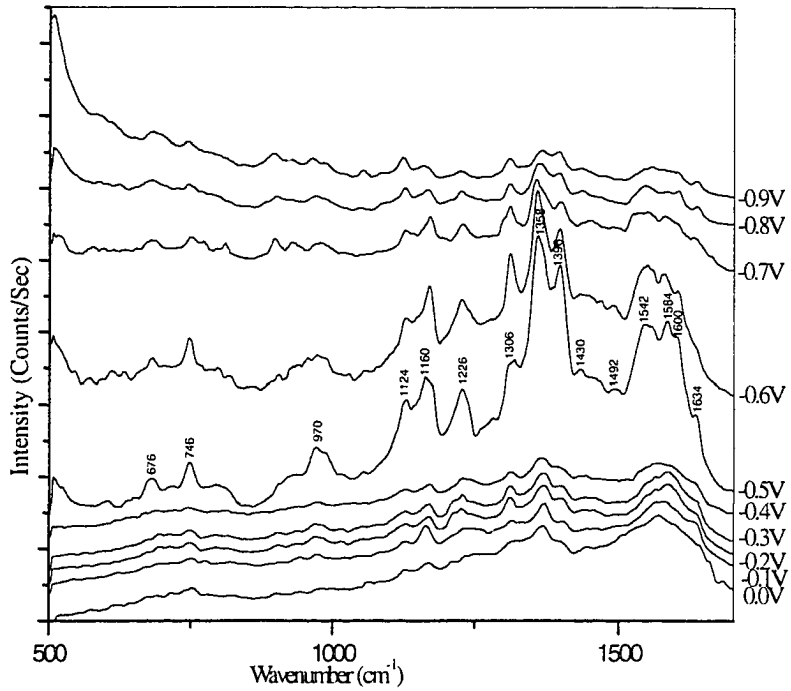

Fig 13. Overlay SERS of 1*10^{-6}M Horse Heart Cytochrome C in 0.1 M Na_2So_4 adsorbed on a silver electrode surface.

Table 11.Vibrational Frequencies of the Surface-Enhanced Raman Spectra of Horse heart Cytochrome C adsorbed on a silver (Ag) electrode surface as a Function of Voltage in the 500 –1700 cm^{-1} region.

-0.1V	-0.2V	-0.3V	-0.4V	-0.5V	-0.6V	-0.7V	- 0.8V	-0.9V	Assignments[a]
				598	606				
694	694		688	680	680	678	680	682	(C_a- C_b-N) bent & (C_a- C_b) SStrch
752	748	748	748	746	746	748	744	742	(C_a- C_a-N) bent & (C_b- Et) SStrch
						808			(C_a- C_m-C_a) bent & (C_a-N) SStrch
						894	898	892	
974	970	970	976	970	972	984	968	924	
				988	988			984	
	1016	1016	1020	1016	1016				
				1054	1056		1048	1054	
1128	1128	1128	1128	1126	1126	1126	1124	1120	(C_a-N) AStretch &(C_b- Et) AStrch
1162	1168	1168	1168	1160	1168	1168	1164	1158	(C_b-E_t) AStretch & (C_a-N) AStrch
		1208							
1234	1226	1226	1230	1226	1226	1228	1224	1222	(C_m-H) Sbent & (Ca-C_b) SStrch
1314	1310	1312	1314	1306	1310	1310	1310	1308	(C_m-H) Abent & (Ca-C_b) AStrch
1370	1368	1368	1362	1358	1356	1354	1360	1366	(C_a-N) SStretch & (C_a-C_m) Sbent
1402	1400	1400	1394	1396	1396	1394	1392	1396	(C_a-N) AStretch &(C_b- Et) AStrch
1446	1438	1438	1442	1432	1432	1446	1434	1430	
		1460			1468				
1494				1492	1490	1484	1498		(C_a-C_m)SStretch & (C_a- C_b) SStrch
	1550					1524			
1566	1560	1548	1534	1546	1548	1548	1546	1556	(C_b-C_b)SStretch & (C_b-E_t) SStrch
1584	1584	1584	1586	1584	1580	1582	1584		(C_a-C_m)AStretch &(C_a-C_b) AStrch
				1600	1600		1602	1600	(C_b-C_b) Stretch & (C_b-E_t) Strch
1634	1628	1636	1634	1632	1634	1634	1636	1636	(C_a-C_m) Stretch &(C_a-C_b) Strch

AStrch = Asymmetrical stretch ; Abent = Asymmetrical bending ; SStretch = Symmetrical stretching ; Sbent = Symmetrical bending ; Assignments[a] = reference 2 .

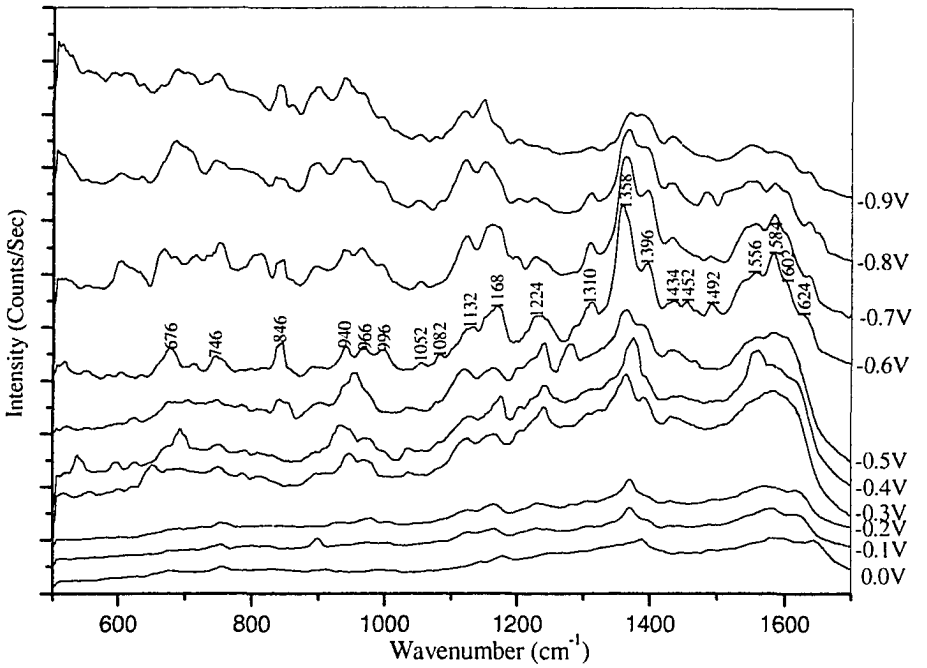

Fig 14 . Overlay SERS of 0.5 mM Horse Skeletal Muscle Myoglobin in 0.1 M Na_2So_4 adsorbed on a silver electrode surface .

Table 12.Vibrational Frequencies of the Surface-Enhanced Raman Spectra of Horse skeletal muscle myoglobin adsorbed on a silver (Ag) electrode surface as a Function of Voltage in the 500 –1700 cm^{-1} region.

-0.1V	-0.2V	-0.3V	-0.4V	-0.5V	-0.6V	-0.7V	- 0.8V	-0.9V	Assignments[a]
		598	600	624		604	602	592	
678	680	652		676	676	668			
			694	704		684	686	688	(C_a- C_b-N) bent & (C_a- C_b) SStrch
						716			
						732			
754	752	750	750	748	746	750	746	748	(C_a- C_a-N) bent & (C_b- Et) SStrch
				842	846	848	836	840	
				854					
898		898		900	892	894	898	898	
		946	934	936	940	936	936	938	
972	978	968	968	958	966	966	960	966	
1004	1006		998		996	994	994	998	
		1036	1036	1032					
			1056		1054	1054	1052	1052	
			1082	1078	1084		1086	1076	
1126	1126	1124	1130	1120	1132	1124	1122	1120	(C_a-N) AStretch &(C_b- Et) AStrch
1166	1164	1164	1174	1166	1168	1166	1152	1148	(C_b-E_t) AStretch & (C_a-N) AStrch
				1202		1196	1204	1202	
1230	1230	1238	1238	1240	1230	1226	1224		(C_m-H) Sbent & (Ca-C_b) SStrch
				1278	1290				
1306	1306	1308	1316		1310	1310	1312	1310	(C_m-H) Abent & (Ca-C_b) AStrch
1370	1370	1364	1374	1364	1358	1362	1366	1370	(C_a-N) SStretch & (C_a-C_m) Sbent
1398	1394	1388	1392	1386	1396	1396	1390	1386	(C_a-N) AStretch &(C_b- Et) AStrch
1430	1430	1432	1436	1428	1436	1432	1434	1432	
				1466	1454				
1490	1490	1486	1488						(C_a-C_m)SStretch & (C_a- C_b) SStrch
						1546			
			1560	1556	1558	1558	1546	1550	(C_b-C_b)SStretch & (C_b-E_t) SStrch
1582	1572		1580	1586	1584	1584	1584	1588	(C_a-C_m)AStretch &(C_a-C_b) AStrch
		1586		1600	1602	1598	1600		(C_b-C_b) Stretch & (C_b-E_t) Strch
1622	1618		1610		1624	1636	1634	1634	(C_a-C_m) Stretch &(C_a-C_b) Strch

AStrch = Asymmetrical stretch ; Abent = Asymmetrical bending ; SStretch = Symmetrical stretching ; Sbent = Symmetrical bending ; Assignments[a] = reference 2 .

Table 13.
Oxidation state and spin state of the iron in the heme chromophore of Horse Heart Cytochrome C as a function of voltage.

Voltage (V)	Oxidation state	Spin state
0.0V	1372 cm^{-1} (s) Fe^{3+}	1632 cm^{-1}
-0.1V	1376 cm^{-1} (s) Fe^{3+}	1624 cm^{-1}
-0.2V	1368 cm^{-1} (s) Fe^{3+}	1628 cm^{-1} L.S
-0.3V	1370 cm^{-1} (s) Fe^{3+}	1632 cm^{-1}
-0.4V	1368 cm^{-1} (s) Fe^{3+}	1618 cm^{-1}
-0.5V	1368 cm^{-1} (S) Fe^{3+}	1602 cm^{-1}
-0.6V	1358 cm^{-1} (S) Fe^{2+}	1602 cm^{-1} L.S
-0.7V	1358 cm^{-1} (S) Fe^{2+}	1600 cm^{-1}
-0.8V	1358 cm^{-1} (S) Fe^{2+}	1604 cm^{-1}
-0.9V	1358 cm^{-1} (S) Fe^{2+}	1578 cm^{-1}

Table 14.
Oxidation state and spin state of the iron in the Heme chromophore of Horse Skeletal Muscle Myoglobin as a function of voltage.

Voltage (V)	Oxidation state	Spin state
0.0V	1370 cm^{-1} (s) Fe^{3+}	1610,1638 cm^{-1}
-0.1V	1370 cm^{-1} (s) Fe^{3+}	1588,1626 cm^{-1}
-0.2V	1370 cm^{-1} (s) Fe^{3+}	1560,1590,1624cm^{-1} H.S
-0.3V	1364 cm^{-1} (s) Fe^{3+}	1584 cm^{-1}
-0.4V	1374 cm^{-1} (s) Fe^{3+}	1560,1608 cm^{-1}
-0.5V	1358,1366 cm^{-1} (S) Fe^{2+}, Fe^{3+}	1554,1582,1604cm^{-1}
-0.6V	1358 cm^{-1} (S) Fe^{2+}	1560,1584,1620cm^{-1}
-0.7V	1362 cm^{-1} (S) Fe^{2+}	1558,1586,1638cm^{-1}
-0.8V	1362 cm^{-1} (S) Fe^{2+}	1546,1586,1632cm^{-1}
-0.9V	1362 cm^{-1} (S) Fe^{2+}	1552,1596,1638cm^{-1}

F. References

[1].Cotton,T. M.; Schultz, S . G.;Van Duyne, R . P. *J . Am . Chem.Soc . 1980, 102,7962 –7965 .*

[2].Spiro,T. G . in "*Biological applications of Raman Spectroscopy " 1988 Volume 3 , by John Wiley & Sons Inc .*

[3].Carey, P.R. in " *Biological applications of Raman and Resonance Raman Spectroscopies " 1982 Academic Press Inc .*

[4].Strekas,T . C.; Spiro,T. G . *Biophys . Biochim .Acta , 1972, 263, 830*

[5].Strekas,T . C.; Spiro,T. G . *Biophys . Biochim .Acta , 1972, 278,188*

[6].Strekas,T . C.; Spiro,T. G . *Proc . Natl .Acad .Sci ., 1972, 69, 2622*

[7].Sunder, S.; Bernstein, H . *J. Raman Spectroscopy ., 1976, 5, 351*

[8].Burke, J . M .; Kincaid, J . R .; Spiro,T . G . *J . Am . Chem . Soc., 1978, 100,6077*

[9].Stein, P.; Ulman, A.; Spiro, T. G. *J . Phys . Chem ., 1984, 88,369-374*

[10].Kitagawa,T.; Abe, M .; Ogoshi, H . *J . Chem . Phys ., 1978, 69, 4516*

[11].Abe, M .; Kitagawa, T.; Kyogoku, Y. *J . Chem. Phys ., 1978, 69 , 4526*

[12].Choi, S .; Spiro, T. G.; Langry, K. C.; Smith, K. M. *J. Am. Chem. Soc.,* 1982, 104,4337

[13].Choi, S.; Lee, J. J.; Wei, Y. W.; Spiro, T. G. *J. Am. Chem. Soc., 1983, 105,3707*

[14].Choi, S.; Spiro, T. G. *J. Am. Chem. Soc., 1983,105, 3683*

[15].Spiro, T. G. in " *Resonance Raman spectroscopic studies of Heme proteins" Biochimica et Biophysica Acta , 1975, 416, 169 –189*

[16].Spiro, T. G.; Strong, J. D.; Stein, P. *J. Am. Chem., 1979,101,2648*

[17].Strong, J. D.; Burke, J. M.; Daly, P.; Wright, P.; Spiro,T.G. *J. Am. Chem. Soc., 1980, 102, 5815*

[18].Teraoka, J.; Kitagawa, T. *J. Phys. Chem., 1980, 24, 1928 –1955*

[20].Kincaid, J.; Stein, P.; Spiro, T. G. *Proc. Natl. Acad. Sci. USA, 1979, 76, 549-4156*

[21].Spiro, T. G.; Burke, J. M.; J. *Am. Chem. Soc., 1976, 98, 5482 –5489*

[22].Babcock, G. T.; Callahan, P. M. *Biochemistry, 1983, 22, 2314*

[23].Choi, S .; Spiro, T. G.; Langry, K. C.; Smith, K. M.; Budd, L. D.; Lamar, G . M. *J. Am. Chem. Soc., 1982, 104,4345*

[24].Wright, P. G.; Stein, P.; Burke, J. M. *J. Am. Chem. Soc.,1979, 101,3531 – 3535*

[25].Spiro, T. G.; Strekas, T. C. *J. Am. Chem. Soc., 1974, 96, 338*

[26].Simpson ,W. T. ; *J. Chem. Phys., 1949, 17, 1218-1221*

[27].Hori, H.; Kitagawa, T. *J. Am. Chem. Soc. 1980, 102, 3608 –3613*

[28].Eaton, S . S.; Eaton, G. R. *J. Am. Chem. Soc., 1975, 97, 3660*

[29].Spiro,T. G .; Strong, J. D.; Stein, P. J. Am. Chem. Soc., 1979, 101, 2648

[30].Brunner, H.; Mayer, A.; Sussner, H. *J. Mol. Biol. 1972, 70,153 –156*

[31].Brunner, H . *Biochem . Biophys . Res . Commun . 1973, 51 , 888-894*

[32].Brunner, H.; Sussner, H. *Biochim . Biophys. Acta 1973,310, 20-31*

[33].Strekas, T. C.; Spiro, T. G. *J. Raman Spectroscopy 1973, 1 , 197-206*

[34].Strekas, T. C.; Spiro, T. G. *J. Raman Spectroscopy 1973, 1 , 387-392*

[35].Pezolet, M.; Nafie, L. A.; Peticolas, W. J. J. Raman Spectroscopy 1973, 1, 455-556

[36].Nestor, J.; Spiro, T. G. *J. Raman Spectroscopy 1973, 1, 539 –550*

[37].Friedman, J. M.; Hochstrasser, R. M. *Chem. Phys. 1973, 1, 457*

[38].Strekas, T. C.; Spiro, T. G. *J . Biochim . Biophys . Acta 1974, 351, 237-245*

[39].Adar, F.; Erecinska, M. *Arch. Biochem. Biophys. 1974, 165, 570*

[40].Behringer, J. in " *Raman Spectroscopy (Szymanski , H . A., ed.) " Vol . 1, Chap 1, Plenum Press, New York*

[41a].Spiro,T .G . *Acts . Chem . Res . 1974, 1, 339-344*

[41b].Spiro, T .G. in *Chemical and Biochemical Applications of Lasers (Moore C.B., ed.) Chap. 2, Academic Press New York*

[42].Tang, J.; Albretch, A. C. in " *Raman Spectroscopy (Szymanski, H. A., ed .) Vol. 2, Chap 2, Plenum Press, New York*

[43].Peticolas, W. L.; Nafie, L.; Stein, B.; Franconi, B.; J. *Chem. Phys. 1970, 52,_1576-1584*

[44].Albretch, A. C. *J. Chem. Phys. 1961, 34, 1476-1484*

[45].Albretch, A. C.; Hutley, M. C. *J. Chem. Phys. 1971, 55, 4438*

Chapter 4

SERS of Surfactants in Monolayer and Multibilayer forms on an Electrified Ag Surface.

A. Abstract

The Raman spectra of several surfactants such as didodecyldimethylammonium bromide (DDAB), cetyltrimethylammonium bromide (CTAB), dimyristoylphosphatidylcholine (DMPC), cetylpyridinium chloride (CPC), dihexadecyl phosphate (DHP) and sodium laurate (NaLs) have been investigated in the solid, multilayer, micellar and multibilayer forms. The first four are cationic surfactants while DHP and NaL are anionic. Raman spectra show that they all exist in an all-trans configuration in the crystalline state while their structure in the multilayer, micellar and multibilayer (film) forms is a mixture of gauche and trans configuration. Previously, we studied[4] the SERS of CTAB on a silver electrode surface in the monolayer form with a variety of other surfactants and it was shown that these surfactants have a head-on orientation at potentials positive to the point of zero charge (pzc). SERS of all the above surfactants (with the exception of CPC) support the claim that these surfactants show an unexpected enhancement for C-H stretching modes at potentials more negative than – 0.8 V vs. SCE and the appearance of two new SERS vibration bands at 2710 and 2815 cm^{-1} in the stretching region. However, in the multibilayer film, the SERS spectra of some of these surfactants (DDAB, CTAB, DMPC) are dominated by two intense bands located in the 1130 cm^{-1} and 1530 cm^{-1} region. The first band (1130 cm^{-1}) corresponds to the all–trans alkyl structure which is common in the Raman spectra of all these surfactants while the 1530 cm^{-1} band

is a totally new band and we associate it with the orientation of the quaternary nitrogen coupled with methyl groups adsorbed on the silver surface.

B. Introduction

Surfactant molecules having a single or double chain aliphatic "tail" and an ionic, zwitterionic, or neutral "head" group have been shown to form ordered monolayers and bilayers membranes in solution and on surfaces[1]. The bilayer films when cast on metal and carbon electrodes can be used in an electrochemical environment[2] and also have applications in chemical sensor technology[3] and as a medium for electrochemical catalysis[4] . Furthermore, these bilayer membranes serve as models for biochemical membranes . Indeed, the study of surfactants adsorbed on a metal surface can provide insights in related fields such as adhesion, lubrication, detergency, and corrosion inhibition. Recently, it has been shown that a surface film of multibilayers forming molecules can enhance electron transfer rates a thousand fold for heme proteins (Myoglobin-DDAB) on a pyrolytic graphite electrode[4]. At concentrations above the critical micelle concentration, cmc, surfactants self aggregate to form micelles which have been shown by AFM to adsorb on positively charged Au(III) surfaces to form hemi-cylindrical monolayer[5] and bilayers[6] . Our previous surface enhanced Raman scattering (SERS) study of surfactants formed by adsorption from solution on Ag showed that the spectral bands are all depolarized indicating that the spectra originate from a monolayer or at most a bilayer at the electrode surface[7]. In the present work, we extend the study of

surface Raman spectra of surfactants on silver electrodes to include cast bilayer films that have been used to enhance the reversibility of electron transfer between proteins and metal surfaces.

In addition to the cationic surfactants , cetyltrimethylammonium bromide (CTAB) and cetylpyridinium chloride (CPC) , that we previously studied as a function of voltage on a silver electrode surface, we include in our present SERS studies the double-chain cationic surfactants didodecyldimethylammonium bromide (DDAB) and the zwitterionic dimyristoylphosphatidylcholine (DMPC) in addition to the anionic surfactants dihexadecyl phosphate (DHP) and sodium laurate (NaL). The structures of these molecules are given in Fig 15. Both surfactant films formed by adsorption from solution on Ag during the roughening procedure and cast multibilayers films of these surfactants have been studied under electrode potential control. Most studies of cast surfactant thin layers on electrode surfaces have been made on metals like copper and gold that form quite stable monolayers or multilayers upon adsorption. These surfactants adhere less strongly to a silver metal surface, and as a result there exists fewer studies of the multibilayer films on a silver electrode surface , an exception being the exsitu SERS study of Suga, Bradley, and Rusling[8]. However, Ag gives the highest surface enhanced Raman signals and allows a wide range in the negative voltage region (potentials negative to SCE reference voltage) for insitu studies. Thus in this paper, we use SERS from Ag electrodes as a probe to study the Raman spectra of surfactant film structures either adsorbed from solution or in cast films, a multibilayer form. We have also

compared some of the SERS spectra with their normal Raman counter parts in the solid and micellar forms.

We have found that their structure varies from the all-trans configuration in the solid to a mixture of gauche and trans configuration in the monolayer, multibilayer film as-well-as in the micellar form. The nature of the surfactant film on the metal surface was studied by performing depolarization measurements which show that all bands of surface spectra are depolarized as in the typical SERS spectrum. Each of the surfactants examined in this paper (cationic and anionic), with CPC as an exception, forms an interfacial structure whose spectra increase dramatically at potentials negative to –1.3 V vs. the SCE on the Ag electrode as we have previously observed[7]. This increase in SERS intensity occurs in a potential region where the current-voltage curves show that the overpotential of hydrogen reduction process has been shifted to the more negative potentials . The reasons for these results are interpreted in terms of structural changes in the surfactant layer.

C. Experimental Section

Didodecyldimethylammonium bromide, DDAB,[$((CH_3\text{-}(CH_2)_{11})_2\text{-}N^+(CH_3)_2Br^-)$]; cetyltrimethylammonium bromide , CTAB , [$CH_3\text{–}(CH_2)_{15}\text{ –}N^+(CH_3)_3\ Br^-$]; dimirystoylphosphatidyl choline , (DMPC) , [$(CH_3)_3N^+(CH_2)_2OPO_3\text{-}CH_2\text{-}CH\text{-}CH_2(COO)_2\text{-}((CH_2)_{12}\text{-}CH_3)_2$]; cetylpyridinium chloride , CPC , [$CH_3\text{–}(CH_2)_{15}\text{ -}N^+C_5H_5Cl^-$] ; dihexadecyl phosphate , DHP,[$(CH_3\text{ -}CH_2)_{15})_2\text{-}PO^{4\ -}$] and sodium laurate, NaL ,[$CH_3\text{-}(CH_2)_{10}\text{-}COO^-\ Na^+$] were reagent grade (Fisher Scientific)

and were used without further purification. The electrolyte solution (KCl) was prepared with deionized-distilled water at 0.1 M concentration. Stock solutions of CTAB and NaL were prepared at a 10 mM concentration in 0.1 M potassium chloride (KCl) while DDAB, DHP and DMPC were prepared at a 0.1 mM concentration in the same electrolyte solution (0.1 M KCl). The electrochemical cell for SERS was composed of a silver working electrode (99.999%), a saturated calomel electrode (SCE reference) and a platinum counter electrode. All electrode potentials are cited versus the SCE with the exception of the cyclic voltammetry results where an Ag working electrode was used with a Ag/AgCl/KCl reference. For the surfactant film formed by adsorption from solution during an oxidation-reduction cycle, ORC, the working electrode was pretreated with a potential step to +0.3V for approximately 1 second with the surfactant in the electrochemical cell (insitu pretreatment). The potential steps applied for the ORC pretreatment were from – 0.2 V to + 0.3 V and then back to – 0.3 V. The roughened Ag electrode with adsorbed surfactant was then placed at the open circuit potential and the surfactant solution washed out of the electrochemical Raman cell and replaced with electrolyte solution (0.1 M KCl). All subsequent SERS measurements where made under potentiostatic control of the Ag working electrode.

The cast film was prepared in each case by making a 0.1 M of each surfactant in a volatile solvent (chloroform) and sonicated in order to assure complete solvation. A specific volume of about 13 µl or 1.3 µmol was spread onto a previously roughened silver electrode surface (roughened in 0.1 M KCl from –

0.6 V ~ + 0.3 V for 10 seconds and then back to – 0.6 V) and put into a glass chamber and left overnight for complete evaporation of the solvent. The next day, the coated electrode was placed into an electrochemical cell containing a 0.1 M degassed KCl solution, and its SERS spectrum was taken at different voltages. In each case, the geometric surface area of the electrode was approximately 10.8 mm^2 with a 1.7 roughness factor which should allow an approximate estimation of the film thickness and the number of surfactant molecules on surface, e.g., for DDAB this gives a film thickness from 3.5 –7 μm. An argon laser (Ar^+) was used (488 nm line from Spectra-Physics Model 2020) and the SERS spectra of the molecules were obtained with a Spex Model 1401 Double Monochromator with a PM tube and photon counting detection. Typically the laser was operated to give about 200 mW (for pure solids and for SERS) and about 700 mW for the micelle. The spectra were run with either 160-μm-or 100-μm-slit widths giving a resolution of 4 to 2 cm^{-1}, respectively. All spectra were recorded at ambient temperature (25°C) and all electrolytes and additives used were of reagent grade. A thorough description of the electrochemical measurements used in this experiment can also be found elsewhere[9]. All potentials are referenced to the saturated calomel electrode (SCE). A polarizer was placed in the path of a scattered light that was polarized parallel or perpendicular to the scattering plane i.e. p or s polarized. The depolarization ratio defined as $\rho = I_\perp/I_{||}$ where $I_\perp$ and $I_{||}$ are the intensities of the Raman radiation of a given frequency that is polarized, respectively, perpendicular and parallel to the plane normal to the incident beam.

D. Results and Discussion

i) Comparison of the Raman Spectroscopy of Surfactants in the Crystalline (Solid Powder), Micellar, Solution Adsorbed , and cast Multibilayer Film Forms.

The Raman spectra of DDAB, CTAB, DHP, DMPC, NaL and CPC in the crystalline (powder) state are shown in figure 16. All of them indicate the existence of an all-trans extended chain structure. The 1050 – 1150 cm^{-1} and the 2800-3000 cm^{-1} regions of the Raman spectra of surfactants are dominated by skeletal vibrations of the C – C stretching modes and C – H vibrations, which are both sensitive to the conformation of the hydrocarbon chain. Table 19 gives the observed bands and their assignments. The assignments of bands in the 2800 - 3000 cm^{-1} are well established and have been used as a probe for lateral chain-chain interaction and conformational disorder[10]. It is seen in all of the spectra of the powders that the asymmetric C-H methylene stretching vibration (d^-) near 2880 cm^{-1} dominates the symmetric C-H (d^+)stretching vibration near 2850 cm^{-1} which is an indication of highly ordered hydrocarbon chains[10b]. Additional information on the confirmation of the hydrocarbon chains can be obtained from the C-C stretching vibrations. For example, the normal Raman spectra of DDAB and CTAB in the crystalline form has three bands located around 1070, 1082 and 1121 cm^{-1} and they have been assigned to the C – C symmetric and antisymmetric stretching modes with CH_2 wag. The 1070 and 1121 cm^{-1} bands represent the trans (T) conformation while the band at around 1082 cm^{-1} has been used to represent the the presence of gauche (G) conformations. In the Raman spectra of the surfactants in the powder form, the bands for the trans configuration dominate.

Figure 17 shows the normal Raman spectra for aqueous solutions of 0.1 M DDAB and 0.1375 M CTAB which are in the micellar form since at these concentrations both surfactants aggregate to from " spherical" micelles. In the micellar form the normal Raman spectra for both surfactants in Figure 17 shows a relatively high intensity for the 1082 cm^{-1} band and low intensities for the 1065 and 1121 cm^{-1} bands. The new intense band at 1082 cm^{-1} is an indication that in the micellar form the hydrocarbon core remains " fluid" kinked with several gauche isomers present. The more liquid like nature of the hydrocarbon core also is illustrated by the ratio of the 2846 cm^{-1} to 2886 cm^{-1} bands where now the symmetric C-H stretch at 2846 cm^{-1} dominates the asymmetric C-H stretch at 2886 cm^{-1} . Table 20 gives the complete set of Raman frequencies with assignments for the bands observed for CTAB and DDAB.

The SERS spectra of CTAB, DDAB, DHP, DMPC, NaL and CPC adsorbed from solution on a silver electrode surface during the ORC is shown in Figures 18, 19, 20, 21, 22, and 23 in the 2600-3100 cm^{-1} region as a function of voltage where the spectra are particularly intense. The band around 2846 cm^{-1} in the C – H stretching region is more intense than the 2884 cm^{-1} band in all of these spectra. The ratio of these bands is similar to those observed in the single-walled bilayer vesicles [10b], in micelles[11] and in cast bilayers[8] which has been interpreted as indicating a liquid like hydrocarbon chain region. As previously mentioned, a reversed situation is observed in the solid or crystalline state of these surfactants where the highly ordered hydrocarbon chains give a very sharp band at 2884 cm^{-1} which is about three times as intense as the band at 2846 cm^{-1} However, on

a hydrocarbon phase transition from solid to liquid, the sharp band at 2884 cm^{-1} loses intensity, broadens, and shifts upwards by 4-5 cm^{-1} [10d,12]. Thus, we can conclude from the SERS spectra of the surfactants presented in figures 18 through 23 where in the -.1 V to –0.7 V region the 2884 cm^{-1} band is less or equal in intensity to the 2846 cm^{-1} band that the adsorbed film on a silver electrode surface has a fluid like hydrocarbon region. Although the relative intensities of the bands around 2846 and 2884 cm^{-1} can be used to investigate the overall disorder in the hydrocarbon region of the surface film , conclusions involving the amount of conformational disorder due to a distribution of trans and gauche isomers and disorder due to lateral packing of extended tail groups of the hydrocarbon chain cannot be made by taking the ratio of the intensities of the 2884 – 2846 cm^{-1} bands[10b,10 d].

Unfortunately, the nature of many of the bands in the C-H region of the Raman spectrum of surfactants are difficult to determine because of Fermi resonance interactions between the C-H stretching fundamental modes and overtones of the HCH scissors modes giving rise to some ambiguity in assignments especially in the band around 2930 cm^{-1} [10a]. The SERS spectra in Figures 4-9 in the potential range –0.1V to –0.7V all show a broad band around 2920 -2930 cm^{-1} which has been assigned by Snyder et al. [10a] to a combination of Fermi resonances with the symmetric C-H modes of methylene and terminal methyl groups. In the solid and micelles the ratio I_{2850}/I_{2930} is significantly large than one as seen in Figure 16 and Figure 17 but in the SERS spectra (Figures 18-23) in the potential range –0.1V to –0.7V it is less than one. According to Snyder et

al.[10a], this indicates considerable conformational disorder in the hydrocarbon chains.

As the electrode potential is moved passed –0.8 V , the entire spectrum in the CH stretching region grows in intensity and new bands become observable at about 2710 and 2814 cm^{-1} for all surfactants except cetylpyridinium chloride, CPC. An interpretation of this phenomenon is discussed in a later section.

ii) Depolarization Studies to Distinguish the Surface-Specific nature of the Spectra.

Establishing the difference between Raman spectrum of various surfactant structures on Ag electrodes from the surfactant in the solution phase is crucial when one is trying to know the exact nature of spectra from surface films. To this end , a depolarization ratio (ρ_n) study of the Raman scattering can help differentiate between surface- enhanced Raman scattering and normal Raman scattering from the solution phase. The normal Raman spectrum of molecules in solution when an average is taken over molecular orientations gives $\rho_n = 0.75$ for non- totally symmetric modes while $0 \leq \rho_n < 0.75$ for totally-symmetric modes[13]. However, ρ_n is often very close to zero for totally-symmetric modes, i.e., they are polarized. Many SERS studies have shown that spectral bands for both totally symmetric and non-totally-symmetrical modes are depolarized. Thus vibrational bands in SERS of totally-symmetric modes from adsorbed molecules all have ρ_n values that are much larger than for the same bands in solution. This has been interpreted as due to a two dimensional averaging of molecular orientations of surface adsorbed species[14].

Tables 15-18 show depolarization ratios for DDAB, CTAB, DMPC, DHP, NaL, and CPC from normal Raman scattering, NRS, in solution and from surface Raman at different conditions. If we compare depolarization ratios of the totally-symmetric C-H stretching vibration at 2850 cm^{-1} of the micellar form of the surfactants in solution in Table 15 with the depolarization ratio of the surfactants on a silver electrode surface, Tables 16-18, we find that they are all nearly twice as large in the surface Raman spectra. We take this to indicate that in both the cast multibilayers films (Table 16) and in the solution adsorbed films (Table 17 & 18), the spectra are SERS spectra originating from the surface film. For the NRS spectra of the micelles presented in Table 15, both of totally - symmetric C – H stretching modes at around 2850 and 2920 cm^{-1} have a relatively very low depolarization ratio (i.e. close to zero) for all the surfactants, e.g., DDAB shows a depolarization ratio of 0.18 and 0.17 for these bands, respectively. On the other hand, the spectra of DDAB for these bands taken at –0.7 V and –1.3 V show depolarization ratio between 0.3 and 0.6 V (see Table 16). A further comparison of the values obtained in Table 15 with those in Tables 16-18 confirm that the Raman spectra originating from the electrode surface are the result of a Raman process from molecules adsorbed at the metal surface.

We found that the surfactants DDAB, CTAB, DMPC can form stable multibilayer films when dissolved in a volatile organic solvent like chloroform and cast on a silver electrode surface. The depolarization ratios of the surfactants which can form the cast mulitibilayer film on activated Ag are given in Table 16. Rusling and coworkers[8] have studied SERS from DDAB

multibilayers films on dry and wet silver island surfaces. However, to our knowledge, no one has studied these cast films of surfactants in the multibilayer film for a metal surface under electrode potential control. Table 16 shows a depolarization study of the multibilayer films for DDAB, CTAB and DMPC at – 0.4 and – 0.6 V. The depolarization ratios in the multibilayers film (Table 16) can be compared with their normal Raman for micelles in Table 15 and the SERS of the solution adsorbed species in Table 17. This comparison of the data shows that the depolarization ratios on the surface are substantially higher than in solution indicating that the surface Raman spectra for DDAB, CTAB and DMPC in the multibilayer film at the Ag electrode surface are depolarized and have characteristics similar to the SERS bands of molecules adsorbed from solution during a typical SERS pretreatment. This is good evidence that the multibilayers films are oriented with respect to the silver surface.

iii) *Potential Dependence of Surfactants Adsorbed on the Silver Electrode Surface.*

The potential dependence of a variety of surfactants has been investigated using Surface – Enhanced Raman spectroscopy. At a specific voltage, molecules studied on a silver electrode surface can take different orientation and this is due partly to the nature (i.e. positive or negative) of the charges that predominates at a particular potential on the electrode surface. Table 17 shows that even the anionic surfactants NaL and DHP show depolarized bands for totally symmetric modes. The fact that these surfactants give SERS spectra indicates that the anionic species are adsorbed from solution during an ORC with their head

groups at the surface interacting with positive Ag adion sites created during the ORC at the more positive potentials. On the other hand, for the cationic surfactants, halide counter ions are adsorbed on the Ag adion sites which then attract the positive surfactant head group. As the potential is moved past the point of zero charge (pzc), about –0.7 V on Ag, the halide ions are repelled from the surface and then the cationic head groups are thought to be directly adsorbed at the negatively charged surface. However, the head groups of the anionic surfactants, DHP and NaL, should be repelled from the surface but the SERS spectra show that the surfactant film is still at the surface (Figures 19 and 22) indicating that the head groups must be distant from the negatively charged surface.

In Figures18 thru 23, the SERS spectra as a function of voltage for DMPC, DHP, CPC, CTAB, NaL, and DDAB show two spectral regions in the 2600 – 3000 cm^{-1} range which behave differently as the voltage is varied for all of the surfactants studied with the exception of CPC. In the potential range from – 0.1 V to –0.7, the spectra are dominated by CH stretching modes from 2840 to 3000 cm^{-1}. As the potential is moved to values more negative than –0.8V, the spectral bands at ca. 2710 cm^{-1} and ca. 2814 cm^{-1} grow in as-well-as an increase in intensity of the 2840 cm^{-1} and 2904 cm^{-1} bands until they all reach a maximum around –1.4 V. At –1.4 V, the intensity of the C –H stretching vibrations is much higher (about 2-20 times) than that at –0.6 V and this fact is an indication of an additional enhancement at a very negative potentials. The same phenomenon was observed by Sun et al[7] for CTAB and Brij-35. With the exception of CPC, similar results

have been obtained for other surfactants having a long hydrocarbon chain in their structure.

This type of unusual enhancement at a very negative voltage can be explained by considering the following factors. The 2720 cm^{-1} is observed in the powder Raman spectra in Figure 1 and its appearance at the negative potentials seems to indicate that the surface film has certain features similar to the solid. In fact, electrocapillary studies on an Hg electrode of CTAB and MTAB, myristyltrimethylammonium bromide, show that at potentials negative to the pzc, the surface films become very rigid with very low compressibility[15]. Furthermore, the SERS spectra for MTAB as a function of potential show the exact same phenomenon in the 2600 – 3000 cm^{-1} range as we've observed in Figures 18, 19, and 21-23. The films that form at these negative voltages show vibrational bands for gauche bonds, and thus appears to have liquid crystalline properties. This film is also a protective layer against hydrogen evolution on the roughened Ag surface and shifts the current–voltage (I/V) curve (not shown) for reduction of hydrogen ion to molecular hydrogen about 250 mV negative to the I/V curve in the absence of the surfactants .

At a potential beyond –0.9 V, the intensities of the tail group of most of the surfactants have an identical spectrum in the CH stretching region at the very negative potentials. We reason that the large enhancement in this region of the spectrum could be due to a change in the adsorption geometry, i. e, orientation, which would favor vibrations enhanced by the electromagnetic (EM) surface enhancement effect. The selection rules for this effect have been discussed by

Creighton[16] and Moskovits and Suh[17]. More recently Bryant and Pemberton[18] discussed this effect for the SERS of 1-alkanethiol SAMs absorbed at Ag, and they point out that the C-H stretching vibrations for long chain alkane groups would have a larger polarizibility tensor component along the axis of the vibration and that for most orientations of surface adsorbed species, the C-H stretching modes will have a component perpendicular to the surface. For small spheroid models of the roughened SERS active Ag surface[19] , the highest electric field of the surface enhanced exciting light is directed perpendicular to the spheroid surface (i.e., to the electrode surface) and decays with distance from the surface. Thus if as the potential is made more negative the tail region of the surfactants move closer to the surface and more stretching modes are oriented perpendicular to the surface (aligned with the enhanced EM field) , the Raman intensity in the entire C-H stretching region as-well-as new bands should grow as is observed experimentally. The new feature in the SERS spectra obtained at negative potential in the C-H stretching region is the band around 2816 cm^{-1} . We find that this band can be assigned by *ab initio* frequency calculations to C-H vibrations in the gauche bond region of the tail which would be more enhanced as the surfactant molecule tilts more parallel to the Ag surface.

The *ab initio* Hartree –Fock vacuum frequency calculations with Raman activity were done using Gaussian 98 for CTAB in two configurations, one with all-trans bonds and one with three gauche bonds between carbon number 7 and 12 , where the terminal methyl is carbon 1. The frequency calculation followed a full geometry optimization both with the 6-311G basis set and the default convergence

criteria of Gaussian 98. After scaling the calculated frequencies by the usual 0.900 factor, we found C-H vibrational modes showing significant Raman activity at 2816 (94) and 2822 (82) cm^{-1} for the gauche configuration molecule and at 2823 (23) and 2824 (97) cm^{-1} for the molecule with all-trans configuration, the values in parentheses indicating the Raman activity. For the gauche configuration, the 2816 cm^{-1} vibration is an asymmetrical C-H stretching mode in the gauche bond region and the 2822 cm^{-1} vibration is a C-H stretching mode for the trans methylene groups extending from the terminal methyl to the first gauche bond. In the all-trans configuration, the above modes are for the C-H stretching vibrations along the entire chain including the terminal methyl group . These latter modes would have their largest polarizability component perpendicular to the electrode surface if the molecules is aligned parallel to the surface.

For comparison, some of the other characteristic calculated vibrations with high Raman activity are found for the gauche configuration at 1479 (36), 2842 (231) , 2850 (347), 2895 (97) , 2905 (326) , and 2988 (114) cm^{-1} with the corresponding modes for the all-trans configuration at 1483 (157) , 2830(235) , 2846 (245), 2894 (101), 2905 (328), 3001(137) cm^{-1}. These C-H vibrations correspond respectively to CH_2 scissor bending, an asymmetrical C-H stretching mode in the chain, a symmetrical C-H stretching mode in the chain, an asymmetrical C-H stretching mode in the terminal $-CH_2-CH_3$ group, and symmetrical and asymmetrical C-H stretching modes for the methyl groups in the CTAB head group. A number of other modes from C-H stretching vibrations in the polar head group are in 2979 to 3006 cm^{-1} range . For all of modes except the one at 2905 cm^{-1}, these calculated

frequencies and assignments agree well with experimental results and assignments for CTAB micelles[11] and for intercalated CTAB[20] which is noteworthy since the model does not take into account the counter ions and the water molecules at the head group nor lateral interactions of molecules. The calculated mode at 2905 cm^{-1} which is the strongest Raman mode in the whole frequencies calculation is for the symmetrical C-H stretch in the N^{+}-CH_3 head group. Raman assignments in the literature[11,20] place this mode at higher frequency 2960-3021 cm^{-1} which may be the effect of the water and counter ion on this frequency. All other calculated bands for the CH vibrations in the alkane chain are reasonable. The band we observe to grow at 2905 cm^{-1} most likely is the C-H stretching mode for the terminal -CH_2-CH_3 group calculated at 2895 cm^{-1}. Thus, it is seen in the figures that for all the surfactants studied, the bands near 2814, 2840, and 2905 cm^{-1} all grow in intensity at negative potential with the exception of cetylpyridinium chloride (CPC). We have observed this phenomenon now for surfactants with cationic, anionic, and zwiterionic head groups at roughened Ag electrodes. Only for CPC does the SERS spectrum disappears at potentials more negative than –1.0V. Our interpretation of these spectral results is that beginning at –0.8V there is a reorientation of the surfactant at the surface so that the head group is moved away from the surface relative to the tail group and the molecules are tilted mainly parallel to the surface so that C-H bonds directed perpendicular to the surface with a corresponding perpendicular directed polarizibility tensor component are surface enhanced. Apparently CPC can not reorient at the Ag surface and does not show this phenomenon which

amounts to a phase change. Cetylpyridiniumchloride shows a large SERS enhancement with maximum intensity around –0.8 , Figure 20. The strongest band in its SERS spectrum is at 3076 cm^{-1} which is the well known in-plane C-H stretching vibration in the pyridinium ring. This band is surface enhanced if the pyridinium ring is oriented perpendicular to the Ag surface where the positively charged nitrogen interacts with specifically adsorbed bromide[21]. For such an orientation with the pyridinium group edge on to the surface, an adsorption geometry has been suggested[22] with the first two methylene groups out from the N-alkyl directed parallel to the surface and the rest of the alkane chain perpendicular to the surface. It appears that from this adsorption geometry, the CPB molecules can not reorient to form a new tightly packed film as in the other cases studied.

iv) The SERS of DDAB, CTAB and DMPC in the Multibilayer film adsorbed on a Silver Electrode surface. The appearance of a new band around 1530 cm^{-1}.

Another feature of surfactants films that requires comment is the ability of some to form stable multibilayer films when cast on a metal surface. Observations of sharp phase transitions suggested that such films have ordered bilayer structures[1].Despite many studies on these amphiphile molecules, their structure in multibilayer films at electrode surfaces and orientation toward the metal surface have not definitely been determined. Electrochemical studies of casts of surfactant films have been carried out previously by Rusling et al[2] on silver island film on glass but not on Ag metal surface and not under potential control. Evaporation of the water from the cast films they prepared took place in

the air while in our case we put the coated electrode in a glass chamber overnight for a hopefully better film preparation.

The SERS spectra of DDAB, CTAB and DMPC in the multibilayer film are mostly dominated by two intense bands in the 1000-1550 cm^{-1} region and four bands in the 2800-3000 cm^{-1} region and this is clearly demonstrated in figures 25, 26, and 27 which show the SERS spectra of these surfactants as a function of voltage. The asymmetric C-C stretch + wag mode at 1130 cm^{-1} is still observed in the multibilayer film and it is one of the most intense bands probably due to the fact that in the film C – C stretching modes are well-ordered as a stack of bilayers arranged on the top of each other pointing away from the metal surface. In the SERS spectra of the multibilayers structure for these surfactants, the well known modes ca. 1300 cm^{-1} and 1440 cm^{-1} corresponding to CH_2 twisting and scissors bending modes are only weakly observed but a mode at 1530 cm^{-1} dominates the spectra. In the case of DMPC (Fig. 26) the Raman spectrum of the phosphatidylcholine molecule is seen in the 500 to 2000 cm^{-1} region but here also the 1100 cm^{-1} and 1530 cm^{-1} bands still dominant the spectrum.

In addition, in the multibilayer films, the 2884 cm^{-1} band is even lower in intensity than the 2846 cm^{-1} and once again, we can conclude that several gauche isomers are present in the structure of these surfactants in the multibilayer film. It is not surprising since water molecules and counter anions must penetrate the film and influence the structure and orientation of the surfactant molecules within the film. The appearance of the mode around 1530 cm^{-1} in the multibilayer film of surfactants is a new phenomenon. A possible assignment for

this band is the bending mode in the methyl groups attached to the nitrogen head group, which would have a head - on orientation toward the metal surface. In fact, the highest frequency band with Raman activity before the C-H stretching region is found in the ab initio calculations with this assignment. The HF/6-311G calculation shows scaled bands at 1486 (51) cm^{-1} and 1485 (36) cm^{-1} for trans and gauche configurations, respectively. Similar to the C-H stretching vibrations attached the nitrogen this frequency could be up-shifted by the same ca. 50 cm^{-1} which gives a band around 1535 cm^{-1}. Other effects may contribute to the appearance of that band and additional research is currently under way in our laboratory to detect if there is any other factors, which give, rise to the 1530 cm^{-1} band observed in the SERS of multibilayer film of surfactants.

E. Conclusion

Raman spectroscopy was used to elucidate the structure and orientation of surfactants in the solid, micellar, multilayer and multibilayer form. Results collected from experiments suggest that these surfactants exist as an all-trans configuration in the crystalline (solid) state while their structure is a mixture of trans and gauche configuration in the micellar, multilayer and multibilayer form. A head-on orientation toward the metal surface with their hydrocarbon tail pointing away from the surface is most likely. In the multibilayer film, the arrangement of molecules within the film is totally different from the multilayer since molecules that make up the multibilayer are arranged into stack of bilayer film. As a result, arrangement of the surfactants molecules combined with

orientation and interaction with the metal surface and among themselves can contribute to the new band that we have experienced around 1530 cm^{-1} when the multibilayer of surfactants are adsorbed on a silver metal surface.

The Structures of some Surfactants (DDAB, CTAB, DMPC, CPC, DHP, and NaL in the solid crystalline state.

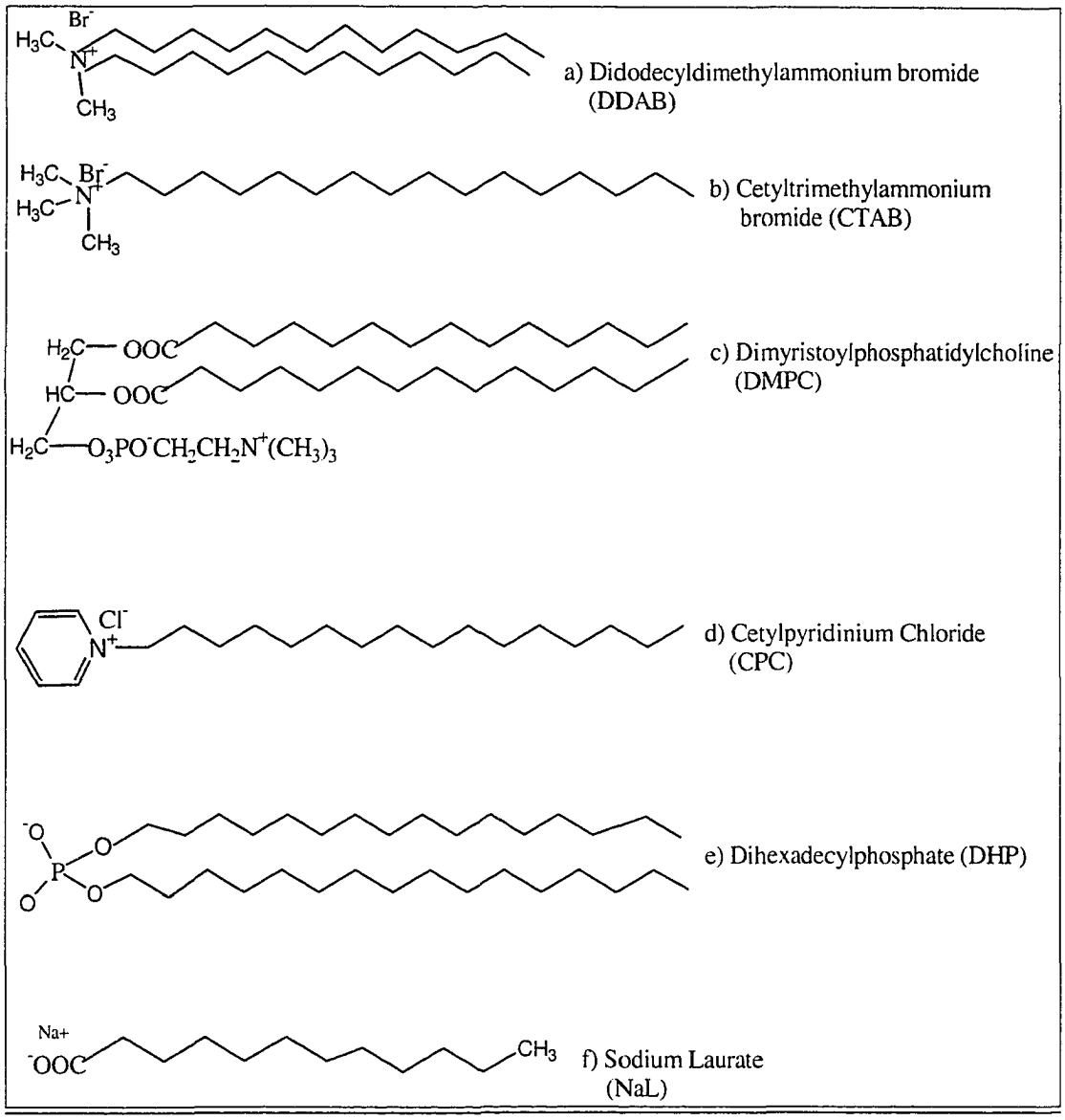

Fig 15.

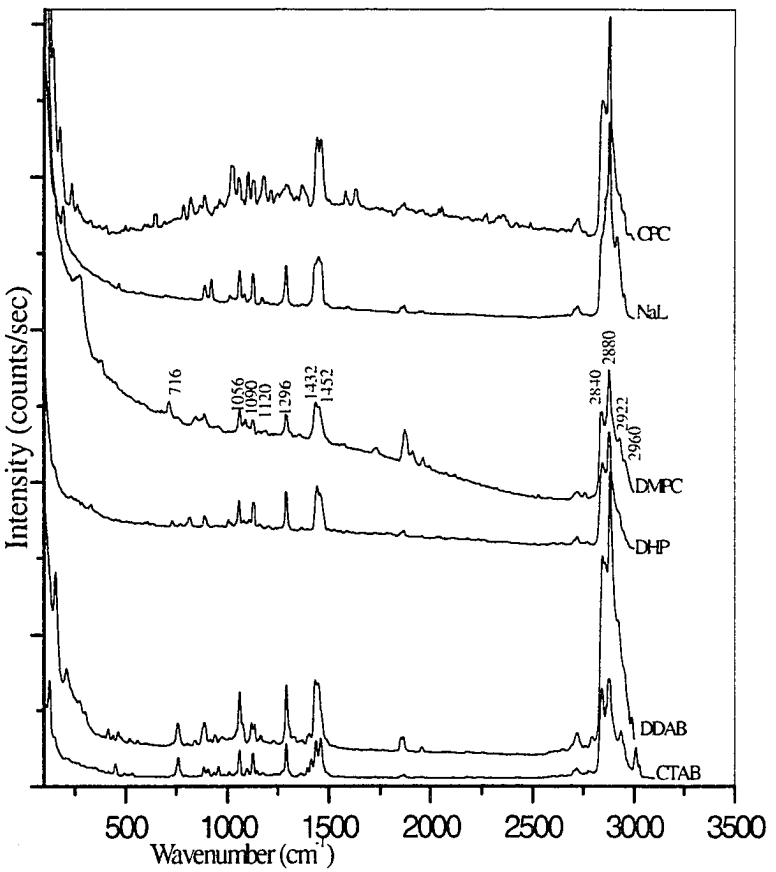

Figure 16.Normal Raman Spectra of CPC, NaL, DMPC, DHP, DDAB and CTAB in the crystalline (solid) form in the 100 - 3100 cm^{-1} region.

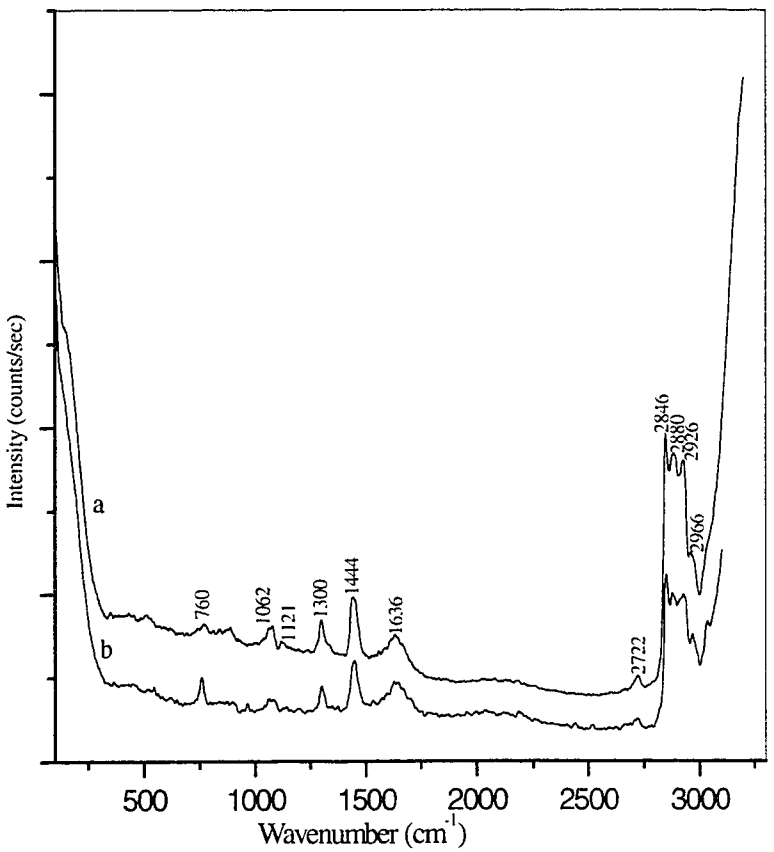

Figure 17. (a) Normal Raman spectra of 0.1mM DDAB in aqueous solution and (b) 0.1375 M CTAB in aqueous solution.488 nm line was used. 100 - 3000 cm^{-1} region (Micellar form).

SURFACE-ENHANCED RAMAN SPECTRA OF SURFACTANTS (CTAB, DDAB, CPC, DHP, DMPC and NaL) AS A FUNCTION OF VOLTAGE ON A SILVER ELECTRODE SURFACE IN THE 2600-3100 CM^{-1} REGION (Figs 18-23).

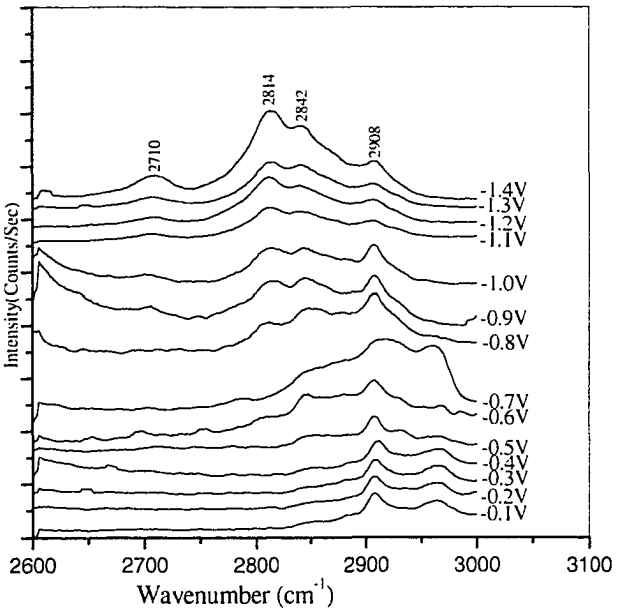

Figure 18. SERS spectra of 0.1 mM DMPC in 0.1M KCl on a Ag electrode surface in the 2600- 3000 cm^{-1} region at different potentials.

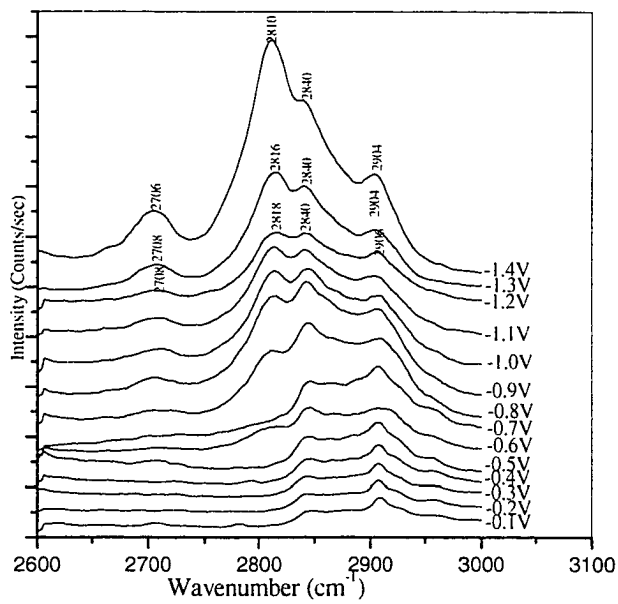

Figure 19. SERS spectra of 0.1 mM DHP in 0.1M KCl on a Ag electrode in the 2600 - 3000 cm^{-1} region at different potentials.

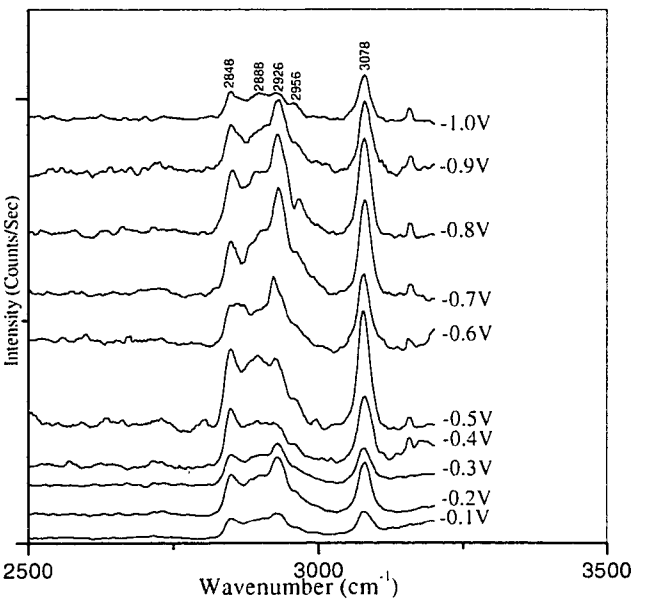

Figure 20. SERS of 10 mM CPC in 0.1 M KCl adsorbed on a Ag electrode surface in the 2600 - 3100 cm^{-1} region at different potentials.

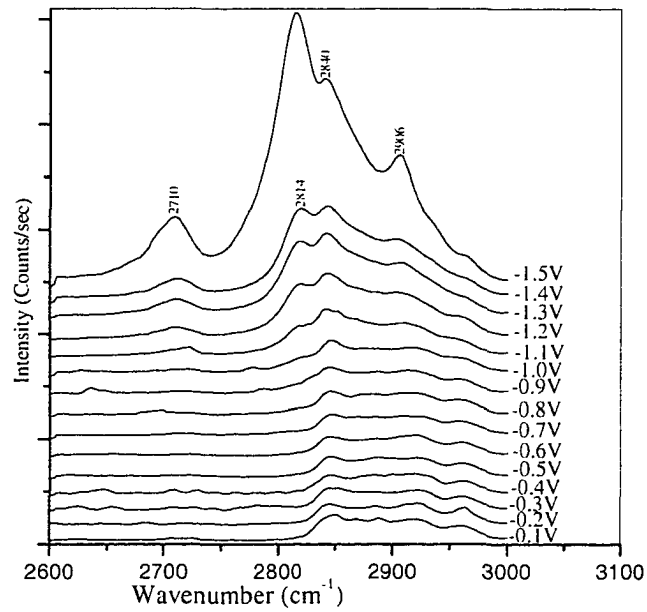

Fig 21. SERS spectra of 10 mM CTAB in 0.1 M KCl on a Ag electrode surface in the 2600-3000 cm^{-1} region at different potentials.

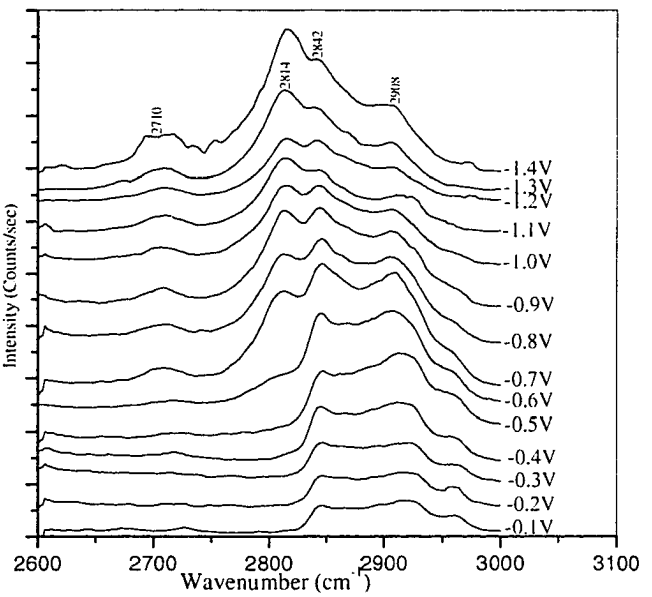

Figure 22. SERS spectra of 10 mM sodium laurate (NaL) in 0.1M KCl on a Ag electrode surface in the 2600 - 3000 cm^{-1} region at different potentials.

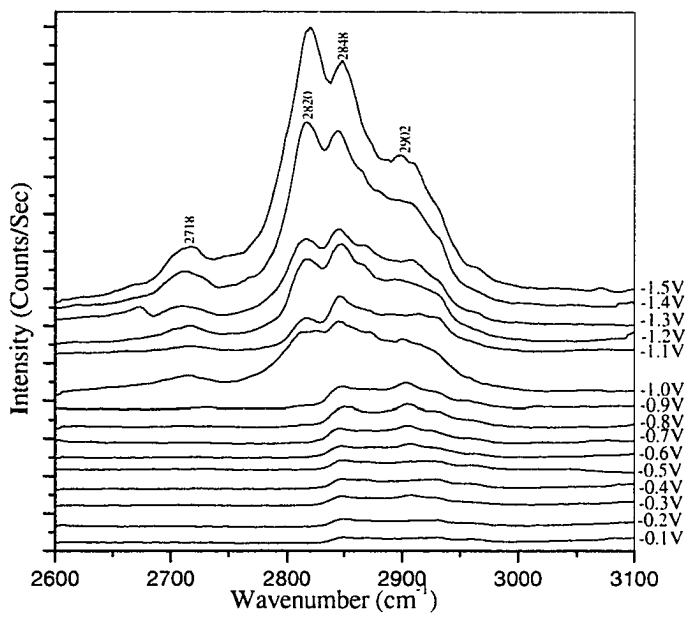

Figure 23. SERS of 10 mM DDAB in 0.1M KCl (2600-3100cm^{-1}) as a function of voltage on a silver electrode surface.

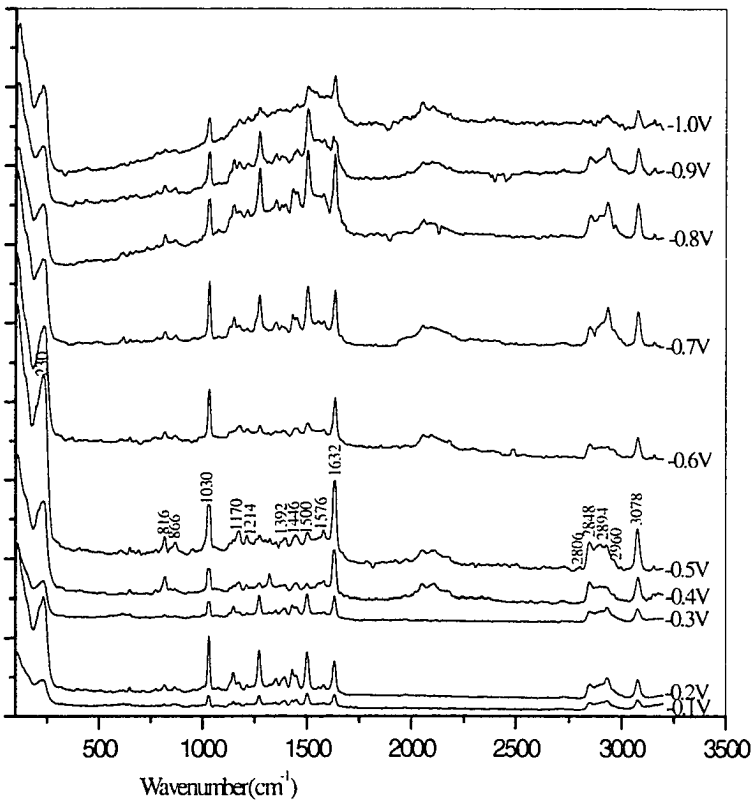

Fig 24 . SERS of 10 mM CPC in 0.1 M KCl (100 -3200 cm^{-1} region)as a function of voltage on a silver electrode surface .

SURFACE-ENHANCED RAMAN OF SOME SURFACTANTS (DDAB, CTAB, DMPC) AS A FILM ADSORBED ON A SILVER ELECTRODE SURFACE (Figures 25, 26, 27)

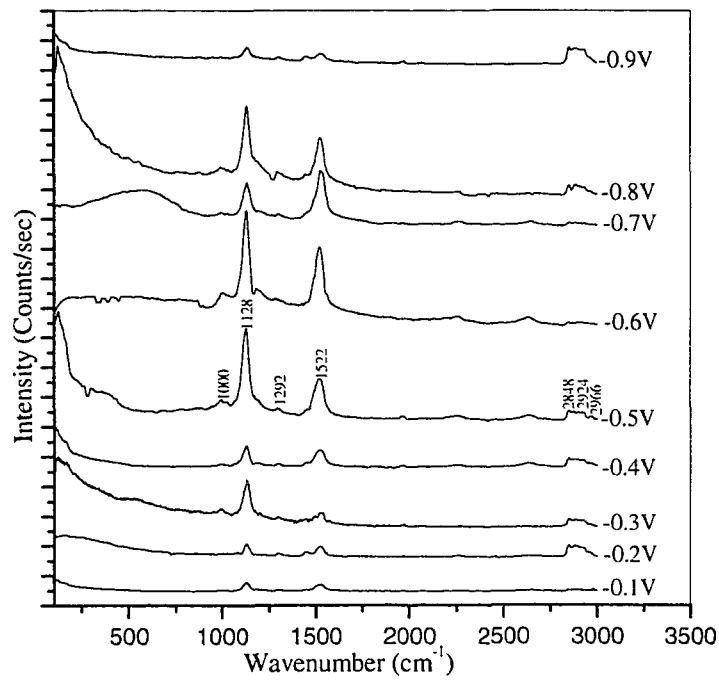

Figure 25. SERS spectra of a multibilayer film of 0.1M DDAB on a Silver (Ag) electrode surface.

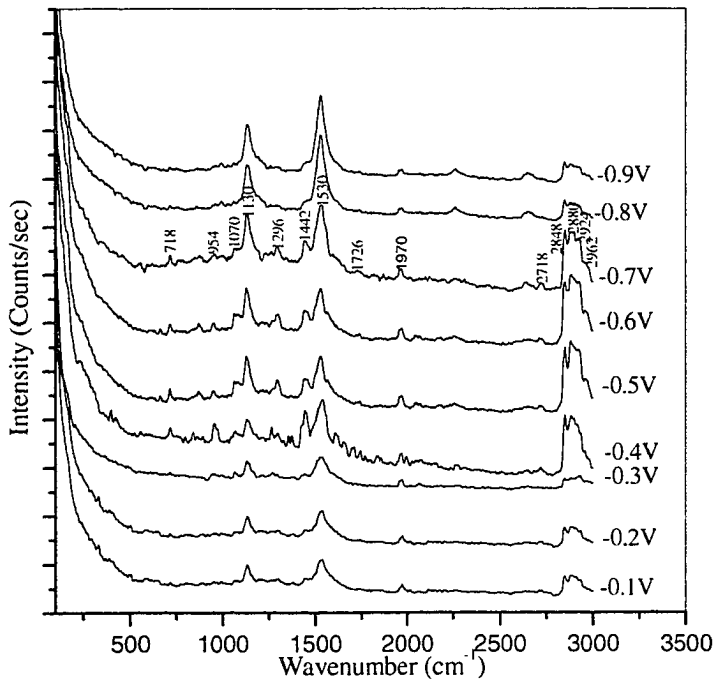

Figure 26. SERS spectra of a multibilayer film of 0.1M DMPC on a Silver (Ag) electrode surface.

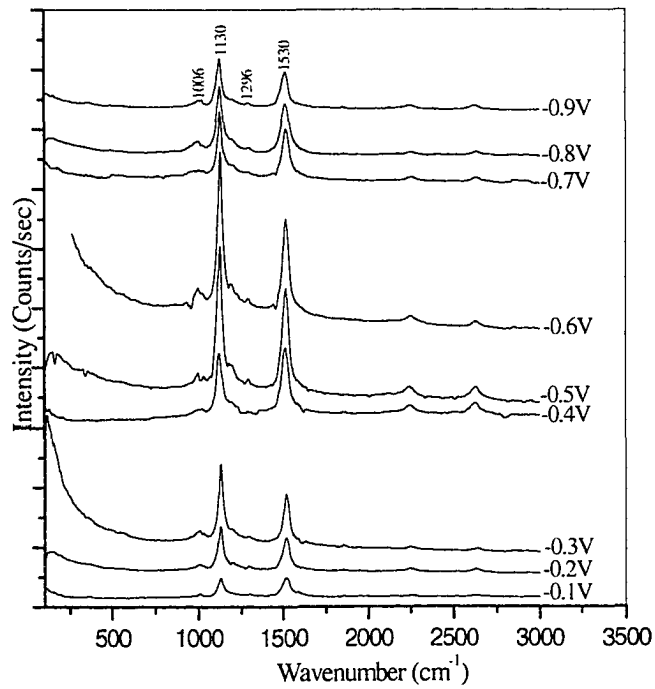

Figure 27. SERS spectra of a multibilayer film of 0.1M CTAB on a Silver (Ag) electrode surface.

TABLE 15: Depolarization ratio ($I_\perp/I_\parallel$) of the normal Raman of DDAB, CTAB, CPC, DMPC, DHP, NaLs dissolved in water using the 488 nm line.

Assignments	Freq (cm^{-1})	DDAB	CTAB	CPC	DMPC	DHP	NaL
sym and trigonal ring breathing	1032	___	___	0.08	___	___	___
C-C asym str + CH_2 wag from (TG_MT) with M large	1126	0.04	0.035	___	___	___	___
CH_2 sym str	2850	0.18	0.07	0.064	0.04	0.22	0.10
CH_2 asym str	2884	0.21	0.11	0.13	0.04	0.15	0.08
CH_2 sym str & overtone	2922	0.17	0.01	0.08	0.11	0.02	0.21
CH_2 scissoring	2960	0.15	0.1	0.38	0.06	0.04	0.10
Ring str	3076	___	___	0.15	___		___

CTAB and NaLs at 0.1M concentrations, CPC at 0.5M, DMPC at 1mM, DHP and DDAB at 0.1mM

All of them were prepared in aqueous solution (distilled water)

___ Means this band is not present in this molecule.

TABLE 16: Depolarization ratio ($I_\perp/I_\parallel$) of the SERS of 0.1 M DDAB, CTAB and DMPC in $CHCl_3$ (Multibilayer film) on a silver (Ag) electrode surface with the 488 nm line.

Depolarization ratio of the surfactants at –0.4 V and –0.6 V on Ag surface

Freq (cm^{-1})	DDAB (-0.4V)	DDAB (-0.6V)	CTAB (-0.4V)	CTAB (-0.6V)	DMPC (-0.4V)	DMPC (-0.6V)
1126	0.54	0.57	0.42	0.45	0.18	0.23
1530	0.57	0.56	0.39	0.40	0.23	0.26
2850	0.50	0.48	0.42	0.40	0.27	0.21
2880	0.50	0.43	0.41	0.43	0.21	0.17
2920	0.47	0.41	0.38	0.39	0.19	0.14
2960	0.30	0.34	0.45	0.42	0.28	0.14

TABLE 17: Depolarization ratio ($I_\perp/I_\parallel$) of the SERS of DDAB, CTAB, DMPC, DHP and NaL in 0.1M KCl (Adsorption from solution) on a silver (Ag) electrode surface with the 488 nm line.

Depolarization ratio of the surfactants at –0.7 V and –1.3 V on Ag surface

Freq (cm^{-1})	DDAB (-0.7V)	DDAB (-1.3V)	CTAB (-0.7V)	CTAB (-1.3V)	DMPC (-0.7V)	DMPC (-1.3V)	DHP (-0.7V)	DHP (-1.3V)	NaL (-0.7V)	NaL (-1.3V)
2850	0.32	0.60	0.31	0.56	0.35	0.57	0.36	0.61	0.39	0.53
2888	0.35	0.56	0.37	0.58	0.32	0.62	0.31	0.58	0.36	0.54
2920	0.30	0.57	0.41	0.59	0.32	0.54	0.30	0.61	0.39	0.55
2960	0.20	0.52	0.41	0.60	0.32	0.55	0.28	0.52	0.37	0.53

TABLE 18: Depolarization ratio ($I_\perp/I_\parallel$) of the SERS of 0.01 M CPC in 0.1M KCl (Adsorption from solution) and the normal Raman (NR) of 0.5M CPC in H_2O with the 488 nm line.

	Voltages and depolarization ratio of 0.01M CPC in 0.1M KCl									NR
Freq (cm^{-1})	-0.1V	-0.2V	-0.3V	-0.4V	-0.5V	-0.6V	-0.7V	-0.8V	-0.9V	
1032	0.50	0.51	0.48	0.34	0.42	0.58	0.29	0.26	0.19	0.08
2850	0.44	0.52	0.38	0.22	0.40	0.48	0.48	0.52	0.61	0.064
2884	0.42	0.45	0.35	0.28	0.39	0.47	0.49	0.51	0.57	0.13
2922	0.45	0.41	0.32	0.29	0.36	0.47	0.42	0.54	0.60	0.08
2960	0.37	0.32	0.37	0.33	0.40	0.42	0.31	0.67	0.65	0.38
3076	0.23	0.22	0.27	0.18	0.24	0.57	0.30	0.48	0.52	0.15

Table 19. Raman Frequencies for the Anionic and Cationic Surfactant Solids CTAB, DDAB, DHP, DMPC, NaL and CPC in the 100 –3100 cm^{-1} region.

CTAB	DDAB	DHP	DMPC	NaL	CPC	assignments (ref. 11)
126 (s)	158 (s)	152 (w)		154 (m)	138 (m)	
	236 (m)	326 (vw)		192 (m)	174 (m)	
	274 (w)		272 (m)		234 (w)	Longitudinal accordion modes
	412 (w)		378 (w)		260 (w)	
450 (w)	436 (vw)				324 (w)	
	460 (w)					
492 (w)				468 (vw)	498 (w)	
502 (w)						
518 (w)	516 (vw)		536 (w)	536 (vw)		
532 (vw)	558 (vw)		572 (w)	582 (vw)		
752 (m)	756 (m)	730 (w)	714 (m)	696 (vw)		
760 (w)			764 (vw)			CH_3 rock from $N^+(CH_3)_3$ group
774 (vw)						
796 (w)	794 (vw)				784 (w)	
830 (w)	840 (vw)	816 (w)			818 (w)	
886 (w)	888 (m)	890 (w)	876 (w)	890 (m)	828 (vw)	
906 (w)	914 (w)		912 (w)	920 (m)	866 (vw)	
934 (vw)	940 (w)	928 (vw)			886 (m)	
956 (w)			954 (w)		964 (m)	CH_2 rock
984 (vw)	972 (w)	1004 (vw)	984 (vw)		1002 (vw)	
1010 (vw)		1018 (vw)	1028 (vw)	1014 (w)	1024 (s)	
1044 (vw)		1056 (m)		1034 (vw)		CH_2 twist crystalline
1062 (m)	1056 (m)	1062(sh)	1062 (m)	1060 (m)	1060 (m)	C-C sym stretch + CH_2 wag
1098 (w)		1106 (w)	1086 (w)	1084 (w)	1074 (vw)	
1124 (m)	1116 (w)	1120 (m)	1126 (vw)	1108 (vw)	1102 (m)	
1146 (vw)	1132 (m)	1136 (vw)	1126 (m)		1130 (m)	C-C asym stretch +CH_2 wag from (TG_mT) with m large

1162 (w)	1170 (w)	1154 (w)				
1174 (w)	1164 (vw)	1174 (vw)	1180 (vw)		1180 (m)	CH_2 wag, crystalline
1190 (w)	1198 (w)			1194 (vw)		
1210 (w)			1216 (w)		1214 (w)	
1226 (vw)	1224 (w)			1230 (vw)	1234 (vw)	
1246 (w)	1246 (w)	1254 (vw)			1250 (vw)	
1272 (w)						
1292 (m)	1290 (m)	1292 (m)	1294 (m)	1294 (m)	1298 (vw)	CH_2 Twist
	1330 (w)	1322(vw)				
		1342(vw)	1350 (w)	1344 (vw)	1338 (vw)	CH_2 wag
1366 (vw)	1366 (vw)	1366(vw)	1378 (vw)	1366 (vw)	1368 (m)	C-CH_3 sym bending
1394 (vw)	1402 (vw)	1396(vw)	1396 (vw)		1392 (vw)	C-H sym bend from N $(CH_3)_3$ group
1412 (w)				1434 (s)		
1438 (s)	1434 (m)	1442 (m)	1436 (m)	1440 (sh)	1440 (s)	-CH_2 bend
1462 (sh)	1448 (sh)	1460 (sh)	1450 (sh)	1450 (sh)	1462 (sh)	-CH_2 bend
1492 (vw)		1502 (vw)		1464 (sh)	1502 (vw)	
			1672 (vw)	1488 (vw)	1584 (w)	
2672 (vw)			2672 (vw)		1634 (m)	
2704 (vw)				2708 (vw)	2704 (vw)	
2718 (m)	2716 (m)	2716 (w)	2720 (w)	2722 (w)	2728 (m)	
2774 (vw)		2774 (vw)	2758 (vw)		2742 (vw)	
2782 (vw)	2784 (w)					
2844 (s)	2846 (s)	2848 (s)	2846 (s)	2840 (m)	2848 (s)	C-H sym stretch of $-CH_2-$
2876 (vs)	2882 (vs)	2880 (vs)	2878 (vs)	2880 (vs)	2878 (vs)	C-H sym stretch of $-CH_3$
2938 (w)	2922 (sh)	2928 (vw)	2928 (vw)	2916 (m)	2932 (w)	C-H asym stretch of $-CH_2-$
2954 (w)		2948(vw)	2954 (vw)	2954 (vw)	2956 (w)	
2966 (w)	2988 (vw)	2968 (vw)			2980 (w)	

Table 20. Raman Frequencies for the Cationic Surfactants (micelle) CTAB, and DDAB and Ab Initio Calculations in the 100 –3100 cm^{-1} region.

CTAB	(0.9)HF/6-311G	for CTAB	DDAB	Assignments from ref. 11 in bold
	Trans	Gauche	*HF Gauche assignments in italics*	
156 (w)	110(5)			
		152 (vw)		
216 (w)		274(3)	352 (vw)	
366 (vw)	329(2)	352(7)	388 (vw)	Longitudinal modes
400 (vw)			430 (vw)	
			454 (vw)	
544 (vw)	526(3)	539(3)	514 (vw)	
760 (m)	714(13)	714(4)	760 (w)	*CH_3 rock from $N^+(CH_3)_3$ group*
		770(16)		*CH_2 rock in tail methyl and methylene*
798 (vw)		797(9)	814 (vw)	*CH_2 rock along the tail*
892 (m)	861(13)	863(10)	842 (vw)	*CH_2 rock in CH_2-$N(CH_3)_3$*
896 (vw)	869(9)	872(11)	890 (vw)	*CH_3 rock (terminal methyl) C-N^+ stretch*
912 (vw)	927(8)	912(9)	912 (vw)	*C-N^+ stretching*
940 (vw)	927(8)	934(11)		*C-N^+ stretching*
968 (vw)	977(6)	964(3)	970 (vw)	
		1000(10)		*C-C sym stretch +CH_2 wag*
1064 (m)	1032(52)	1033(22)	1062 (m)	C-C sym stretch +CH_2 wag
1082 (sh)	1084(32)	1085(6)	1078 (m)	*CH_2 twist*
1102 (vw)	1110(26)			
1122 (w)	1131(11)	1145(6)	1118 (vw)	
1138 (vw)				C-C asym stretch +CH_2wag inTG_mT
1162 (vw)	1175(5)	1175(4)	1160 (vw)	CH_2 rock
1194 (vw)		1216(4)	1238 (vw)	CH_2 wag crystalline and CH_2 twist
1302 (m)	1300(44),	1306(6)		
	1301(89)	1312(25)		*CH_2 twist at end of tail*

	1314(9)	1326(94)		*CH_2 wag*
1350 (vw)				CH_2 wag
1370 (vw)	1350(4)			C-CH_3 sym bending
1446 (m)	1436(3)	1436(3)	1442 (m)	*N-CH_3 sym bending*
1450 (vw)	1477(19)	1476(18)	1450 (sh)	*N-CH_3 asym bending*
1492 (vw)	1481(35)	1478(35)		*CH_2 scissors*
	1483(157)	1481(20),1483(16)		sym *CH_2 scissors*
1532 (vw)	1485 (51)	1485(36)	1532 (vw)	"
	1486(17)			
1570 (vw)	1500(8)	1494(15), 1497(12)	1566 (vw)	*CH_2 rock in tail and* $N^+(CH_3)_3$ group
1628 (m)			1636 (m)	
1646 (vw)				
1708 (vw)				
2720 (w)			2724 (w)	
	2823(23), 2824(97)	2816(94), 2822(82)		*C-H asym stretch of -CH_2-*
	2826(287)	2827(178)		*C-H sym stretch of -CH_2-*
	2828(156)	2831(144)		*C-H asym stretch of -CH_2-*
2850 (s)	2830(235), 2836(263)	2842(231), 2849(347)	2846 (s)	*C-H asym stretch of -CH_2-*
2874 (s)	2892(25)	2861(161)	2864 (w)	*C-H asym stretch of -CH_2-*
2880 (s)	2894(102)	2895(97)	2886 (s)	*C-H sym stretch of -CH_3*
2926 (sh)	2905(328)	2905(326)	2924 (s)	*C-H sym stretch of N^+-$(CH_3)_3$*
2968 (sh)	2987(43), 2988(115)	2988(114), 3006(54)	2960 (sh)	*C-H asym stretch of N^+-$(CH_3)_3$*
	3001(137), 3006(54)	"		
3036 (w)				C-H sym stretch of N^+-$(CH_3)_3$

[a] Assignments taken from reference 11

Table 21. Raman Frequencies for the Surfactants (Multibilayer) CTAB, DDAB, and DHP in the 100 –3100 cm^{-1} region.

CTAB (-0.6V)	DDAB (-0.6V)	DMPC (-0.6V)	Tentative assignments[a]
152 (vw)	152 (vw)	152 (w)	
220 (vw)	220 (vw)	220 (w)	
562 (vw)	562 (vw)	562 (w)	Longitudinal accordion mode
812 (vw)	812 (vw)	812 (w)	
866 (vw)	866 (vw)	866 (w)	
898 (vw)	898 (vw)	898 (w)	
934 (w)	942 (w)	946 (m)	CH_2 rock
		988 (vw)	
1000 (m)	994 (m)	1004 (vw)	
1030 (vw)	1062 (vw)	1062 (w)	C-C sym stretch + CH_2 wag
1128 (s)	1128 (s)	1132 (s)	C-C asym stretch + CH_2 wag from (TG_mT) with m large CH_2 rock
1198 (w)	1190 (w)	1196 (vw)	CH_2 wag , crystalline
1290 (w)	1294 (w)	1244 (w)	
1374 (vw)		1268 (vw)	
		1294 (m)	
		1366 (vw)	C-CH_3 sym bending
		1388 (vw)	
1446 (vw)	1440 (w)	1438 (sh)	-CH_2 bend
1518 (s)	1520 (s)	1528 (s)	
2248 (vw)	2252 (vw)	2252 (vw)	
2630 (vw)	2636 (vw)	2636 (vw)	
2768 (vw)	2728 (vw)	2726 (vw)	
2848 (vw)	2852 (w)	2848 (m)	C-H sym stretch of -CH_2-
2872 (vw)	2866 (w)	2868 (m)	
2894 (vw)	2892 (w)	2878 (m)	C-H sym stretch of CH_3 -
2928 (vw)	2926 (w)	2922 (m)	C-H asym stretch of –CH_2-
2966 (vw)	2962 (w)	2956 (sh)	C-H asym stretch of CH_3 -

[a] Assignments taken from reference 11

Table 22. Raman Frequencies of the SERS for the Anionic and Cationic Surfactants CTAB, DDAB, DHP, DMPC, NaL and CPC in the 2600 –3100 cm^{-1} region at – 0.6 V.

CTAB	DDAB	DHP	DMPC	NaL	CPC	Tentative assignments[a]
			2706		2718	
2802	2804	2804	2802	2804	2794	
2846	2846	2846	2848	2846	2848	CH_2 sym str
2872	2864	2872	2874	2866	2872	
2884	2884	2886	2880	2884	2894	CH_2 asym str
2906	2910	2906	2908	2906		
2920	2920	2920	2928	2930	2922	CH_2 sym str and overtone
2960	2954	2954	2966	2958	2960	CH_2 scissoring
					3078	Ring CH str
					3154	

a Assignments taken from reference 11

F. References

[1].(a)Kunitake, T; Okahata *J. Am.. Chem. Soc.* 1977, 99, 3860-3861.

(b) Kunitake, T.; Tsuge, A. Nakashima, N *Chem. Letts* 1984, 1783-1786. for review see (c) Kunitake, T " *Synthetic Bilayer Menbranes* " *Comprehensive Supermolecular Chem.* 1996, 9, 351-406.

[2].Rusling, J. F. Acc. *Chem. Res.* 1998, 31, 363—369.

[3].Okahata, Y.; Ebato, H. *Anal. Chem.* 1991, 63, 203-207.

[4].Rusling, J. F., Zhang, H. *Langmuir* 1991 , 7, 1791-1796 .

[5].(a) Jaswchke, M.; Butt, H.-J.; Gaub, H. E.; Manne, *Langmuir* 1997, 13, 1381-1384.

[6].Tang, Z.; Wang, E. *J. Electroanal. Chem.* 2001, 496, 82-87 .

[7].Sun, S.; Birke, R. L.; Lombardi, J.R. *J. Phys. Chem.* 1990 , 94 , 2005 –2010.

[8].Suga, Kosaku.; Bradley, Michael.; Rusling , J. F. . *Langmuir* 1993, 9, 3063-3066 .

[9].Faria, P.A.; Chen, X., Lombardi, J. R.; Birke, R. L. *Langmuir* 2000, 16, 3984-3992.

[10].(a) Snyder, R. G.; Strauss , H. L.; Elliger *J. Phys. Chem.* 1982 , 86 , 5145 – 5150.
(b) Garber, B. P.; Peticolas, W. L. *Biochim. Biophys. Acta* 1977, 465, 260-274.
(c) Snyder, R. G.; Scherer, J. R. *J. Chem. Phys* 1979 , 72 , 3221. (d) Snyder, R. G.; Hsu, S. L.; Krimm, S. Spectrochim. Acta, Part A 1978, 34, 395-406.

[11].Kalyanasundaram, K.; Thomas, J. K. *J. Phys. Chem.* 1976, 80, 1462 – 1473.

[12].Zerbi, G.; Roncone, P.; Longhi, Wunder, S. L. *J. Chem. Phys* 1988 , 89 , 166-173.

[13].Carey, P. R. in *"Biological Applications of Raman and Resonance Raman Spectrocopies"* 1982, Academic Press, p. 40.

[14].Van Dutne, R. P., in " *Chemical and Biological Applications of Laser*

Raman Spectroscopy " ed. C. Bradely Moore

[15].Chan, S. Y-Y, " Adsorption of Surfactants at Solid/Liquid and Liquid/ Liquid Interfaces for Dewetting Process" , Ph. D. Thesis , The City University of New York, 1988

[16].Creighton; J. A. *Surf. Sci.* 1983 124, 209-219.

[17].Moskovits;M.; Suh , J.S. *J Chem. Phys.* 1984, 88, 5526.

[18].Bryant, M. A.; Pemberton J. E. *J. Am.. Chem. Soc.* 1991, 113, 3629-3637.

[19].Birke, R. L. ; Lombardi, J. R., In *Spectroelectrochemistry:Theory and Practice;*Gale, Ed. Plenum, Ch.6, 1988.

[20].Venkataraman, N.V.; Vassudevan, S. *J. Phys. Chem.* 2001, 105, 1805 – 1812.

[21].Sun, S.C., Bernard, I., Birke, R. L., Lombardi, J. R. *J. Electroanal. Chem.* 1985, 196, 359-374.

[22].Kreisig, S. M.; Tarazona, A., Koglin, E., and Schwuger, M. J. *Langmuir* 1996, 12, 5279-5288.

Chapter 5

UV –Vis, Surface-Enhanced Raman, and Cyclic Voltammetric Studies of Heme Proteins (Horse Heart Cytochrome C and Horse Skeletal Muscle Myoglobin) in the Presence of Surfactants.

A. Abstract

Heme proteins, such as horse skeletal muscle myoglobin and horse heart cytochrome c, were incorporated into bilayers of surfactants. Both proteins have the protoporphyrin IX structure in their backbone but different side chains. Our interest is to study the behavior of these heme proteins in the presence of surfactants using UV-visible, cyclic voltammetry and Surface-Enhanced Raman Spectroscopy (SERS). For the UV-visible experiments, the heme proteins were incorporated into surfactants at concentrations that are below, above, and at their critical micelle concentration (cmc). It has been observed that at low porphyrin to surfactant molar ratios, i.e. less or equal to $6.7 * 10^{-3}$ for DDAB (see table 24) and less or equal to $1.1 * 10^{-4}$ for CTAB (see table 24), the Soret band in myoglobin shifted from 410 nm to 400 nm. However , no such change has been observed in the case of horse heart cytochrome c. For myoglobin, the shift observed in its Soret band can be attributed to the histidyl- F_8 side chain that is very sensitive to the overall heme environment. Cyclic voltammograms of these heme proteins confirm that electron transfer occurs at a much faster rate between the molecules (heme proteins) and the electrode surfaces such as glassy carbon (GC), silver (Ag) and gold (Au) when these proteins were incorporated in surfactant films. On a glassy carbon electrode, electron transfer occurs between – 0.2V and –1.1V. These voltages correspond to the reductions of Fe^{3+} to Fe^{2+} at – 0.2V and a second reduction at -1.1V respectively. In addition, surface-enhanced Raman spectroscopy on cast films of

didodecyldimethylammoniumbromide(DDAB) surfactant revealed an intensity change in the 1390 cm^{-1} and 1630 cm^{-1} bands, while anew band appears at 3070 cm^{-1}. The first one is a shoulder band associated with the ligand binding to the central metal atom .The second band , at approximately 1630 cm^{-1}, gives us some insight about the orientation of the polypeptide chain of the heme protein. The band at 3070 cm^{-1} corresponds to the C-H aliphatic vibration of the heme protein that connects the tetrapyrrole ring.

B. Introduction

Considerable attention is currently dedicated to the biomimetic chemistry of heme proteins on electrode surfaces in relation with the development of biosensors and biotechnological process[1,2]. The porphyrins in heme proteins play a central role in some important biological processes such as light energy conversion, oxygen transport, and catalysis[3]. In all these chemical processes the porphyrin molecule has had a variety of functions such as electron transport; charge separation, reversible binding of the oxygen molecule and the reductive activation of dioxygen. The nature of the central metal ion in the porphyrins is partly responsible for the diverse chemical and photophysical properties of these molecules[3]. In addition, the central metal ion in the porphyrins of these heme proteins is very sensitive to their environment. In the past, a variety of studies have been carried out in which the main characteristics of the porphyrin molecules are controlled by directly modifying these molecules and / or by changing the surrounding of the

reaction medium of the porphyrins[3,4]. Our goal is to study the behavior of these heme proteins (horse heart cytochrome c and Horse skeletal muscle myoglobin) when incorporated into micelles and multibilayers of surfactants. It has been shown previously that the incorporation of porphyrins in micelles or multibilayers has considerably altered the rate of metalation of these molecules[5]. Electrochemistry of proteins has been combined with spectroscopy[6-9] to investigate changes in the structure of these heme proteins via redox reactions. UV-visible spectroscopy of myoglobin (Mb) and hemoglobin solution revealed structural differences between Fe (III) and Fe (II) forms for the polypeptide backbone and the hemes [7b]. UV- visible spectroscopy can help to uncover changes in the heme environment, while FT-IR spectral band shapes can be used to monitor conformation changes in the proteins. Multibilayer films of surfactants can provide biomembrane-like environments that are useful in the study of protein redox chemistry, as well as for applications in biosensors and catalysis. Rusling et al[11-14]. have reported stable, ordered, liquid crystal surfactant films in which direct electron transfer between electrodes and myoglobin was achieved. Electron transfer rates for these heme proteins especially myoglobin incorporated in these surfactant films were up to 1000- fold larger than for the protein in solution on bare carbon electrodes (GC and PG), gold (Au) , and platinum (Pt) electrodes[15]. Spectroelectrochemistry showed that MbFe(III) was converted quantitatively to MbFe(II) in the absence of oxygen[15].

In this paper, the influence of the surfactant film's concentration (i.e. below, above, and at their critical micelle concentrations) on heme proteins has been investigated using UV- visible spectroscopy. In addition, cyclic voltammetry was used in order to show these surfactant films can considerably increase the rate of electron transfer on glassy carbon (GC), silver (Ag), and gold (Au) electrodes as compared to bare electrode surfaces. Finally, surface-enhanced Raman spectroscopy was used to investigate the structural differences or conformation changes within the protein structure of horse skeletal muscle myoglobin.

C. Experimental

Horse skeletal muscle myoglobin and horse heart cytochrome c were purchased from Sigma and dissolved in distilled and deionized water. Both solutions were passed through Amicon YM30 filters (30,000 MW cutoff)[12a]. The concentrations after filtration were determined by UV-visible spectroscopy. After purification, both heme proteins (horse skeletal muscle myoglobin and horse heart cytochrome c) concentrations' were determined to be 0. 50 mM. The surfactants, didodecyldimethylammoniumbromide (DDAB) and cetyltrimethylammoniumbromide (CTAB) had 99 % purity and were both purchased from Sigma and used without further purification. All other chemicals were reagent grade. Cyclic voltammograms of both heme proteins were taken in 0.1 M phosphate buffer pH 7. For the UV-visible, both proteins were diluted to a lower concentration in 0.1 M sodium sulfate

(Na_2SO_4) at 1.0 $*10^{-6}$ M while the concentrations of DDAB and CTAB surfactants were made many fold above and below their critical micelle concentrations. The SERS spectrum of horse skeletal muscle myoglobin incorporated in DDAB surfactant was taken by mixing and sonicating 3 µl of 0.1 mM DDAB with 7 µl of 0.5 mM of heme protein. Then, we coated a roughened silver electrode (roughened in 0.1 M phosphate buffer with an ORC at –0.6V to ~+0.45 V for 10 seconds and then back to –0.6V) with that mixture and left overnight in a sealed glass chamber. The next morning, the coated electrode was taken out of the glass chamber, exposed to the air for about and hour before putting it into an electrochemical cell containing 0.1 M phosphate buffer and degassed for an hour. A UV-Vis spectrometer, model LAMBDA 18 from PERKIN ELMER , was used for the spectroscopy experiment. The Raman apparatus was described previously elsewhere[16]. Cyclic voltammograms were taken using a CHI instrument, model CHI 720, which is an electrochemical workstation that control data acquisition and voltage. Films were cast onto glassy carbon (GC), silver (Ag), and gold (Au) electrodes from clear vesicle dispersions[13] of 0.1mM DDAB containing 0.5mM Mb. Before casting the films on electrode surfaces, the electrodes were cleanly polished with alumina powder [from Buehler Micropolish (Micron Deagglomerated Alpha Alumina)] of 0.3 and 0.05 microns in size and then the electrode was rinsed in distilled water and sonicated for approximately fifteen minutes. Pretreatment for both silver (Ag) (-0.6V to +0.45V for 10 seconds and then back to – 0.6V in 0.1M phosphate buffer) and

gold (Au) (-0.2V to +1. 3V for 2 seconds and then back to – 0.2V in 0.1M phosphate buffer) were achieved by performing an oxidation-reduction cycle (ORC) and the electrodes consist of reference (SCE), auxiliary (platinum), and working electrode (either Ag, Au, or GC). However, no ORC was performed for the glassy carbon electrode. Oxygen was removed by purging solutions with prepurified nitrogen purchased from T.W. Smith. All experiments were done at 25°C.

D. Results and Discussion

i) UV-Vis of the heme chromophore of Horse Skeletal Muscle Myoglobin in the presence of surfactant [DDAB and CTAB (above , below , and at their critical micelle concentration)] marked by a wavenumber shift of the Soret band while no change was observed in the case of Horse heart cytochrome c.

UV-visible spectroscopy was used to monitor changes in the heme environment as these heme proteins were incorporated into bilayers of surfactants. At a certain protein to surfactant ratio and pH, the heme chromophore of horse skeletal muscle myoglobin in the presence of DDAB or CTAB surfactants has shown a shift in the wavelength in the Soret band while such a shift has not been observed when horse heart cytochrome c was studied in the presence of surfactants (DDAB or CTAB). It has been previously reported that the Soret band caused by visible absorbance of the Fe (III) heme in Mb is sensitive to pH[17,18]. Also, Rusling et al[19]. had demonstrated that between a pH of 6 or 9, the Mb-DDAB λ_{max} is about 415 nm, at slightly longer wavelengths than in Mb films or in solutions. Our results are in complete agreement with them since at a pH relatively greater

than 6 (see tables 24 and 27), the Mb-DDAB and Mb-CTAB λ_{max} are about at 410 nm. At that particular wavelength, that value corresponds to a myoglobin mixed with DDAB or CTAB surfactant at equal volumes but at concentration lower than their critical micelle concentrations (cmc). However, when horse skeletal muscle myoglobin was mixed in DDAB or CTAB surfactants at concentrations that are above their critical micelle concentrations (cmc), the Mb-DDAB and Mb-CTAB λ_{max} shifted to a lower wavelength at 400 nm. For cytochrome C it is worthy to mention that its Soret band has not shown any shift whatsoever , i.e. the Soret band absorbs at λ_{max} = 410 nm whatever the conditions such as pH and protein to surfactant ratio. Protonation of the distal and proximal histidine heme pocket in horse skeletal muscle myoglobin has already been demonstrated to be the main reason for the shift of their Soret band.

ii) Cyclic voltammetric studies of heme proteins in the presence of surfactant (DDAB) .Evidence of electron transfer on glassy carbon(GC) gold (Au) and silver (Ag) electrodes.

Cyclic voltammetry was used to investigate the effect of surfactant (DDAB) on heme proteins (horse skeletal muscle myoglobin and horse heart cytochrome c) adsorbed on electrode surfaces. Cast films mixed with proteins can provide biomembrane-like environments that are useful for the study of protein redox chemistry, as well as for applications in biosensors and catalysis. Stable, well-ordered liquid crystal surfactant films can be used as enhancers of the electron transfer process between electrodes and heme proteins[11-14]. The surfactant films give specific orientation to the heme

proteins that considerably increase the electron transfer rate. Prior to that discovery, in general the sluggish direct electrochemical response of redox proteins with standard techniques makes multi- electron catalysis difficult to initiate and follow. However, during the past decade, dramatic advances in the direct electrochemistry of redox proteins have been made[28-32].

Unfavorable orientation of the heme protein toward the electrode surface and trace amount of oligomers in the proteins have been characterized to be some of the major barriers responsible for poor electron transfer between the electrode surface and the protein. A variety of methods have been used in order to overcome this problem and they include adsorption[30] or covalent attachment[31] of the protein to the electrode surface, and the use of promoters such as alkylthiols and surfactants which coat the electrode surface with chemical functionalities that can directly interact with the protein. As another approach, Rusling et al[31], have developed the use of water-insoluble surfactant films deposited on the electrode surface. Casts of multilayer films form stable, multilayer macrostructures that facilitate the rapid electrochemical response of redox active species contained with them[12, 14,15,20,29(a)] .The surfactant film and the heme proteins form a biphasic system consisting of aqueous and hydrophobic regions similar to the phospholipid membranes in which many vital biological redox reactions occur.

Layered films containing a mixture of surfactant such as didodecyldimethylammoniumbromide (DDAB) and heme proteins (horse skeletal muscle myoglobin and horse heart cytochrome C) can be formed on

electrode surfaces and their electrochemical properties can be studied using the cyclic voltammetric technique. The direct electrochemical response of heme protein (Mb) in these Mb/DDAB films deposited on glassy carbon (GC), silver (Ag), and gold (Au) electrodes is greatly enhanced, a factor of 10^3 , over the protein on bare electrode surface. Cyclic voltammetric study showed that Mb (Fe III) can be converted quantitatively to Mb(FeII) in the absence of oxygen[14]. Two electrochemical reductions from ferric Mb are seen in the cyclic voltammogram of Mb/DDAB in fig 33, the first is assigned to the [Fe (III)]/[Fe (II)] couple, and a second can be tentatively assigned to the reduction of a radical anion of the porphyrin ring .Our main objective was to examine the electrochemical behavior of these Mb/DDAB and HHCytC/DDAB films as background material for the SERS study . In the presence of DDAB surfactant, Mb/DDAB and HHCytC/DDAB films exhibit reversible electron transfer on glassy carbon electrode. In addition, Mb/DDAB films have shown reversible electron transfer on silver and gold electrodes while the HHCytC/DDAB mixture could not form a film on gold and silver electrode surfaces and as a result, we have not observed any appreciable electron transfer for HHCytC/DDAB on these electrodes.

iii) Surface-Enhanced Raman spectra of heme protein in DDAB surfactant film cast on a silver electrode surface.

It has been reported by Rusling et al[8] that surface-enhanced Raman spectral band shapes can be used to monitor changes in protein conformation. The pH dependence of the protoporphyrin heme in the presence of surfactant has been studied previously using ESR, absorption spectroscopy and linear

dichroism[11-14]. Those studies showed that myoglobin in DDAB and PC films are in the high spin MbFe (III)-H_2O form at solution pH between 5.5 and 7.5[19] . This native state features a proximal histidine bound to iron below the plane of the heme and distal histidine hydrogen bonded to ligated water above the heme[19]. The heme protein resides within the surfactant films and only a fraction of the proteins are electrochemically active inside those films due to the specific orientation of the heme proteins inside of the films. In addition, the properties of these heme proteins (Mb) are partly controlled by the acidity of the overall environment of the proteins. At a specific pH, partial unfolding of the protein can occur and Rusling et al[11-14] showed that at a pH between 5.5 and 7.5 , Mb in the surfactant film has a secondary structure similar to the native state , with about 75% helix[19]. However, they have also reported a partial unfolding of the myoglobin secondary structure at a pH less than 5.5.

In this paper, the Surface-Enhanced Raman spectral of heme protein (Mb) embedded in DDAB surfactant film was studied as a function of voltage while keeping the pH of the overall mixture at 7.60. Some Raman bands are very sensitive to chemical environment and our purpose was to investigate the behavior of those bands within the films as we vary the voltage. The following bands; 1392 cm^{-1} , 1630 cm^{-1}, and 3076 cm^{-1} , are the major focus of our investigation because they can provide meaningful information about the conformation of our protein within the surfactant film. The first one (1392cm^{-1}) has shown an unusual growth in intensity in the presence of

surfactant and this phenomenon can be attributed to a water molecule acting as a ligand attached to the central iron atom[11]. The 1630 cm^{-1} band is associated with the porphyrin asymmetric ring stretch <(C_α-C_m) .This band (1630 cm^{-1}) started to appear at -0.5V and its intensity grows as we move into a more negative voltage range. At a relatively lower negative voltage, (-0.1V to -0.4V see table 23) , the band in the vicinity of 1630 cm^{-1} does not show up but at a relatively greater voltage (-0.5 V to -1.0V) it started to appear. Rusling et al[11] have correlated this band in FTIR to the pathway for reduction of native MbFe (III) –H_2O to MbFe (III) involving the partial unfolding of protein helices but in SERS it is due to the protoporphyrin IX.

Finally, the band at approximately 3070 cm^{-1} can be attributed to the in plane C-H stretching vibration of the aliphatic hydrocarbon <(C_m-H) that connects the tetrapyrrole rings. Since there exist four of them which are part of a ring current created by conjugated double bonds, the intensity of the 3070 cm^{-1} band is relatively strong. In addition, this band is surface enhanced when the tetrapyrrole ring takes a specific orientation within the surfactant film. We assume that the tetrapyrrole ring is oriented perpendicular to the Ag surface i.e. within the path of the ring current and according to SERS selection rules there is an enhancement of that band. At a relatively negative voltage, like -1.0V, the 3070 cm^{-1} band disappears because at this voltage the heme protein takes a different orientation within the surfactant film that is not favorable for the enhancement of that band.

E. Conclusion

UV-visible spectroscopy, cyclic voltammetry, and surface-enhanced Raman spectroscopy were used to monitor the behavior of heme proteins in the presence of surfactants. Results suggest that the pH of micelle concentration has a direct effect on the position of the Soret band in the UV-Visible spectrum of myoglobin when both surfactant and heme protein were mixed together. However, the Soret band of the UV-Visible spectrum of horse heart cytochrome c did not shown any change in the presence of different micelle concentrations.

The electrochemistry of both proteins in surfactant film (DDAB) is unique in several ways. Especially significant, in the case of myoglobin, is the ability to stabilize a second electron transfer reaction on a glassy carbon electrode and still undergo facile binding and exchange of aqueous ligands. For horse heart cytochrome C, chemical transformations accompanying reversible electron transfers has been detected on a glassy carbon electrode surface. Therefore, this type of system (Mb/DDAB and CytC/DDAB) is very promising for the study of biomimetic catalysis electrochemically within a modifiable protein environment.

Finally, the SERS of these heme proteins (HHCytC and HSMM) within surfactant film (DDAB) give us some insight into the change in conformation and orientation of the heme of the protein inside of the surfactant films and this fact has been supported by the change in intensity and /or wavenumber of some Raman bands.

UV–Vis spectra of Heme proteins (HSMM and HH CYTC) in the presence of surfactants (DDAB and CTAB) Figs 28,29, 30, 31.

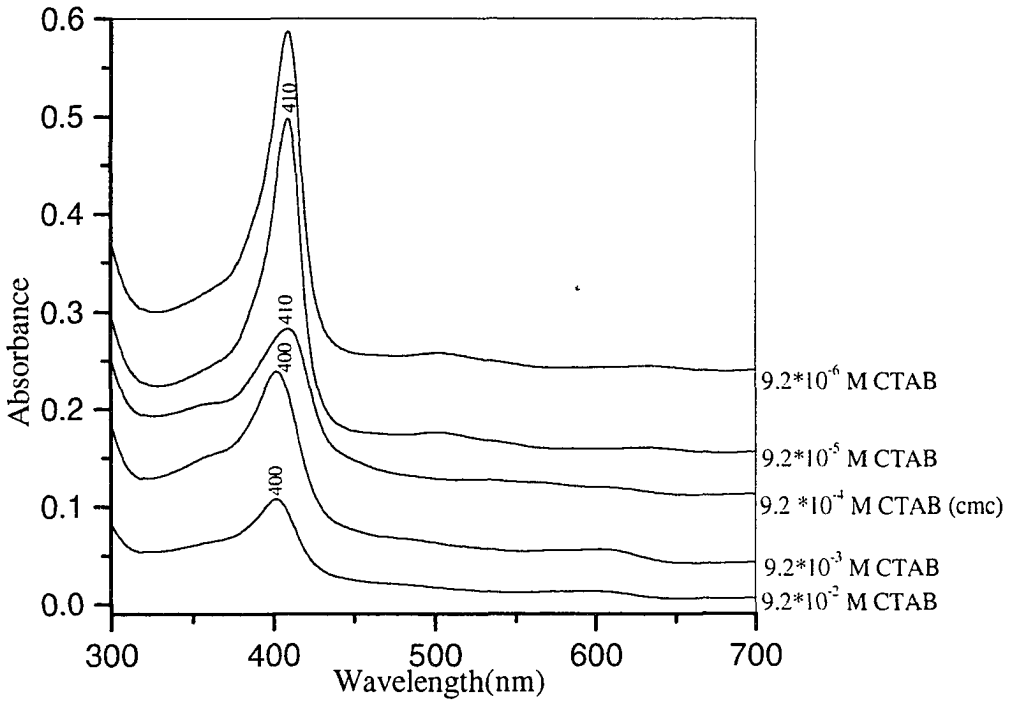

Fig 28 . UV-Vis of $1*10^{-6}$M horse skeletal muscle myoglobin mixed with an equal volume of CTAB surfactant solution.

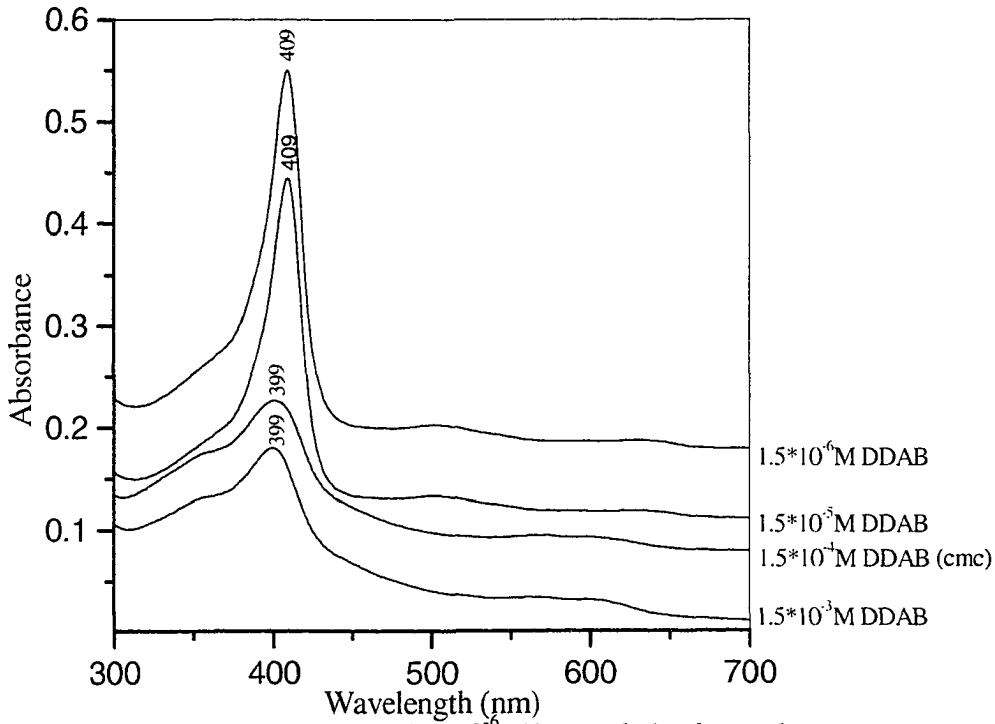

Fig 29.UV-Visible absorption spectra of $1*10^{-6}$M horse skeletal muscle myoglobin in mixed with an equal volume of DDAB surfactant solution.

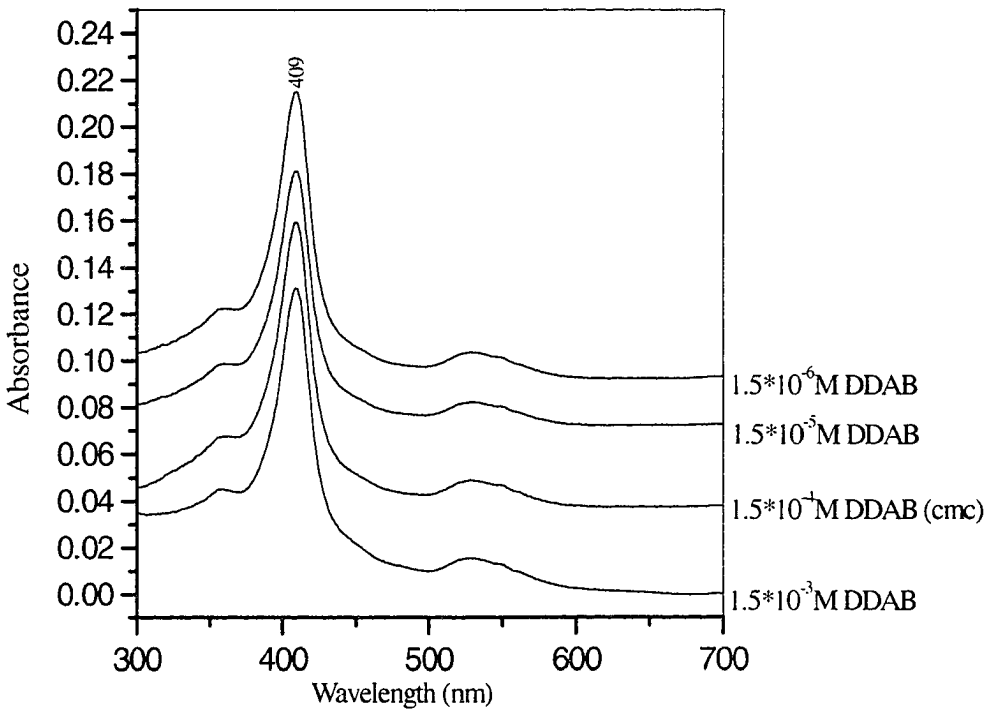

Fig 30.UV -Visible spectra of $1*10^{-6}$ M Horse Heart cytochrome C mixed with an equal volume of DDAB surfactant solution.

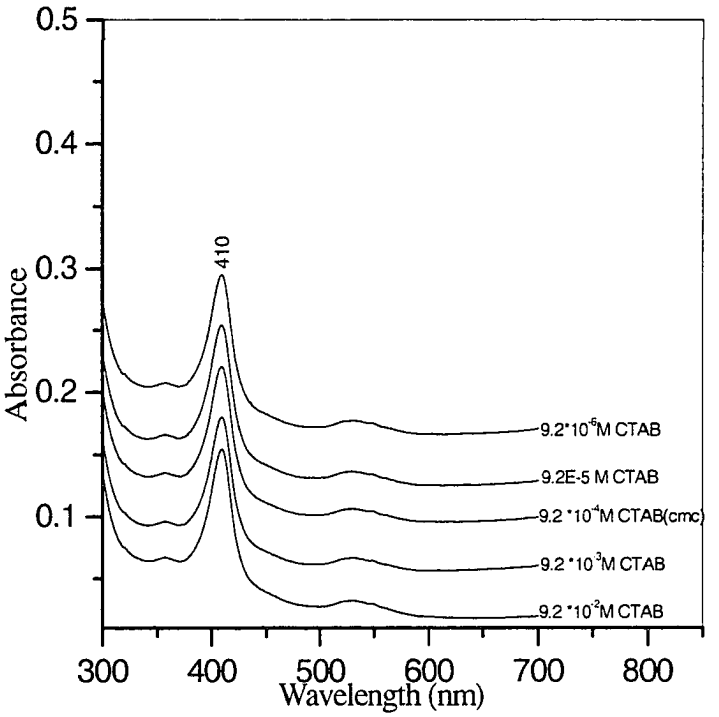

Fig 31. UV - Vis Spectra of $1*10^{-6}$ M Horse Heart Cytochrome C mixed with an equal volume of CTAB surfactant.

Cyclic voltammogram of heme proteins (Horse heart cytochrome c and horse skeletal muscle myoglobin) in the presence of DDAB surfactant adsorbed on Glassy carbon (GC),Silver (Ag) and Gold (Au) electrodes surface.

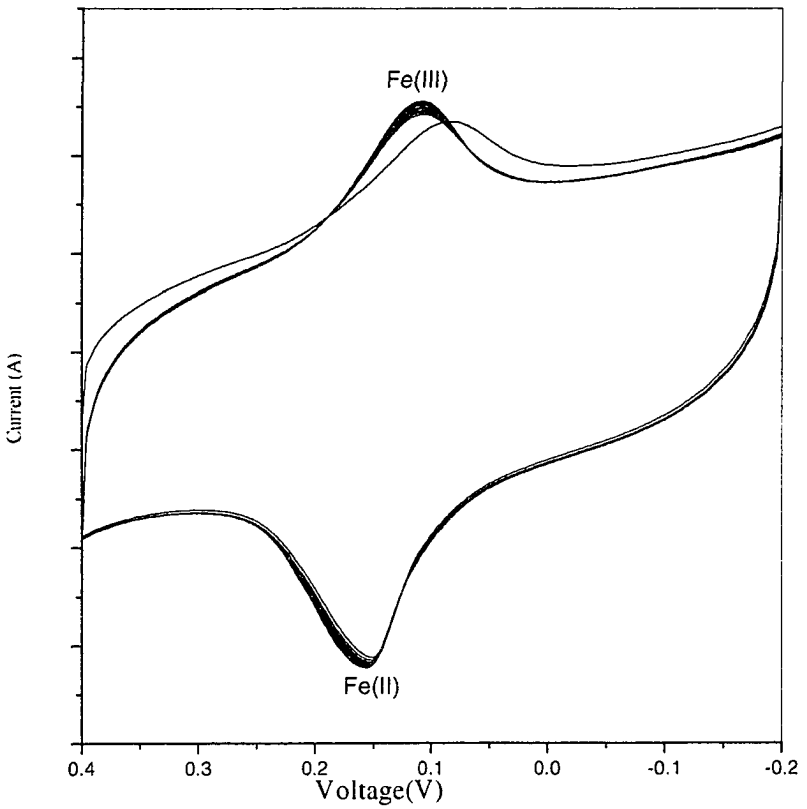

Fig 32. Cyclic voltammogram of 0.5mM of horse heart cytochrome C in 0.1mM DDAB on a glassy carbon electrode. Phosphate buffer pH =7 and Scan rate 0.05 v/s.

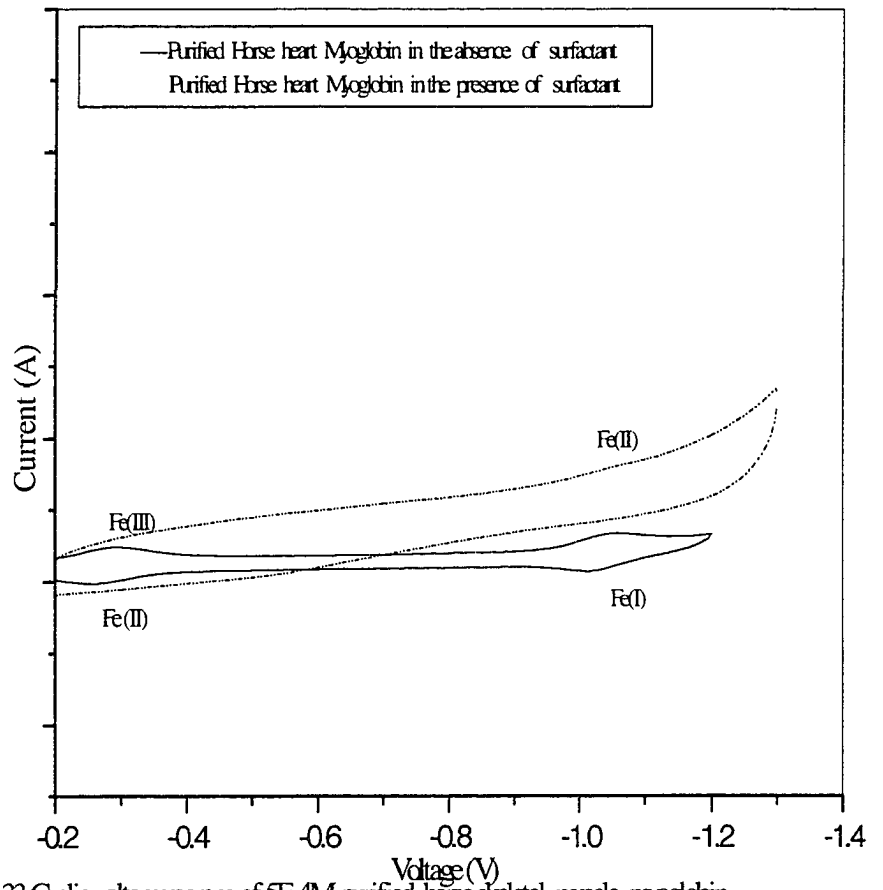

Fig 33. Cyclic voltammogram of 5E-4M purified horse skeletal muscle myoglobin in 0.1mM DDAB surfactant on a glassy carbon electrode in phosphate buffer pH=7 and scan rate 0.05 V/s.

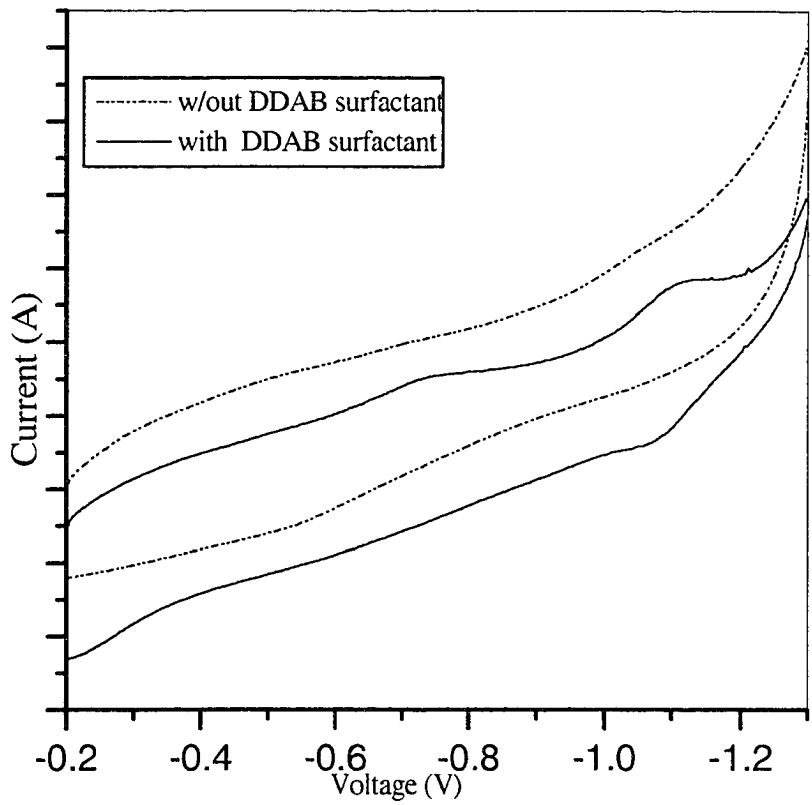

Fig 34 .Cyclic Voltammogram of 0.5mM horse skeletal muscle myoglobin in the presence and absence of surfactant on a silver (Ag)electrode surface. Phosphate buffer, pH =7, Scan rate = 0.05 v/s.

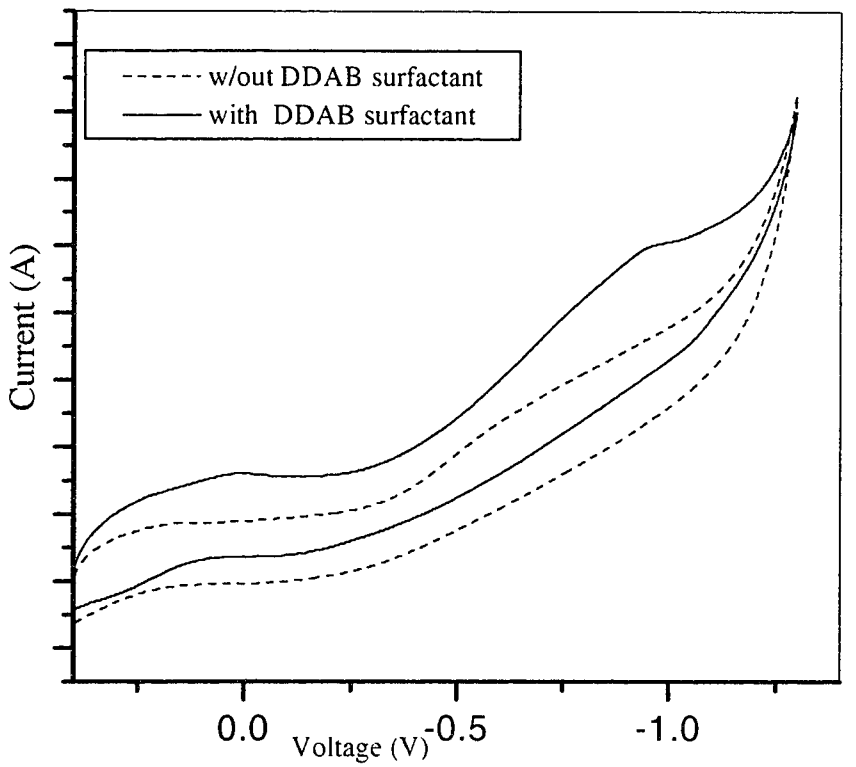

Fig 35. Cyclic Voltammogram of 0.5mM of horse skeletal muscle myoglobin on a gold electrode surface.Phosphate buffer pH =7, Scan rate = 0.05 v/s.

Surface-enhanced Raman spectra of heme proteins adsorbed on a silver electrode surface in the presence of surfactants .

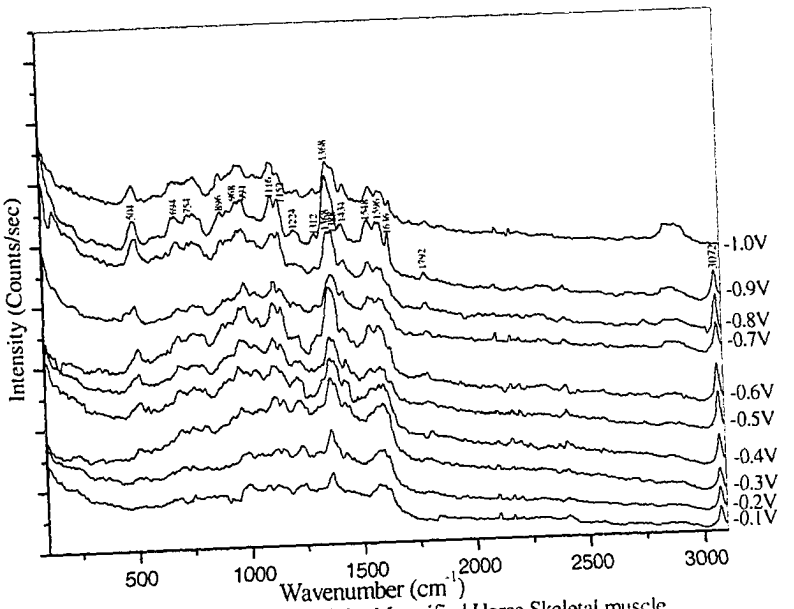

Fig 36.Surface-enhanced Raman Spectra of 0.5 mM purified Horse Skeletal muscle Myoglobin incorporated in 0.1mM DDAB surfactant on a silver electrode surface as a function of voltage in the 100-3100 cm^{-1} region.

Table 23.Vibrational Frequencies of the Surface-Enhanced Raman Spectra of Horse skeletal muscle myoglobin incorporated in multibilayer film of DDAB (Surfactant) as a Function of Voltage in the 100 –3100 cm^{-1} region on a silver (Ag) electrode surface.

-0.1V	-0.2V	-0.3V	-0.4V	-0.5V	-0.6V	-0.7V	- 0.8V	-0.9V	-1.0V	Assignments[a]
520	506	510	522	518	520	506	508	504	506	
694	696	702	696	700	700	696	702	694	690	(C_a- C_b-N) bent & (C_a- C_b) SStrch
754	748	756	764	758	770	764	750	754	782	(C_a- C_a-N) bent & (C_b- Et) SStrch
888	894	896	898	900	900	900	898	896	896	
		934	922	936		936	920	932		
974	970	972	962	970	970	968	970	968	972	
998	994	998			996		992	990		
		1048	1040	1034	1046	1040	1044	1050	1048	
1114	1116	1114	1106	1114	1114	1128	1128	1126	1114	(C_a-N) AStretch &(C_b- Et) AStrch
1136	1150	1156	1152	1152	1152	1150	1152	1152	1156	(C_b-E_t) AStretch & (C_a-N) AStrch
1224	1232	1218	1218	1236	1232	1216	1224	1222	1240	(C_m-H) Sbent & (Ca-C_b) SStrch
1326	1314	1312	1336	1334	1314	1312	1312	1314		(C_m-H) Abent & (Ca-C_b) AStrch
1370	1366		1366	1370	1368	1368	1362	1368	1372	(C_a-N) SStretch & (C_a-C_m) Sbent
1390	1384		1386	1384	1388	1380		1384	1394	(C_a-N) AStretch &(C_b- Et) AStrch
1432	1432	1430	1430	1440	1434	1436	1442	1428	1444	
		1480	1488							(C_a-C_m)SStretch & (C_a- C_b) SStrch
		1554		1548	1548	1542	1548	1548	1560	(C_b-C_b)SStretch & (C_b-E_t) SStrch
1572	1572	1574	1582	1584	1588		1588	1584		(C_a-C_m)AStretch &(C_a-C_b) AStrch
	1596	1594	1600	1608		1602			1600	(C_b- C_b) Stretch & (C_b-E_t) Strch
1618	1624			1632	1636	1636	1638	1636	1648	(C_a-C_m) Stretch &(C_a-C_b) Strch
		1802	1808	1794	1796	1798	1796	1794	1804	
2408	2406	2408	2408	2408	2406	2408	2408	2406		
3074	3072	3074	3076	3074	3074	3076	3074	3072		(C-H) in plane vibration of conjugated π bond of tetrapyrrole ring

AStrch = Asymmetrical stretch ; Abent = Asymmetrical bending ; SStretch = Symmetrical stretching ; Sbent = Symmetrical bending ; Assignments[a] = reference 26 .

Table 24. Spectroscopic Data of Protoporphyrins IX (Horse skeletal muscle Myoglobin) incorporated in DDAB and CTAB bilayers.

[Myoglobin] / [CTAB] (Ratio)	UV-Vis Spectrum λ_{Soret} / nm	[Myoglobin] / [DDAB] (Ratio)	UV-Vis Spectrum λ_{Soret} / nm
0.11	410	0.67	410
0.011	410	0.067	410
0.0011	410	0 .0067	400 (at cmc)
0.00011	400 (at cmc)	0.00067	400 (above cmc)
0.000011	400 (above cmc)	0.000067	400

[Myoglobin] = $1 * 10^{-6}$ M; T = 25 °C; [CTAB] = from $9.2 * 10^{-2}$ M to $9.2 * 10^{-6}$ M
[DDAB] = from $1.5 * 10^{-2}$ M to $1.5 * 10^{-6}$ M. cmc = critical micelle concentration

Table 25: Spectroscopic Data of Protoporphyrins IX (Horse heartCytochrome C) incorporated in DDAB and CTAB bilayers.

[Cytochrome C] / [CTAB] (Ratio)	UV-Vis Spectrum $\lambda_{Soret\,/\,nm}$	[Cytochrome C] / [DDAB] (Ratio)	UV-Vis Spectrum $\lambda_{Soret\,/\,nm}$
0.11	410	0.67	410
0.011	410	0.067	410
0.0011	410	0 .0067	410 (at cmc)
0.00011	410 (at cmc)	0.00067	410 (above cmc)
0.000011	410 (above cmc)	0.000067	410

[Cytochrome C] = $1 * 10^{-6}$ M; T = 25 °C; [CTAB] = from $9.2 * 10^{-2}$ M to $9.2 * 10^{-6}$ M
[DDAB] = from $1.5 * 10^{-2}$ M to $1.5 * 10^{-6}$ M; cmc = critical micelle concentration

Table 26: A pH dependence study of Protoporphyrins,(Horse heart Cytochrome C and Horse skeletal muscle Myoglobin) DDAB, and CTAB individually .

DDAB Concentration	pH Values	CTAB Concentration	pH Values	Protoporphyrin IX Concentration	pH Values
DDAB ($1.5*10^{-2}$ M)	4.62 ± 0.07	CTAB ($9.2*10^{-2}$ M)	5.40 ± 0.06	HSMM ($1*10^{-6}$ M)	6.32 ± 0.1
DDAB ($1.5*10^{-3}$ M)	5.54 ± 0.03	CTAB ($9.2*10^{-3}$ M)	5.43 ± 0.005	HH CytC ($1*10^{-6}$ M)	6.32 ± 0.1
DDAB ($1.5*10^{-4}$ M)	5.82 ± 0.005	CTAB ($9.2*10^{-4}$ M)	5.57 ± 0.06		
DDAB ($1.5*10^{-5}$ M)	6.04 ± 0.03	CTAB ($9.2*10^{-5}$ M)	5.63 ± 0.03		
DDAB ($1.5*10^{-6}$ M)	6.05 ± 0.04	CTAB ($9.2*10^{-6}$ M)	5.83 ± 0.10		

DDAB = dimethyldidodecylammoniumbromide; CTAB = Cetyltrimethylammoniumbromide
HSMM = Horse skeletal muscle myoglobin; HHCytC = Horse Heart Cytochrome C

Table 27: A pH dependence study of Horse skeletal muscle Myoglobin Incorporated in DDAB and CTAB Bilayers.

HSMM & DDAB (3ml each)	pH Values	HSMM & CTAB (3ml each)	pH Values
[$1*10^{-6}$ M] & [$1.5*10^{-2}$ M]	5.39 ± 0.23	[$1*10^{-6}$ M] & [$9.2*10^{-2}$ M]	5.15 ± 0.06
[$1*10^{-6}$ M] & [$1.5*10^{-3}$ M]	5.95 ± 0.15	[$1*10^{-6}$ M] & [$9.2*10^{-3}$ M]	5.74 ± 0.05
[$1*10^{-6}$ M] & [$1.5*10^{-4}$ M]	6.10 ± 0.10	[$1*10^{-6}$ M] & [$9.2*10^{-4}$ M]	5.91 ± 0.06
[$1*10^{-6}$ M] & [$1.5*10^{-5}$ M]	6.24 ± 0.03	[$1*10^{-6}$ M] & [$9.2*10^{-5}$ M]	6.07 ± 0.08
[$1*10^{-6}$ M] & [$1.5*10^{-6}$ M]	6.25 ± 0.08	[$1*10^{-6}$ M] & [$9.2*10^{-6}$ M]	6.13 ± 0.10

Table 28: A pH dependence study of Horse skeletal muscle Myoglobin Incorporated in DDAB and CTAB Bilayers.

HHCytC & DDAB (3 ml each)	pH Values	HHCytC & CTAB (3 ml each)	pH Values
[$1*10^{-6}$ M] & [$1.5*10^{-2}$ M]	5.18 ± 0.07	[$1*10^{-6}$ M] & [$9.2*10^{-2}$ M]	5.48 ± 0.12
[$1*10^{-6}$ M] & [$1.5*10^{-3}$ M]	5.79 ± 0.12	[$1*10^{-6}$ M] & [$9.2*10^{-3}$ M]	5.80 ± 0.07
[$1*10^{-6}$ M] & [$1.5*10^{-4}$ M]	5.97 ± 0.13	[$1*10^{-6}$ M] & [$9.2*10^{-4}$ M]	5.96 ± 0.17
[$1*10^{-6}$ M] & [$1.5*10^{-5}$ M]	6.07 ± 0.06	[$1*10^{-6}$ M] & [$9.2*10^{-5}$ M]	6.07 ± 0.06
[$1*10^{-6}$ M] & [$1.5*10^{-6}$ M]	6.04 ± 0.08	[$1*10^{-6}$ M] & [$9.2*10^{-6}$ M]	6.05 ± 0.14

Table 29.
Oxidation state and spin state of the iron in the heme chromophore of purified Horse skeletal muscle myoglobin into bilayers of DDAB surfactant as a function of voltage.

Voltage	Oxidation State	Spin State
-0.1V	1370	1572, 1594, 1618
-0.2V	1360	1572, 1596, 1618
-0.3V	1366, 1386	1566, 1594, 1618
-0.4V	1370, 1384	1582, 1600, 1616
-0.5V	1370, 1386	1548, 1588, 1632
-0.6V	1368	1548, 1588, 1636
-0.7V	1382	1542, 1590, 1634
-0.8V	1368, 1388	1548, 1590, 1634
-0.9V	1368	1548, 1602, 1636
-1.0V	1368, 1394	1548, 1600, 1648

F. References

[1].Turner, A. P.F.; Karube, I.; Wilson, G.S. *Biosensors; Oxford University Press:Oxford, U.K., 1987.*

[2].(a) Simon, H.; Bader, J.; Gunther, H.; Newman, S.; Thomas, J.Agnew. *Chem. Int. Ed.Engl. 1985, 24, 529.*
(b) Laane, C.; Pronk, W.; Franssen, M.; Veeger, C. *EnzymeMicrob.Technol. 1984, 6, 165.*
(c) Bourdillon, C.; Lortie , R.; Laval , *J.M.Biotechnol.Bioeng. 1988,31, 553.*

[3].Collman, J.P.; Gagne, R.R.; Reed, C.A.; Halbert, T,R.; Lang , G.; Robinson, W.T. *J. Am. Chem.Soc.1975, 97,1427-1439.*

[4].Tabushi, I.; Kodera, M.; Yokohama, M. *J. Am.Chem.Soc.1985, 107,4466-4473.*

[5].Barber, D.C.; Whitten. D.G. *J. Am. Chem. Soc. 1987, 109, 6842-6844.*

[6].(a) Simone, M.J.; Kreishman, G.P. *Anal. Biochem. 1983, 132, 142-146.*

(b) Hildebrandt , P.; Stockburger, M. *Biochemistry 1989, 28, 6710-6721.*

[7].(a) Moss, D.; Nabedryk, E.; Breton, J.; Mantele, W. *Eur. J. Biochem. 1990, 187, 565-572.*
(b) Schlereth, D.D.; Mantele W. *Biochemistry 1992, 31, 7494-7502.*

(b) Schlereth, D.D.; Fernandez, V. M.; Mantele W. *Biochemistry 1993, 32, 9199-9208.*

[8].Battistuzzi, G.; Borsari , M.; Ferretti, S.; Sola, M.; Soliari, E . *Eur. J. Biochem.1995, 232, 206-213.*

[9].(a) Yuan , X.; Sun, S.; Hawkridge, F.M .; Chlebowski, J.F.; Taniguchi, I. *J. Am.Chem. Soc. 1990 , 112 , 5380-5381.*
(c) Nishiyama , K.; Hawkridge, F.M. *Biochem. Biophys. Res. Commun. 1994 , 205 1724- 1728.*

[10].Rusling, J. F.; Nassar, A.-E.F. *J. Am . Chem. Soc. 1993, 115, 11891-11897.*

[11].(a) Nassar, A. -E. F.; Willis, W. S.; Rusling , J.F. *Anal.Chem. 1995, 67, 2386-2392.*
(b) Rusling, J.F.; Nassar, A. -E. F. *Langmuir. 1994, 10, 2800-2806.*

[12].(a) Nassar, A. -E. F.; Narikiyo, Y.; Sagara, T.; Nakashima, N.; Rusling, J.F. *J. Am. Chem. Soc.; Faraday Trans. 1995, 91, 1775-1782.*

(b) Zhang, Z.; Rusling, J.F.; *Biophys.Chem.; in press.*

[13].Nassar, A. -E. F.; Zhang, Z.; Chynwat, V.; Frank, H.A.; Rusling, J.F.; Suga, K. *J. Phys. Chem. 1995, 99, 11013-11017.*

[14]. Nassar, A. -E. F.; Bobbitt, J.M.; Stuart, J.D.; Rusling, J.F. *J. Am. Chem. Soc. 1995, 117, 10986-10993.*

[15].Sun, S. C. Bernard, I.; Birke, R. L.; Lombardi, J. R. *J. electroanal. Chem. 1985, 196, 359.*

[16]. (a)Theorell, H.; Ehrenberg, A. *Acta Chem.Scand. 1951, 5, 823-848.*
(b)George, P.; Hanania, G. *Biochem. J. 1952, 52, 517-523.*
(c)Herskovits, T.T.; Jaillet, H. *Science 1969, 163, 282-285.*

[17].(a) Brunori, M.; Giacometti, G.M.; Antonini, E.; Wyman, J. *J.Mol.Biol. 1972,63,*139-152.
(b) Takahashi-Ushijima, E.; Kihara, H. *Biochem.Biophys. Res.Commun. 1982, 105, 965-968.*

[18].Nassar, A-E.F.; Zhang, Zhe.; Hu, Naifei.;Rusling, J.F. *J. Phys. Chem B 1997, 101, 2224-2231.*

[19].(a) Puett, D. *J. Biol.Chem. 1973, 248, 4623-4634.*
(b) Tang, H-L.; Chance, B.; Mauk. A . G.; Powers, L.S.; Reddy, K.S.; Smith, M. *Biochem. Biophys. Acta. 1994, 1206, 90-96.*

[20].Yang, A-S.; Honig, B. *J.Mol.Biol. 1994, 237, 602-614.*

[21].(a) Goto, Y.; Fink, A.L. *J.Mol.Biol. 1990, 214, 803-805.*
(b) Stigter, D.; Alonso, D.O.V.; Dill, K.A. *Proc.Natl. Acad. Sci. USA. 1991, 88, 4176- 4180.*

[22].Friend, S.H.; Gurd, F.R.N. *Biochemistry 1979, 18, 4612-4619; 4620-4630.*

[23].Bashford,D.; Case, D.A.; Dalvit, C.; Tennant, L.; Wright, P.E.*Biochemistry 1993, 32, 8045-8056.*

[24].Cocco, M. J.; Kao, Y-H.; Phillips, A-T.; Lecomte, J.T. *J.Biochemistry 1992, 31, 6481-6491.*

[25]. Spiro,T. G . in "*Biological applications of Raman Spectroscopy* " *1988 Volume 3 , by John Wiley & Sons Inc .*

BIBLIOGRAPHY

Chapter 1

[1].Albrecht, A . C. *J. Chem. Phys.* 1961 , 34 , 1436 .

[2].Syzmanski, H. A . in " *Raman spectroscopy, Theory and Practice" Vol. 1, Plenum Press, 1967 pages 7& 31.*

[3].Faquharson, S. K .; Guyer, L.; Lay, P. A.;Maynuson, R .H. *Gov.Rep.Announce., Index (U.S)1984, 20, 64 .*

[4].Lombardi, J. R.; Birke, R. L.; Sanchez,L. A.; Bernard, I.;Sun, S. C. *Chem. Phys.Letter.1984, 104 ,240 .*

[5].Lombardi, J. R.; Birke, R. L .;Lu, Tianhong.; Xu, Jia *J. Chem. Phys. 1986, 84 ,4174 .*

[6].Furtak,T. E .;Reyes, J. *Surface Science 1980, 93, 351 .*

[7].Pettinger, B.; Wenning , U.;Wetzel, H. *Chem. Phys. Letter. 1979, 67, 192 .*

[8].Albrecht, M. G.; Creighton, J. A. *J. Am. Chem. Soc., 1977, 99, 5215.*

[9].Jeanmaire, D. J.; Van Duyne, R. P. *J. Electroanal. Chem. 1977,84, 1.*

[10].Manzel, K.; Schutze, W.; Moskovits, M. *Chem. Phys. Letter. 1982, 85, 183 .*

[11].Gao, P.;Weaver, M. J. *J. Phys. Chem. 1985, 89, 5040 .*

[12].Moskovits, M.;Dillela, D.P. *Chem. Phys. Letter. 1983,73,500 .*

[13].Dilella, D. P.;Moskovits, M. *J. Phys. Chem. 1981, 85,2042 .*

[14].Moskovits, M.; and Dilella, D. P. in " *Surface-enhanced Raman Scattering" (R. K. Chang and T. E. Furtak, eds) pages 243-273 Plenum Press. New York (1982) .*

[15].Raman,C. V.; Krishnan, K. S. *Nature 1928, 121, 501 .*

[16].Sun, S. *PhD. Dissertation City University of New York. (1987) .*

[17].Moskovits, M . *J.Chem . Phys. 1960, 44, 310 .*

[18].Lombardi, J. R.; Birke, R. L. in " *Surface- Enhanced Raman scattering "*

from spectroelectrochemistry: Theory and Practice Edited by R. J. Gale

[19].Moskovits, M.; Suh, J .S. *J. Phys. Chem. 1984, 88, 5526 .*

[20].Creighton, J. A . *Surface Science 1983, 124, 209-219 .*

[21].Fleischmann,M .; Hendra, P. J.;Mc Quillan, A. J. *J. Chem. Soc. Chem. Comm. 1973, 80*

[22].Kimura, F.; Umemura, J.; Takenaka, T. *Langmuir 198, 2 , 96 .*

[23].Busby, C.C.; Creighton, J. A. *J. Electroanal. Chem. 1982 , 140 , 379 .*

[24].Moskovits, M . in " *Surface roughness and the enhanced intensity of Raman scattering by molecules adsorbed on metals" J. Chem. Phys 1978, 69, 4159.Enhanced Raman Scattering by molecules adsorbed on electrodes. A theoretical Model, Solid State Commun. 32: 59 (197) .*

[25].Weitz, D. A.; Gramila,T. J.; Genack, A. Z.; Gersten, J. I. in "*Anomalous low- frequency Raman Scattering from rough metal surfaces and the origin of surface-enhanced Raman scattering" Phys. Rev. Letter. 1980, 45 , 355 . Inelastic Mie Scattering from rough metal surfaces: Theory and Experiment, Phys. Rev. 1980, B 22, 4562.*

[26].Carey, P. R . in " *Biochemical applications of Raman and resonance Raman spectroscopies" Academic Press Inc. (1982)*

[27].Chang, R . K .;Furtak,T.E. in " *Surface- Enhanced Raman scattering" Library of Congress Cataloging in Publication Data. Plenum Publishing Corporation (1982) .*

[28].Fleischmann,M.;Hendra, P. J.;Mc Quillan A . *J. Chem. Phys. Letter. 1974, 26 ,163 .*

[29].Van Duyne, R . P. in " *Chemical and Biochemical Applications of Lasers" C. B. Moore Editor, Academic Press, New York 1974, 4, Ch. 5 .*

[30].Birke, R .L .;Lombardi, J.R.;Sanchez, L. A. in " *Advances in Chemistry Series" No 201, Karl M. Kadish, Editor, ACS 4 (1982) 69 .*

[31].Furtak, T. E.; Reyes-Corona *J. Surf. Sci. 1980, 93, 382 .*

[32].Otto, A . *Appl. Surf. Sci. 1980 ,6 , 309 .*

[33].Bockris, J. O'M ;Reddy, A . K. N . *in "Modern Electrochemistry" 1970, Vol. 2, Plenum Press, New York .*

[34].Diem, M. in *"Introduction to Modern Vibrational Spectroscopy " New York , John Wiley and Sons: (1993) .*

[35].Baranska, H .;Labudzinska, A .;Terpinski, J . in *"Laser Raman Spectroscopy " Trans . J .R .Majer . Chichester (England): Ellis Harwood Ltd: (1987) .*

[36].Heller, E . J. in *"The Semiclassical way to Molecular Spectroscopy." Accounts of Chemical Research. 1981, 14 , 368-375 .*

[37].Heller E. J.; Sundberg, R .L. Tannor, D. in *"Simple Aspects of Raman Scattering" Journal of Physical Chemistry. 1982, 86, 1822-1833 .*

[38].Levine, I . N. *"Quantum Chemistry" 4th ed. New York: Prentice Hall : 1991 .*

[39].Merzbacher, E . *"Quantum Chemistry" New York: John Wiley and Sons, 1962 .*

[40].Parson, R . *J. Electroanal. Chem., 1981, 3, 118.*

[41].Valette, G. *J. Electroanal. Chem.,1982, 132, 31 .*

[42].Kotz, R .; Yeager, E . *J. Electroanal . Chem .,1981, 123, 335 .*

[43].Anderson, A. B.; Kotz, R .; Yeager,E . *Chem. Phys. Letter. 1981, 82, 130 .*

[44].King ,F. W.; Van Duyne,R . P.; Schatz, G. C. *J.Chem. Phys. 1978, 69 ,4472 .*

[45].Macomber, S.H .;Furtak, T. M . *Surf. Sci. in press .*

[46].Pettinger, B.; Moere, L . *J. Electroanal. Chem. in press .*

[47].Hosten, C. *Ph.D. Dissertation The City University of New York. (1991).*

[48].Pettinger, B.;Tadjeddine, A .;Kolb, D. M. *Chem. Phys. Lett.1978, 66, 544.*

[49].Furtak, T. E. ; Kester, J.J. *J. Phys. Rev. Lett. 1980, 45 , 1652 .*

[50].Kester, J. J .;Furtak, T. E. *Solid State Commun.1982, 41, 457 .*

[51].Murray, C. A. in *" Surface Enhanced Raman Scattering ", R. K. Chang and T. G.Furtak editors, Plenum, New York 1982, p. 203 .*

[52].Trott, G. R .; Furtak, T. E . *Solid State Commun 1980, 36, 1011 .*

[53].Creighton, J. E. in " *Surface Enhanced Raman Scattering*", *R. K. Chang and T. E . Furtak editors , Plenum , New York , 1982, p. 315 .*

[54].Chen, C. K .; de Castro, A . R . B.; Shen, Y. R . *Phys. Rev . Lett .1981, 46, 145 .*

[55].Pettinger , B.; Wenning, U.; Kolb, D.M .; Bunsenges, B. *Phys. Chem.1978, 82, 1326 .*

[56].Loo, B. H. *J. Phys. Chem. 1982, 86 ,433 .*

[57].Fleischmann, M .;Hendra, P. J.;Hill, I . R .; Pemble, M .E . *J. Electroanal. Chem.1981, 117, 243 .*

[58].Pettinger, B .; Philpott, M.; Gordon, H . *J. Surf. Sci. 1981, 105 ,469 .*

[59].Chen, T. T.; Owen, J. F.; Chang, R . K. *Chem. Phys. Lett. 1982, 89 ,356 .*

[60].Macomber, S.H .; Furtak, T. E.; Devine, T. M . *Surf . Sci . in press.*

[61].Macomber, S.H .; Furtak, T. E.;Devine, T. M . *Chem . Phys. Lett .1982, 90 ,439*

[62].Barz, F. G .; Gordon, J. G .; Philpott, M . R. Weaver, M. *J. Chem. Phys. Lett 1982, 91 (4) ,291 .*

[63].Chen ,T. T.; van Rabeu, K . U .; Owen, J . F.;Chang, R . K. Laube, B. L . *Chem. Phys. Lett.1982, 91 (6), 494.*

[64].Demuth, J. E .; Sanda Warlaumont, J. M .;Tsang , J . C.Christman, K . in *"Vibrations at Surfaces" editors R . Candano, J. M . Gilles and A . A . Lueas Plenum, New York, 1982, p. 391 .*

[65].Woodand,T. H.; Klein, M . V. *J. Vac. Sci. and Tech .1979, 16, 459 .*

[66].Furtak,T. E .; Trott, G .;Loo, B . H . *Surf . Sci 1980, 101,374 .*

[67].Gersten, J. I .; Birke, R .L.Lombardi, J . R . *Phys. Rev . Lett.1979, 43 ,147*

[68].Furtak,T. E.;Macomber, S . H. *Chem. Phys. Lett. 1983, 95 , 328 .*

[69].Creighton, J . A .;Albrecht, H . G.;Hester, R . E.;Matthew, J .A .D. *Chem. Phys . Lett . 1978 , 55, 55 .*

[70].Wenning, U .; Pettinger, B.;Wetzel, H. *Chem. Phys. Lett. 1980, 70 , 49 .*

[71].Schmeisser,D.; Demuth, J . E . Avouris, P . H. *Chem . Phys . Lett . 1982,8 , 324 .*

[72].Person, B . N. J . *Chem . Phys . Lett . 1981, 82, 561 .*

[73].Wood, T. H.;Klein, M . V. *Solid State Commun. 1980, 35,263 .*

[74].Furtak, T. E.; Macomber, S . H . *Chem . Phys . Lett . 1983, 95, 328 .*

[75].Allen, C . S.; Schatz, G . C.; Van Duyne, R . P. *Chem . Phys . Lett . 1980 , 75 ,201 .*

[76].Otto, A. *Surf . Sci . 1978, 75, L 392 .*

[77].Pettinger, B.;Wetzel, H . *Chem . Phys . Lett . 1981, 78, 398 .*

[78].Busby, C. C.;Creighton, J. A. *J . Electroanal. Chem . 1982,133,183 .*

[79].Fleischmann, M .; Hendra, P. J .; Hill, I . R .; Pemble, M .E . *J. Electroanal . Chem . 1981,117, 243 .*

[80].Allen, C . S.; Van Duyne, R. P. *J. Am . Chem . Soc. 1981,103,7497 .*

[81].Wetzel, H.; Gerischer , C. *Chem . Phys . Lett . 1980, 76, 460 .*

[82].Cotton, T . M. *J. Am . Chem . Soc., 1980, 102,7960 .*

[83].Cotton,T. M .; Schultz, S. G.; Van Duyne, R . P. *J . Am . Chem . Soc . 1981, 102, 7960.*

[84].Bernard, I .*Ph.D. Dissertation The City University of New York. (1987).*

[85].Gersten , J. I.; Nitzan, C. *J.Chem .Phys.1980, 73 , 3023*

Chapter 2

[1].Fleishman, M.; Hendra, P.J. ; McQuillan, A.J. *Chem. Phys. Lett.* 1974, 26, 163.

[2].(a) Kneipp, K.; Kneipp, H.; Itzkan, I.; Dasari, R. R.; Feld, M. S. *Chem. Rev.* 1999, 99,2957-2956. (b) Campion, A.; Kambhampati P. *Chem. Soc. Rev.* 1998, 27, 241-250.

[3].Doering, W. H. ; Nie, S. *J. Phys Chem. B* 2020, 106, 311-317

[4].Kennedy, B. J.; Spaeth, S.; Dikey, M.; Carron, K. T. *J. Phys Chem. B* 1999, 103, 3640-3646

[5].Hill, W. ; Fallourd, V.; Klocjow, D. *J. Phys Chem. B* 1999, 103, 4707-4713

[6].Cao, Y-W,; Jin, R,; Mirkin, C. A. *Science* 2002, 297 1536-1540.

[7].Birke, R. L.; Lombardi, J. R. *Spectroelectrochemistry: theory and practice*; Gale, R. J., Ed.; Plenum Publishing Corporation: New York, 1988; pp. 263-347.

[8].Bagus, P. S., Pacchioni, G., Philpott, M. R. *J. Chem. Phys.*, 1989, 90, 4287-4295

[9].Rodrigues, J. A. *Surf. Sci.*, 1990, 226, 101-118

[10].Bagus, P. S., Herman,K., Bauschlicher, C. W. Jr. *J. Chem. Phys.*, 1984, 81, 1966-1974

[11].Rodrigues, J. A. *Surf. Sci.*, 1992, 273, 385-404.

[12].Kasser, W.; Kettler, U.; Bechthold, P.S. *Chem. Rev. Let.* 1982, 86, 223-227.

[13].Lombardi, J. R.; Shields Knight, E. A.; Birke, R. L. *Chem. Phys. Lett.* 1981, *79*, 214-218.

[14].Creighton, J. A.; Albrecht, M. G.; Hester, R.E.; Matthew, J. A. D. *Chem. PhysLett.* 1978, *55*, 55-58.

[15].Van Duyne, R. P. *Chemical and biochemical application of lasers*; Moore, C. B.,Ed.; Academic Press: New York, 1979; Vol. 4, Ch 5, pp. 101-185.

[16].Evans, J. F.; Albrecht, M. G.; Ullevig,, D. M.; Hexter, R. E. *J. Electroanal. Chem.* 1980, *106*, 209-234.

[17].Neto, N.; Muniz-Miranda, M.; Sbrana, G. *J. Phys. Chem.* 1996, *100*, 9911 9917.

[18].Muniz-Miranda, M.; Neto, N.; Sbrana, G. *J. Phys. Chem.* 1988, *92*, 954-959.

[19].Creighton, J. A. *Surf. Sci.* 1983, 124, 209-219

[20].Netzer, F. P.; Bertel, E.; Matthew, J. A. D. *Surf. Sci.* 1980, 92, 43-52.

[21].Surman, M.; Bare, S. R.; Hoffman, P.; King, D. A. *Surf.Sci.* 1987, 179, 243-253.

[22].Dudde, R.; Koch, E. E.; Ueno, N.; Engelhardt, R. *Surf. Sci.* 1986, *178*, 646-656.

[23].Bridge, M. E.; Connolly, M.; Lloyd, D. R., Somers, J.; Jakob, P.; Menzel, D. *Spectrochim. Acta A* 1987, 43, 1473-1478.

[24].Moskovits, M. ; Suh, J. S. *J. Chem. Phys.* 1984, 88, 5526

[25].Golab, J. T.; Sprague, J. R.; Carron, K. T.; Schatz, G. C.; Van Duyne, R. P. *J.Chem. Phys.* 1988, *12*, 7942-7951.

[26].Billman, J.; Kovacs, G.; Otto, A. *Surf. Sci.* 1980, *92*, 153-173.

[27].Bunding, K. A.; Birke, R. L.; Lombardi, J. R. *Chem. Phys.* 1980, *54*, 115-121.

[28].(a) Roy, D.; Furtak, T. E. *Chem. Phys. Lett.* 1986, *124*, 299-303 (b) Roy, D.; Furtak, T. E. *Phys. Rev.* B 1986, *344*, 5111-5117

[29].Corni, S.; Thomasi, J. *J. Chem. Phys.* 2002, *116*, 1156-1164.

[30].Cornis S.; Thomasi, J. *J. Chem. Phys.* 2001, *114*, 3739-3751.

[31].Corni, S.; Thomasi, J. *Chem. Phys. Lett.* 2001, *342*, 135-140.

[32].Kwon, Y. J.; Son, D. H.; Ahn, S. J.; Kim, M. S.; Kim, K. *J. Phys. Chem.* 1994, *98*, 8481-8487.

[33].Cardini, G.; Muniz-Miranda, M. *J. Phys. Chem.* 2002, *106*, 6875-6880.

[34].Arenas, J. F.; Soto, J.; López Tocón, I.; Fernández, D. J.; Otero, J. C. *J. Chem.Phys.* 2001, 116, 7207-7216.

[35].Vivoni, A.; Chen S. -P.; Ejeh, D.; Hosten, C. M. *Langmuir* 1999, *16*, 3310-3316.

[36].Aroca, R. F.; Clavijo, R. E.; Halls, M. D.; Schlegel, H. B. *J. Phys. Chem.* A 2000, *104*, 9500-9505.

[37].Yang, W. H.; Schatz, G. C. J. Chem. Phys. 1992, 97, 3831-3845.

[38].Muniz-Miranda, M. *J. Phys. Chem.* 2000, *104*, 7803-7810.

[39].Barlow, A.; Diem, M. *J. Chem. Ed.* 1991, *68*, 35-39.

[40].Vivoni, A.; Birke, R.; Lombardi, J. *Spectrochim. Acta A* 2001, *57*, 535-544.

[41] .Suzuki, S.; Orville-Thomas, W. J. *J Mol. Struct.* 1976, 37, 321-327.

[42].Nilsson, K.; Oskarsson, A. *Acta Chem. Scand. A* 1982, 36, 605-610.

[43].Stidham, H. D.; DiLella, D. P. *J. Raman Spectrosc.* 1980, *9*, 247-256.

[44].M. J. Frisch, G. W. Trucks, H. B. Schlegel, G. E. Scuseria,
M. A. Robb, J. R. Cheeseman, V. G. Zakrzewski, J. A. Montgomery, Jr.,
R. E. Stratmann, J. C. Burant, S. Dapprich, J. M. Millam,
A. D. Daniels, K. N. Kudin, M. C. Strain, O. Farkas, J. Tomasi,
V. Barone, M. Cossi, R. Cammi, B. Mennucci, C. Pomelli, C. Adamo,
S. Clifford, J. Ochterski, G. A. Petersson, P. Y. Ayala, Q. Cui,
K. Morokuma, P. Salvador, J. J. Dannenberg, D. K. Malick,
A. D. Rabuck, K. Raghavachari, J. B. Foresman, J. Cioslowski,
J. V. Ortiz, A. G. Baboul, B. B. Stefanov, G. Liu, A. Liashenko,
P. Piskorz, I. Komaromi, R. Gomperts, R. L. Martin, D. J. Fox,
T. Keith, M. A. Al-Laham, C. Y. Peng, A. Nanayakkara, M. Challacombe,
P. M. W. Gill, B. Johnson, W. Chen, M. W. Wong, J. L. Andres,

[45].Bürig, H.-B.; Dunitz, J. D. *J. Am. Chem. Soc.* 1987, 109, 2924-2926.

[46].Li, X.-Y.; Zgierski, M. Z. *J. Phys. Chem.* 1991, 95, 4268-4287.

[47].Herschbach, D. R.; Laurie, V. W. *J. Chem. Phys.* 1961, 35, 458-463.

[48].Majoube, M. *J. Raman Spectrosc.* 1985, 16, 98-110.

[49].Moskovits, M.; and Di Lella, D. P. *J. Chem. Phys.* 1980, *73*, 6068-6075.

[50].Gao, P.; Weaver, M. J. J. *Phys. Chem.* 1985, 89, 5040-5046.

[51].Faria, P. A.; Chen, X., Lombardi, J. R.; Birke, R. L. *Langmuir* 2000, 16, 3984-3992

[52].Li, W.-H.; Li, X.-Y.; Yu, N.-T. *Chem. Phys. Lett.* 1999, 305, 303-310.

[53].Vekatesan, S.; Erdheim, G; Lombardi, J. R,; Birke, R. L. *Surf. Sci.* 1980, 101, 387

[54].Anderson, A. B.; Kotz, R.; Yeager, E. Chem Phys. Lett. 1981, 82, 130

[55].Lin, W. F.; Tian, Z. Q.; Sun, S. G.; Tian, Z. W. *Electrochimica Acta* 1992, 37, 211-213

[56].Takahasi, H.; Mamola, K.; Plyler, E. K. *J. Mol. Spectrosc.* 1966, *21*, 217-230.

[57].Arenas, J. F.; Woolley, M. S.; López Tocón, I.; Otero, J. C.; Maecos, J. I. *J.Chem. Phys.* 2000, *112*, 7669-7683.

[58].Carter, D. A.; Pemberton, J. E.; Woelfel, K. J. *J. Phys. Chem.* 1998, *102*, 9870-9880.

[59].Watanabe, T.; Kawanami, O.; Honda, K; Pettinger , B. *Chem. Phys. Lett.* 1983, 102 , 565-569.

[60].Bosnick , K.A., Ph.D. Thesis, University of Toronto, 2000

[61].Haslett, T. L.; Bosnick ,K. A.; Moskovits, M. *J. Chem. Phys.* 1998 108, 3453-3457

[62].Eachus, R.S. ; Symons, M.C.R., *J. Chem. Soc. A 1970, 1329-*

[63].Baetzold, R.C.*J.Chem.Phys. 1971,55, 4363- 4370*

[64].Lambert, D.K. *Electrochimica Acta 1996, 5 ,623-630*

[65].Lombardi, J.R.; Birke, R.L., Lu, T., Xu, J. *J.Chem.Phys. 1986, 84, 4147-4180*

[66].Moskovits, M. *Reviews of Modern Physics 1985, 57, 783-826*

[67].Tian, Z.Q.; Li, W. H.; Qiao, Z.H.; Lin, W.F.; Tian, Z.W. *Russian J. of Electrochem. 1995, 31, 935-940.* From Elektrokhimiya. 1995, 31, 1014-1020

Chapter 3

[1].Cotton,T. M.; Schultz, S . G.;Van Duyne, R . P. *J . Am . Chem.Soc . 1980, 102,7962 –7965 .*

[2].Spiro,T. G . in "*Biological applications of Raman Spectroscopy " 1988 Volume 3 , by John Wiley & Sons Inc .*

[3].Carey, P.R. in " *Biological applications of Raman and Resonance Raman*

Spectroscopies " 1982 Academic Press Inc .

[4].Strekas,T . C.; Spiro,T. G . *Biophys . Biochim .Acta , 1972, 263, 830*

[5].Strekas,T . C.; Spiro,T. G . *Biophys . Biochim .Acta , 1972, 278,188*

[6].Strekas,T . C.; Spiro,T. G . *Proc . Natl .Acad .Sci ., 1972, 69, 2622*

[7].Sunder, S.; Bernstein, H . *J. Raman Spectroscopy ., 1976, 5, 351*

[8].Burke, J . M .; Kincaid, J . R .; Spiro,T . G . *J . Am . Chem . Soc., 1978, 100, 6077*

[9].Stein, P.; Ulman, A.; Spiro, T. G. *J . Phys . Chem ., 1984, 88,369-374*

[10].Kitagawa,T.; Abe, M .; Ogoshi, H . *J . Chem . Phys ., 1978, 69, 4516*

[11].Abe, M .; Kitagawa, T.; Kyogoku, Y. *J . Chem. Phys ., 1978, 69 , 4526*

[12].Choi, S .; Spiro, T. G.; Langry, K. C.; Smith, K. M. *J. Am. Chem. Soc.,* 1982, 104,4337

[13].Choi, S.; Lee, J. J.; Wei, Y. W.; Spiro, T. G. *J. Am. Chem. Soc., 1983, 105,3707*

[14].Choi, S.; Spiro, T. G. *J. Am. Chem. Soc., 1983,105, 3683*

[15].Spiro, T. G. in " *Resonance Raman spectroscopic studies of Heme proteins " Biochimica et Biophysica Acta , 1975, 416, 169 –189*

[16].Spiro, T. G.; Strong, J. D.; Stein, P. *J. Am. Chem., 1979,101,2648*

[17].Strong, J. D.; Burke, J. M.; Daly, P.; Wright, P.; Spiro,T.G. *J. Am. Chem. Soc., 1980, 102, 5815*

[18].Teraoka, J.; Kitagawa, T. *J. Phys. Chem., 1980, 24, 1928 –1955*

[20].Kincaid, J.; Stein, P.; Spiro, T. G. *Proc. Natl . Acad. Sci. USA, 1979, 76, 549- 4156*

[21].Spiro, T. G.; Burke, J. M.; J. *Am. Chem. Soc., 1976, 98, 5482 –5489*

[22].Babcock, G. T.; Callahan, P. M. *Biochemistry, 1983, 22, 2314*

[23].Choi, S .; Spiro, T. G.; Langry, K. C.; Smith, K. M.; Budd, L. D.; Lamar, G . M. *J . Am. Chem. Soc., 1982, 104,4345*

[24].Wright, P. G.; Stein, P.; Burke, J. M. *J. Am. Chem. Soc.,1979, 101, 3531 – 3535*

[25].Spiro, T. G.; Strekas, T. C. *J. Am. Chem. Soc., 1974, 96, 338*

[26].Simpson ,W. T. ; *J . Chem . Phys ., 1949, 17, 1218-1221*

[27].Hori, H.; Kitagawa, T. *J. Am. Chem. Soc. 1980, 102, 3608 –3613*

[28].Eaton, S . S.; Eaton, G. R. *J. Am. Chem. Soc., 1975, 97, 3660*

[29].Spiro,T. G .; Strong, J. D.; Stein, P. J. Am. Chem. Soc., 1979, 101, 2648

[30].Brunner, H.; Mayer, A.; Sussner, H. *J. Mol. Biol. 1972, 70,153 –156*

[31].Brunner, H . *Biochem . Biophys . Res . Commun . 1973, 51 , 888-894*

[32].Brunner, H.; Sussner, H. *Biochim . Biophys. Acta 1973,310, 20-31*

[33].Strekas, T. C.; Spiro, T. G. *J. Raman Spectroscopy 1973, 1 , 197-206*

[34].Strekas, T. C.; Spiro, T. G. *J. Raman Spectroscopy 1973, 1 , 387-392*

[35].Pezolet, M.; Nafie, L. A.; Peticolas, W. J. J. Raman Spectroscopy 1973, 1, 455-556

[36].Nestor, J.; Spiro, T. G. *J. Raman Spectroscopy 1973, 1, 539 –550*

[37].Friedman, J. M.; Hochstrasser, R. M. *Chem. Phys. 1973, 1, 457*

[38].Strekas, T. C.; Spiro, T. G. *J . Biochim . Biophys . Acta 1974, 351, 237-245*

[39].Adar, F.; Erecinska, M. *Arch. Biochem. Biophys. 1974, 165, 570*

[40].Behringer, J. in " *Raman Spectroscopy (Szymanski , H . A., ed.) " Vol . 1, Chap 1, Plenum Press, New York*

[41a].Spiro,T .G . *Acts . Chem . Res . 1974, 1, 339-344*

[41b].Spiro, T .G. in *Chemical and Biochemical Applications of Lasers (Moore C. B., ed.) Chap. 2, Academic Press New York*

[42].Tang, J.; Albretch, A. C. in " *Raman Spectroscopy (Szymanski, H. A., ed .) Vol. 2, Chap 2, Plenum Press, New York*

[43].Peticolas, W. L.; Nafie, L.; Stein, B.; Franconi, B.; J. *Chem. Phys. 1970, 52, 1576-1584*

[44].Albretch, A. C. *J. Chem. Phys. 1961, 34, 1476-1484*

[45].Albretch, A. C.; Hutley, M. C. *J. Chem. Phys. 1971, 55, 4438*

Chapter 4

[1].(a)Kunitake, T; Okahata *J. Am.. Chem. Soc.* 1977, 99, 3860-3861.

(b) Kunitake, T.; Tsuge, A. Nakashima, N *Chem. Letts* 1984, 1783-1786. for review see (c) Kunitake, T " *Synthetic Bilayer Menbranes* " *Comprehensive Supermolecular Chem.* 1996, 9, 351-406.

[2].Rusling, J. F. Acc. *Chem. Res.* 1998, 31, 363—369.

[3].Okahata, Y.; Ebato, H. *Anal. Chem.* 1991, 63, 203-207.

[4].Rusling, J. F., Zhang, H. *Langmuir* 1991 , 7, 1791-1796 .

[5].(a) Jaswchke, M.; Butt, H.-J.; Gaub, H. E.; Manne, *Langmuir* 1997, 13, 1381-1384.

[6] Tang, Z.; Wang, E. *J. Electroanal. Chem.* 2001, 496, 82-87 .

[7].Sun, S.; Birke, R. L.; Lombardi, J.R. *J. Phys. Chem.* 1990 , 94 , 2005 –2010.

[8].Suga, Kosaku.; Bradley, Michael.; Rusling , J. F. . *Langmuir* 1993, 9, 3063-3066 .

[9].Faria, P.A.; Chen, X., Lombardi, J. R.; Birke, R. L. *Langmuir* 2000, 16, 3984-3992.

[10].(a) Snyder, R. G.; Strauss , H. L.; Elliger *J. Phys. Chem.* 1982 , 86 , 5145 – 5150.
(b) Garber, B. P.; Peticolas, W. L. *Biochim. Biophys. Acta* 1977, 465, 260-274.
(c) Snyder, R. G.; Scherer, J. R. *J. Chem. Phys* 1979 , 72 , 3221. (d) Snyder, R. G.; Hsu, S. L.; Krimm, S. Spectrochim. Acta, Part A 1978, 34, 395-406.

[11]. Kalyanasundaram, K.; Thomas, J. K. *J. Phys. Chem.* 1976, 80, 1462 – 1473.

[12].Zerbi, G.; Roncone, P.; Longhi, Wunder, S. L. *J. Chem. Phys* 1988 , 89 ,

166-173.

[13].Carey, P. R. in *"Biological Applications of Raman and Resonance Raman Spectrocopies"* 1982, Academic Press, p. 40.

[14].Van Dutne, R. P., in " *Chemical and Biological Applications of Laser Raman Spectroscopy* " ed. C. Bradely Moore

[15].Chan, S. Y-Y, " Adsorption of Surfactants at Solid/Liquid and Liquid/ Liquid Interfaces for Dewetting Process" , Ph. D. Thesis , The City University of New York, 1988

[16].Creighton; J. A. *Surf. Sci.* 1983 124, 209-219.

[17].Moskovits;M.; Suh , J.S. *J Chem. Phys.* 1984, 88, 5526.

[18].Bryant, M. A.; Pemberton J. E. *J. Am.. Chem. Soc.* 1991, 113, 3629-3637.

[19].Birke, R. L. ; Lombardi, J. R., In *Spectroelectrochemistry:Theory and Practice;* Gale, Ed. Plenum, Ch.6, 1988.

[20].Venkataraman, N.V.; Vassudevan, S. *J. Phys. Chem.* 2001, 105, 1805 – 1812.

[21].Sun, S.C., Bernard, I., Birke, R. L., Lombardi, J. R. *J. Electroanal. Chem.* 1985, 196, 359-374.

[22].Kreisig, S. M.; Tarazona, A., Koglin, E., and Schwuger, M. J. *Langmuir* 1996, 12, 5279-5288.

Chapter 5

[1].Turner, A. P.F.; Karube, I.; Wilson, G.S. *Biosensors; Oxford University Press:Oxford, U.K., 1987.*

[2].(a) Simon, H.; Bader, J.; Gunther, H.; Newman, S.; Thomas, J.Agnew. *Chem. Int. Ed.Engl. 1985, 24, 529.*
(b) Laane, C.; Pronk, W.; Franssen, M.; Veeger, C. *EnzymeMicrob.Technol. 1984, 6, 165.*
(c) Bourdillon, C.; Lortie , R.; Laval , *J.M.Biotechnol.Bioeng. 1988,31, 553.*

[3].Collman, J.P.; Gagne, R.R.; Reed, C.A.; Halbert, T,R.; Lang , G.; Robinson, W.T. *J. Am. Chem.Soc.1975, 97,1427-1439.*

[4].Tabushi, I.; Kodera, M.; Yokohama, M. *J. Am.Chem.Soc.1985, 107,4466-*

4473.

[5].Barber, D.C.; Whitten. D.G. *J. Am. Chem. Soc. 1987, 109, 6842-6844.*

[6].(a) Simone, M.J.; Kreishman, G.P. *Anal. Biochem. 1983, 132, 142-146.*

(b) Hildebrandt , P.; Stockburger, M. *Biochemistry 1989, 28, 6710-6721.*

[7].(a) Moss, D.; Nabedryk, E.; Breton, J.; Mantele, W. *Eur. J. Biochem. 1990, 187, 565-572.*
(b) Schlereth, D.D.; Mantele W. *Biochemistry 1992, 31, 7494-7502.*

(b) Schlereth, D.D.; Fernandez, V. M.; Mantele W. *Biochemistry 1993, 32, 9199-9208.*

[8].Battistuzzi, G.; Borsari , M.; Ferretti, S.; Sola, M.; Soliari, E . *Eur. J. Biochem.1995, 232, 206-213.*

[9].(a) Yuan , X.; Sun, S.; Hawkridge, F.M .; Chlebowski, J.F.; Taniguchi, I. *J. Am.Chem. Soc. 1990 , 112 , 5380-5381.*
(c) Nishiyama , K.; Hawkridge, F.M. *Biochem. Biophys. Res. Commun. 1994 , 205 1724- 1728.*

[10].Rusling, J. F.; Nassar, A.-E.F. *J. Am . Chem. Soc. 1993, 115, 11891-11897.*

[11].(a) Nassar, A. -E. F.; Willis, W. S.; Rusling , J.F. *Anal.Chem. 1995, 67, 2386-2392.*
(b) Rusling, J.F.; Nassar, A. -E. F. *Langmuir. 1994, 10, 2800-2806.*

[12].(a) Nassar, A. -E. F.; Narikiyo, Y.; Sagara, T.; Nakashima, N.; Rusling, J.F. *J. Am. Chem. Soc.; Faraday Trans. 1995, 91, 1775-1782.*
(b) Zhang, Z.; Rusling, J.F.; *Biophys.Chem.; in press.*

[13].Nassar, A. -E. F.; Zhang, Z.; Chynwat, V.; Frank, H.A.; Rusling, J.F.; Suga, K. *J. Phys. Chem. 1995, 99, 11013-11017.*

[14]. Nassar, A. -E. F.; Bobbitt, J.M.; Stuart, J.D.; Rusling, J.F. *J. Am. Chem. Soc. 1995, 117, 10986-10993.*

[15].Sun, S. C. Bernard, I.; Birke, R. L.; Lombardi, J. R. *J. electroanal. Chem. 1985, 196, 359.*

[16]. (a)Theorell, H.; Ehrenberg, A. *Acta Chem.Scand. 1951, 5, 823-848.*
(b)George, P.; Hanania, G. *Biochem. J. 1952, 52, 517-523.*
(c)Herskovits, T.T.; Jaillet, H. *Science 1969, 163, 282-285.*

[17].(a) Brunori, M.; Giacometti, G.M.; Antonini, E.; Wyman, J. *J.Mol.Biol. 1972,63,*139-152.
(b) Takahashi-Ushijima, E.; Kihara, H. *Biochem.Biophys. Res.Commun. 1982, 105, 965-968.*

[18].Nassar, A-E.F.; Zhang, Zhe.; Hu, Naifei.;Rusling, J.F. *J. Phys. Chem B 1997, 101, 2224-2231.*

[19].(a) Puett, D. *J. Biol.Chem. 1973, 248, 4623-4634.*
(b) Tang, H-L.; Chance, B.; Mauk. A . G.; Powers, L.S.; Reddy, K.S.; Smith, M. *Biochem. Biophys. Acta. 1994, 1206, 90-96.*

[20].Yang, A-S.; Honig, B. *J.Mol.Biol. 1994, 237, 602-614.*

[21].(a) Goto, Y.; Fink, A.L. *J.Mol.Biol. 1990, 214, 803-805.*
(b) Stigter, D.; Alonso, D.O.V.; Dill, K.A. *Proc.Natl. Acad. Sci. USA. 1991, 88, 4176- 4180.*

[22].Friend, S.H.; Gurd, F.R.N. *Biochemistry 1979, 18, 4612-4619; 4620-4630.*

[23].Bashford,D.; Case, D.A.; Dalvit, C.; Tennant, L.; Wright, P.E.*Biochemistry 1993, 32, 8045-8056.*

[24].Cocco, M. J.; Kao, Y-H.; Phillips, A-T.; Lecomte, J.T. *J.Biochemistry 1992, 31, 6481-6491.*

[25]. Spiro,T. G . in "*Biological applications of Raman Spectroscopy* " *1988 Volume 3 , by John Wiley & Sons Inc .*